LONDON'S GLOBAL UNIVERSITY

Design and synthesis of chimeric fungal luciferins

Author

Minyan Lyu

Thesis submitted for the degree of Doctor of Philosophy

Department of Chemistry
University College London

September 2023

I, Minyan Lyu confirm that the work presented in my thesis is my own. Where information has been derived from other sources, I confirm that this has been indicated in the thesis.

Abstract

Bioluminescence is a common light-emitting activity caused by a chemical reaction in nature performed by numerous species. The reaction is a low-toxicity bio-pathway in living cells and the cold light generated has a high signal-to-noise ratio. It is frequently used in medicinal imaging for studying cell activities *in vitro* and *in vivo* experiments. The most-widely applied bioluminescence is firefly bioluminescence, an oxidative reaction between firefly luciferase and firefly D-luciferin. Our group has worked on firefly bioluminescence for over a decade. We have focussed on improving red shifted bioluminescence wavelength and quantum yield *via* modification of the D-luciferin molecular structure. The thesis is based on expanding our studies in this area by exploring fungal bioluminescence. To explore new structures of bioluminescent molecules that may have superior qualities, different parts of D-luciferin and analogues were combined with different parts of fungal luciferin, to prepare chimeric fungal luciferin molecules.

The research began with the simple modification of the electron-donating groups of fungal luciferin. We developed a highly efficient synthetic pathway towards 3-hydroxyhispidin derivatives. The electron donating part of D-luciferin, benzo[d]thiazol-6-ol, was introduced into the fungal luciferin molecule, making the first chimeric fungal luciferin. The sulphur heteroatom in benzo[d]thiazol-6-ol was substituted with nitrogen and oxygen, making 1H-benzo[d]imidazol-6-ol and benzo[d]oxazol-6-ol type chimeric fungal luciferins. The hydroxyl group on benzo[d]thiazol-6-ol was also substituted by an amino group, making 1H-benzo[d]imidazol-6-amine type chimeric fungal luciferin. The synthetic pathway towards the chimeric fungal luciferins was changed twice during the research to improve the overall yield and *cis/trans* ratio.

The bioluminescence activity of these chimeric fungal luciferins will be tested by our collaborators in due course. Further beneficial modification of chimeric fungal luciferins can then be made based on the bioluminescence testing results to give new and improved luciferins for advanced imaging techniques.

Statement of Impact

Bioluminescence imaging (BLI) offers spontaneous and accurate imaging in tracing and monitoring biological activity in cells and living organisms. Past research has achieved several successful bioluminescence imaging systems with the firefly bioluminescence system emerging as the most successful for near-infrared (nIR) imaging. The development of the nIR imaging market is worth up to USD 1.0 billion since 2023 and is going to reach USD 1.6 billion by 2028. However, the frequency of publishing new bioluminescent structures has slowed down since 2022. Therefore, exploring new analogues of synthetic luciferins is important to academic and industrial areas.

This study explores a new strategy, where different parts of natural luciferins are combined to make a chimeric luciferin. The new chimeric fungal luciferins will broaden the building blocks and synthetic routes towards new fungal luciferin analogues. Moreover, the new convergent synthetic methods developed in this work are beneficial to synthesize trans-alkene linked heterocycles.

Acknowledgements

I would like to thank my supervisor Prof Jim Anderson for inspiration and guiding me in such a new research project. Although chimeric fungal luciferin is not a common topic, we thought, designed, overcome difficulties together and finally brought these molecules to this world.

I would like to thank my parents for financial support. There has been no scientist in the last three generations of my family. Thank you to my parents for respecting my choice and supporting me, although they initially wanted me to be a bank officer.

I would like to thank my lab colleagues, Chia-Hao, Mikhail, Storm and Jude for sharing the lab experience with me. Some experiments were poorly designed in past papers and knowledge from my lab colleagues helped me to improve those experiments a lot.

I would like to thank Martyn from the teaching lab, and people from lab 435 and lab 409 for allowing me to borrow chemicals and glassware.

I would like to thank the mechanical engineer in chemistry department for repairing our vacuum pump so many times.

Also, many thanks to NMR technical support from Prof Abil Aliev and Mass Spectrometry support from Dr Kersti Karu.

Special thanks to my favourite online artists. My working days are a monotonous cycle of simple schedules. Art prevents me from alcohol abuse and smoking when I felt stress in work and life.

Table of Contents

List of Abbreviations

λ max	Maximum wavelength
δ	Chemical shift
a.u.	astronomical unit
AkaLumine	(*S*)-2-((1*E*,3*E*)-4-(6,7-dihydro-5H-thiazolo[4,5-f]indol-2-yl)buta-1,3-dien-1-yl)-4,5-dihydrothiazole-4-carboxylic acid
Ar	aromatic
Aryl	aromatic functional group
ATP	adenosine triphosphate
BOP	(benzotriazol-1-yloxy)tris(dimethylamino)phosphonium hexafluorophosphate
Bn	benzyl
CoASH	Coenzyme A
CPH	Caffeylpyruvate hydrolase
CIEEL	chemically initiated electron exchange luminescence
CycLuc1	(*S*)-2-(6,7-dihydro-5H-thiazolo[4,5-f]indol-2-yl)-4,5-dihydrothiazole-4-carboxylic acid
DBU	1,8-diazabicyclo [5.4.0]undec-7-ene
DCM	dichloromethane
DDQ	2,3-Dichloro-5,6-dicyano-1,4-benzoquinone
DMF	dimethylformamide
DMN	dimethylnaphthalene
DMSO	dimethyl sulfoxide
dmso-d_6	deuterated dimethyl sulfoxide
$DMNO_2$	1,4-dimethylnaphtalene-1,4-endoperoxide
DSLR	Digital single-lens reflex
et al	and others
ESI	electrospray ionisation
E/Z	*trans/cis*
FAAH	fatty acid amide hydrolase
$FMNH_2$	reduced riboflavin phosphate
H3H	hispidin-3-hydroxylase
HRMS	High Resolution Mass Spectrometry
Hz	hertz
HOMO	highest occupied molecular orbital
IR	Infrared
kcal/mol	kilocalorie per mole
LDA	Lithium diisopropylamide
LiHMDS	Lithium bis(trimethylsilyl)amide
LUMO	lowest occupied molecular orbital
Luz	fungal luciferase
MEM	2-Methoxyethoxymethyl ether
MEMCl	2-Methoxyethoxymethyl chloride
MS	Mass Spec
MsCl	Methanesulfonyl chloride
MHz	million hertz
mmol	millimoles
m.p	melting point
NADH	nicotinamide adenine dinucleotide
NADPH	nicotinamide adenine dinucleotide phosphate
n-BuLi	n-butyllithium
NBS	N-bromosuccinimide

nm	nanometer
NMR	Nuclear magnetic resonance
nnluz	N. nambi luciferase
nnh3h	N. nambi hydroxylase
nnhisps	N. nambi polyketide synthase
ngpa	Aspergillus nidulans 4'- phosphopntetheinyl transferase
OAc	acetate
PAL	Phenylalanine ammonia-lyase
Pd-C	palladium-carbon
Ph	phenyl
PKS	polyketide synthase
PLE	pig liver esterase buffer
PPA	Phenylpropanolamine
ppm	parts per million
PPh_3	triphenylphosphine
sat.aq.	saturated aqueous
SET	single electron transfer
TAL	Tyrosine ammonia-lyase
Tf_2O	Trifluoromethanesulfonic anhydride
THF	tetrahydrofuran
TMS	Trimethylsilyl
TBDMS	*Tert*-Butyldimethylsilyl
TLC	Thin layer chromatography
Ts	Tosylate
TEA	triethylamine

1.Introduction

The study of bioluminescence can be traced back to an early stage of science history when in 1667 Robert Boyle found air was essential for bioluminescence. [1] The first milestone experiment was performed by Raphael Dubois in 1885. [2] A portion of crushed bioluminescent clam was placed in cold water and another portion in hot water. In hot water, the bioluminescence of the clam residue disappeared immediately, while the residue dimmed slowly in cold water. After a long time when both bioluminescence had disappeared, the two portions were combined, and bioluminescence was restored. Dubois concluded that hot water denatured the enzyme catalyzing bioluminescence and the substrate molecules necessary for bioluminescence remained. In cold water, the molecules necessary for bioluminescence were consumed and the enzyme catalyzing bioluminescence was still active. When the two portions were combined, the remaining molecules in the hot water portion met the enzyme in the cold water portion and bioluminescence was resumed. The enzyme catalyzing the bioluminescence reaction was named "luciferase" and the precursor molecule required was named "luciferin" by Raphael Dubois in 1885.

In the early 20th century, the discovery and identification of different bioluminescent systems began with common species in nature (**figure 1**). The bioluminescent systems are divided based on luciferins as one luciferin could be found in several different species. Coelenterazine-dependent bioluminescent systems are widely observed in marine species. Several phylogenetically distant species with different luciferases, such as *Renilla*, *Oplophorus*, *Periphylla*, *Gaussia*, *Metridia* and *Conchoecia* all utilize the luciferin coelenterazine to generate blue bioluminescence around 450-500nm. [3,4,5]The Cypridina-dependent bioluminescent system owns a similar tripeptide luciferin as the coelenterazine-dependent system. The luciferin cypridina molecule is observed in ostracod *Cypridina* and midshipman fish *Porichthys*. [6,7] Like the coelenterazine-dependent system, the cypridina-dependent system also generates a blue bioluminescence around 465nm. The D-luciferin-dependent bioluminescent system is mainly found in beetles. [8] One of the classic examples is the green-yellow light from the tail of firefly. Other species such as click beetles and railroad worms also generate bioluminescence with D-luciferin, but the luciferase involved in each species is completely different. The tetra-pyrrole dependent bioluminescent system is observed

in dinoflagellates and euphausiids. [9,10] Unlike previous bioluminescent systems, the luciferins involved in the tetra-pyrrole dependent bioluminescent system are different tetra-pyrrole molecules. Due to the complexity in luciferin synthesis, the study of this category is much less than other bioluminescent systems. The bacterial bioluminescent system has the simplest luciferin molecule, myristic aldehyde, and all the bioluminescent bacteria share the same mechanism of light emission. [11] The myristic aldehyde is metabolized to form reduced riboflavin phosphate ($FMNH_2$) and releases a blue light around 490nm. The Fungal bioluminescent system shares one luciferin, 3-hydroxyhispidin, among all bioluminescent fungi. The phylogency of bioluminescent fungi shows an oval evolution tree, which three genes, *luz*, *h3h* and *hisps*, are found in most of the bioluminescent fungi. [12] The converged bioluminescent fungal family tree indicates a common ancestor may exist for all bioluminescent fungi. Other bioluminescent systems, such as the diplocardia-dependent system, the fridericia-dependent system, the latia-dependent system and the odontosyllis-dependent system were also studied during 20^{th} ~21^{st} centuries and more than millions of bioluminescent creatures have been discovered.[13]

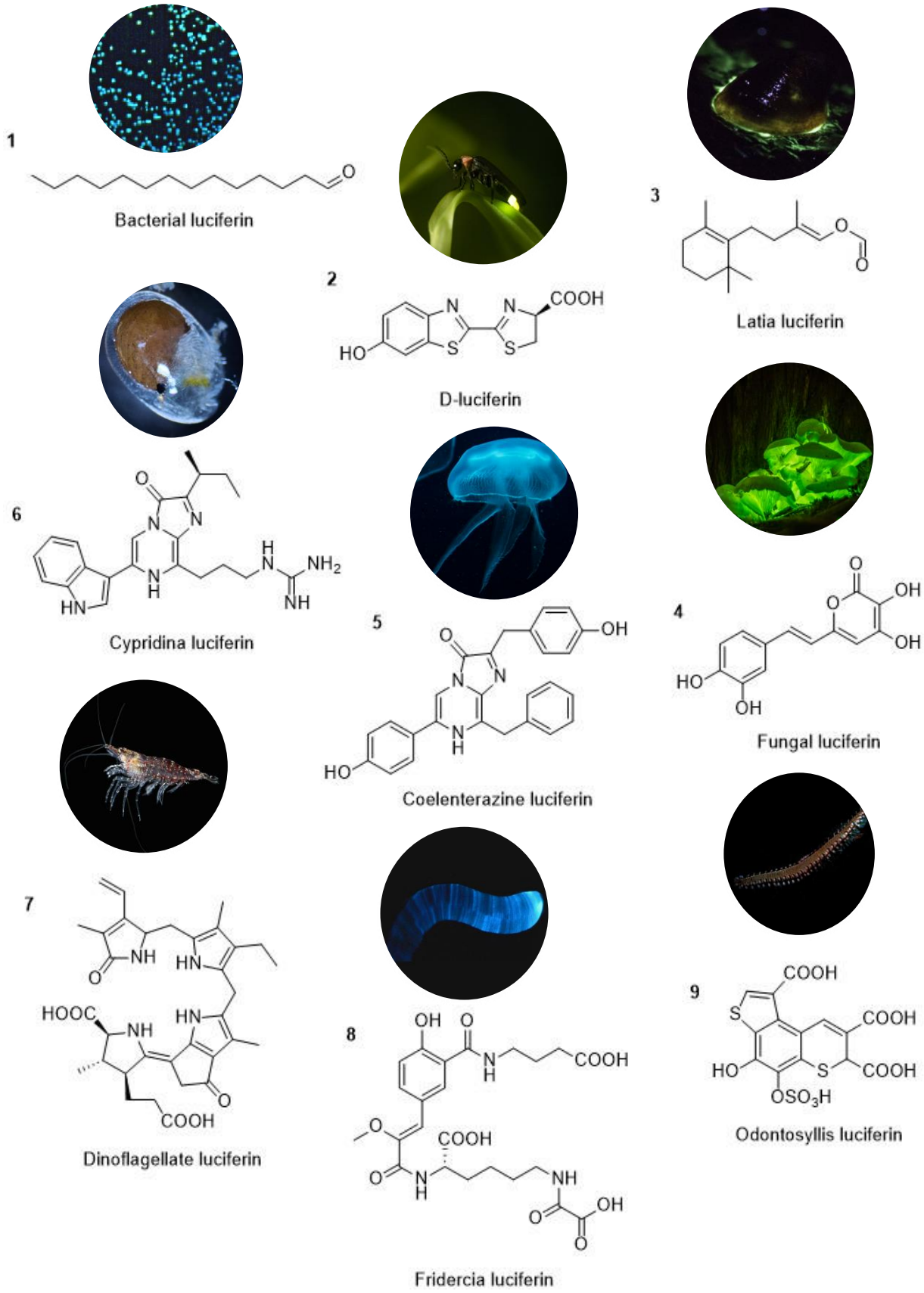

Figure 1: Bioluminescent species and corresponding luciferins

Historically, biological studies consumed vast number of animal samples, because detailed information could only be obtained by anatomical dissection. Non-invasive imaging methods were developed as a substitute for anatomic experiments. For intra-cellular experiments, a sensitive, real-time monitoring methodology is required to measure fast biological processes. Bioluminescence has outstanding properties for intra-cellular imaging as it has a low-toxicity biological pathway to living cells and the cold light generated has a low background signal. These properties attracted a lot of attention in the 20th century and bioluminescence began to be used as source of light in some biological screening experiments.

In 1953, McElory found ATP was necessary for firefly bioluminescence and the bioluminescence intensity was proportional to the concentration of ATP. [14] Later in 1966, firefly bioluminescence imaging was firstly applied to detect blood cell ATP variation. [15] Similar experiments, such as bacterial ATP detection[16] and cell membrane ATP detection[17] were also performed by firefly bioluminescence in the late 20th century. The major barrier of bioluminescence imaging in *vivo,* was from mammalian tissue absorption. In order to measure extra-weak spontaneous bioluminescence from tissue, many efforts were contributed to improving photon counting equipment and thus improve the sensitivity of the optical instrument. [18,19] In 1993, clear tumor cell imaging in dead tissue was achieved using marine bacterial *Vibrio Fischeri* bioluminescence. [20] The overall optical instrument sensitivity and understanding of the bioluminescence mechanism was greatly improved, and more and more bioluminescence imaging research has been carried out since that time.

Modern biological research requires high-resolution imaging technology which can immediately respond to cellular interactions. To achieve this goal, a high tissue penetration of bioluminescence is required so that a clear and stable signal can be sustained. The absorption band of mammalian tissue is between 400nm~ 600nm[21] and bioluminescence wavelengths higher than 600nm (red-shifted) usually have good tissue penetration. Luciferase mutations are one of the most common methods to achieve red-shifted bioluminescence. Mutants of firefly and railroad worm luciferases, such as BgLuc[22] (firefly luciferase mutant) and N351K[23] (railroad worm mutant) both generate red to infra-red bioluminescence. This method, which causes structural changes to the microenvironment of the active site of the luciferase can have a deleterious effect on the binding efficiency of the luciferin which can affect the light output.[24] It is also limited by the inherent electronic character of the natural luciferin. Other methods such

as the modification of luciferin molecule also produces red-shifted bioluminescence. Past research has shown that bioluminescence wavelength is strongly dependent upon electron density and the level of conjugation of the luciferin molecule (See later in **scheme 3** and **scheme 4**). This has become an essential guideline for designing artificial luciferins of which a large number have been made.

1.2 General luciferins and modification methods

1.2.1 Firefly bioluminescence and synthetic firefly luciferins

Firefly luciferin is a bridged heterocyclic ring molecule called D-luciferin or (*S*)-2-(6-hydroxybenzo[d]thiazol-2-yl)-4,5-dihydrothiazole-4-carboxylic acid. During the firefly bioluminescence pathway, Mg^{2+} ion, adenosine triphosphate (ATP) and oxygen are reacted together with D-luciferin by the catalyst firefly luciferase, forming an unstable dioxetanone ring **13** (**scheme 1**).[25] Decomposition of the dioxetanone ring releases a molecule of carbon dioxide and forms the excited state ketone of oxyluciferin **15**. When the excited oxyluciferin relaxes back to its ground state, it releases light of 530~635 nm which is yellow/green to the naked eye. [26]

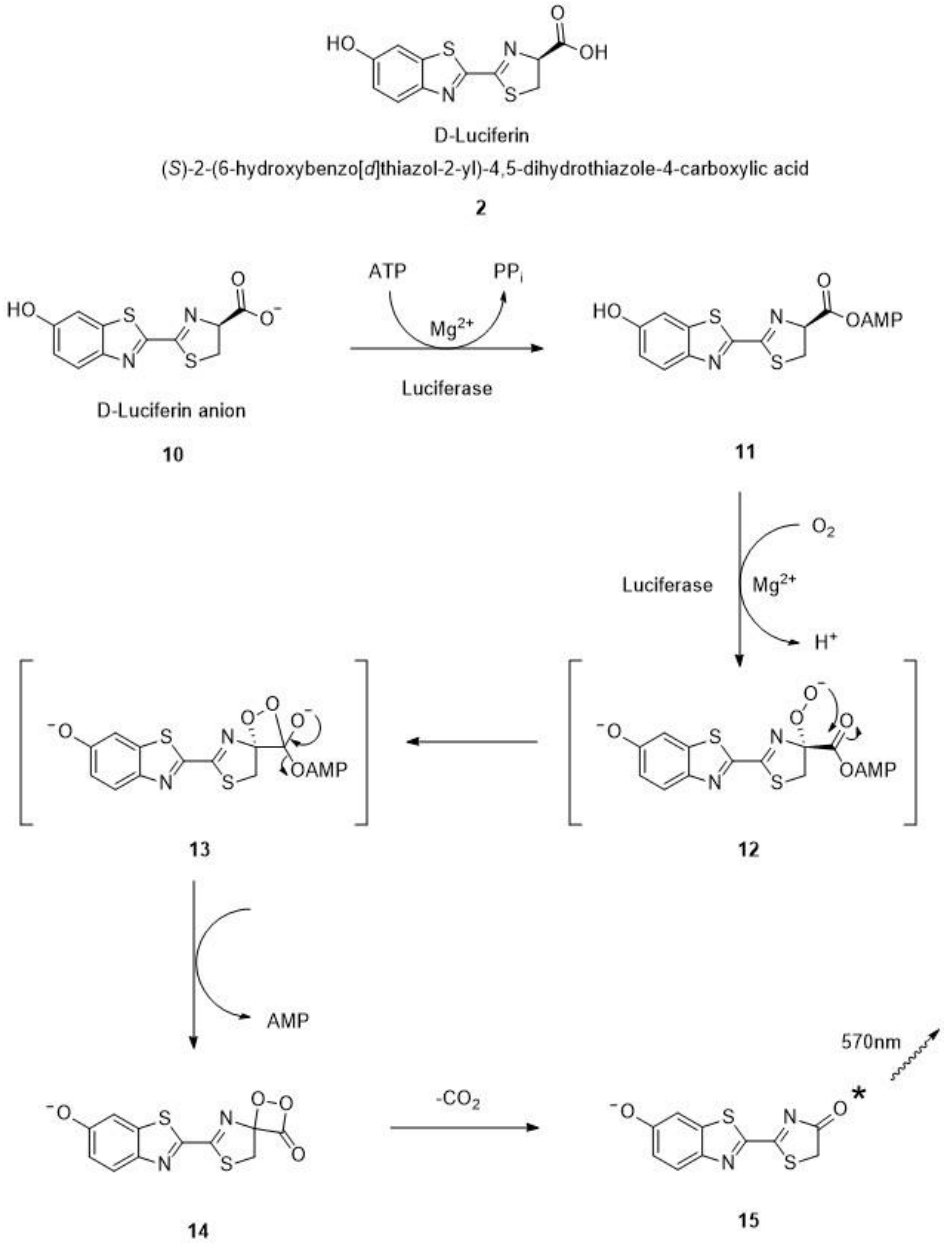

Scheme 1: Firefly luciferin and bioluminescence pathway

One of the interesting steps of this pathway is the formation of peroxide **12** by insertion of a unit of oxygen. However, triplet oxygen is usually unreactive and this process is spin-forbidden. Thus, other mechanisms, such as single electron transfer (SET) is a more likely explanation to this problematic step (**scheme 2**).

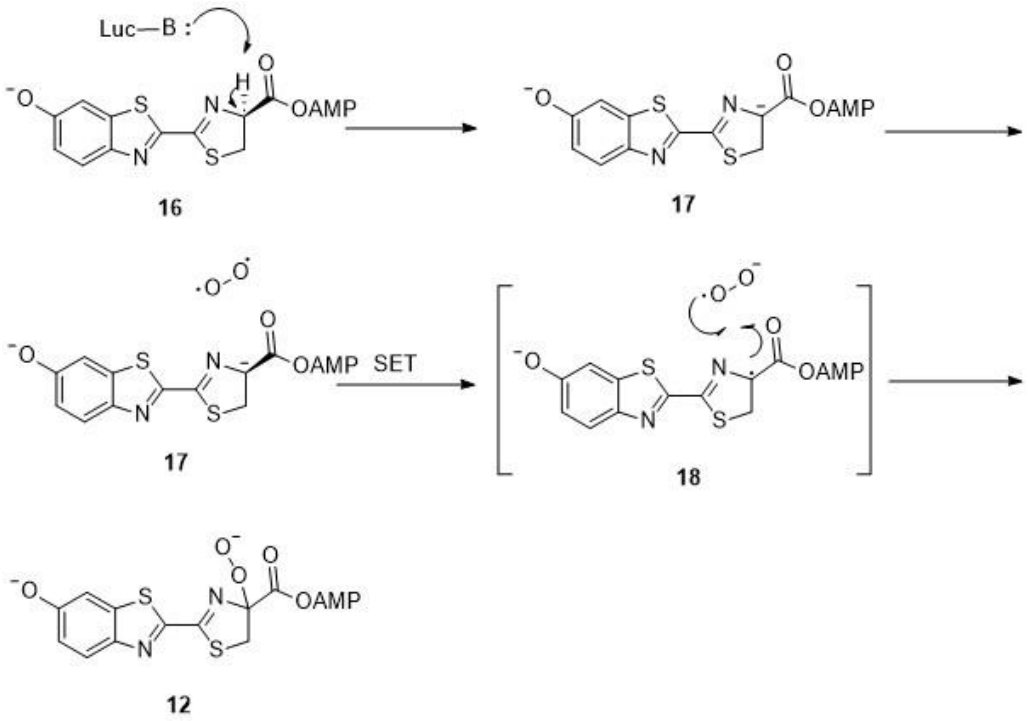

Scheme 2: Single electron transfer of peroxide formation.

The SET reaction mechanism was suggested by Branchini, Bruce R *et al.* [27] The D-luciferin is firstly deprotonated by firefly luciferase. Then, single electron transfer from D-luciferin to oxygen forms radical intermediate **18**. The reaction between **18** and radical oxygen is spin allowed and the combination of the two radicals forms the desired peroxide **12**. Cyclization of peroxide **12** generates unstable dioxetanone ring **13**.

Natural firefly bioluminescence has a wavelength peak around absorption bands (540~600 nm) of haemoglobin.[28] Bioluminescent imaging with natural firefly luciferin usually has a low tissue penetration because absorption band of haemoglobin overlaps with emission band of bioluminescence. Synthetic firefly luciferins were designed to emit red-shifted bioluminescence and avoid absorption by haemoglobin and other tissue parts. White *et al* tried to achieve this goal by replacing hydroxyl electron donating group and introducing additional substituents onto benzothiazole ring (**scheme 3**).[29,30] The resulting synthetic luciferins all had very small change in bioluminescence wavelength (<30nm). Lager wavelength change (>50nm) were

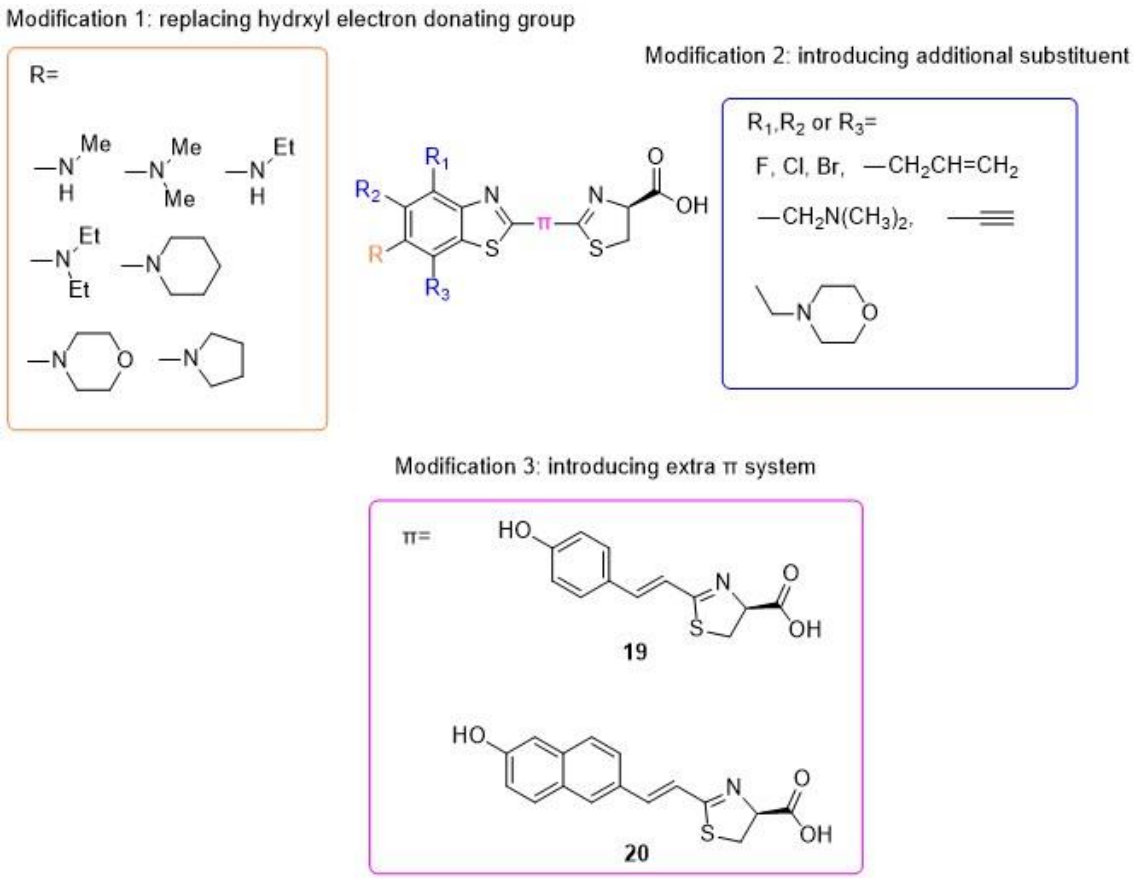

Scheme 3: Examples of past firefly luciferin modifications

achieved by introducing additional double bonds or aromatic rings between benzothiazole and thiazoline ring. [31] Increase in π- π conjugation reduced the energy gap between HOMO and LUMO, and thus increased the wavelength of S_1 to S_0 transition. Classic examples are double bond extended **19** (706nm) or aromatic extended **20** (655nm). Interestingly, this kind of modifications can lead a decrease in

brightness of bioluminescence. Many factors, such as the degrees of freedom of the molecule can lead to this decay. Natural firefly luciferin has rotational freedom across the C-C single bond between two heterocycles. Our group has made synthetic firefly analogues **21** and **22** (**scheme 4**).[32]

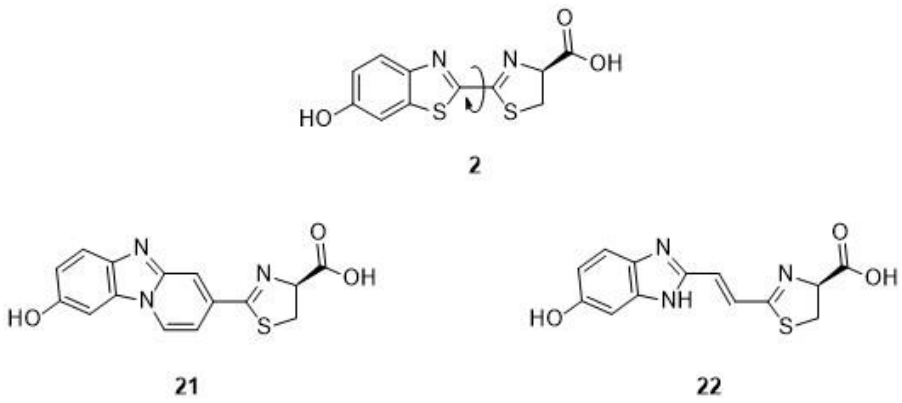

Scheme 4: Rigidness comparison between **2**, **21** and **22**.

Although molecules **21** and **22** both had red-shifted bioluminescence, molecule **21** did not show an improved bioluminescence over **22**. Compared to non-rigid molecule **2**, molecule **21** and **22** both showed a drop in brightness. This result suggested molecule rigidness could have certain enhancement on bioluminescence wavelength, but not a dominant factor to cause change on overall bioluminescence quality.

Other factors such as bioluminescence length, cell permeability and pharmacokinetic properties are also important to consider for *in vivo* experiments. Firefly bioluminescence imaging in brain is difficult because it is hard for D-Luciferin to pass the blood-brain-barrier and direct injection may cause uneven distribution of luciferin molecule. By using similar strategy in drug delivery, a prodrug luciferin CycLuc1 amide **23** was firstly made, and was converted into formal luciferin **24** by fatty acid amide hydrolase (FAAH) after passing the blood-brain-barrier[33] (**scheme 5**). The required dose of prodrug luciferin was 400-fold less and radiance level (x 10^6 p/s/cm^2/sr) was 4-time higher than normal D-luciferin **2**.

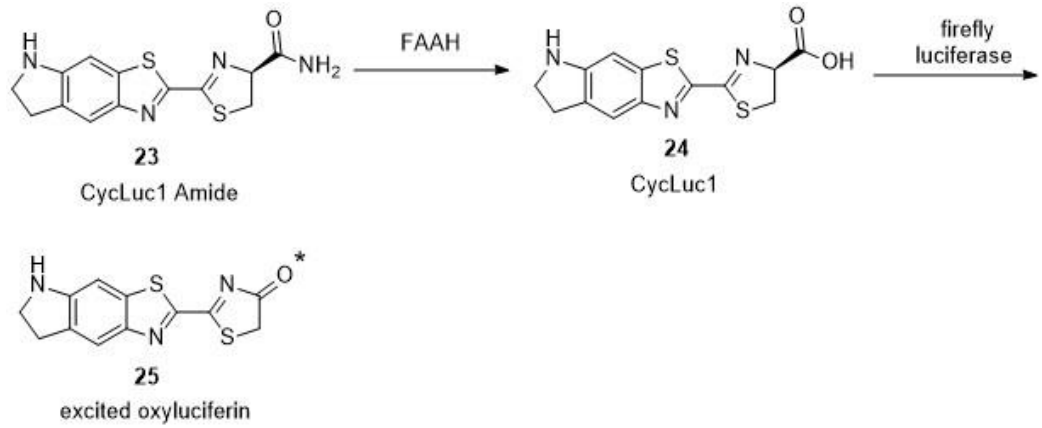

Scheme 5: Prodrug luciferin CycLuc1 amide and its pathway to excited oxyluciferin

Evans *et al* achieved one successful breast cancer imaging in mammary fat of BALB/c mice with synthetic firefly luciferin CycLuc1 (**24**) (**scheme 6**). [34] The synthetic luciferin CycLuc1 had 10- fold higher bioluminescence intensity and double the duration of bioluminescence compared to natural D-Luciferin. The synthetic luciferin CycLuc1 also had better cell permeability and a 20-fold less luciferin injection dose was required to produce clear imaging.

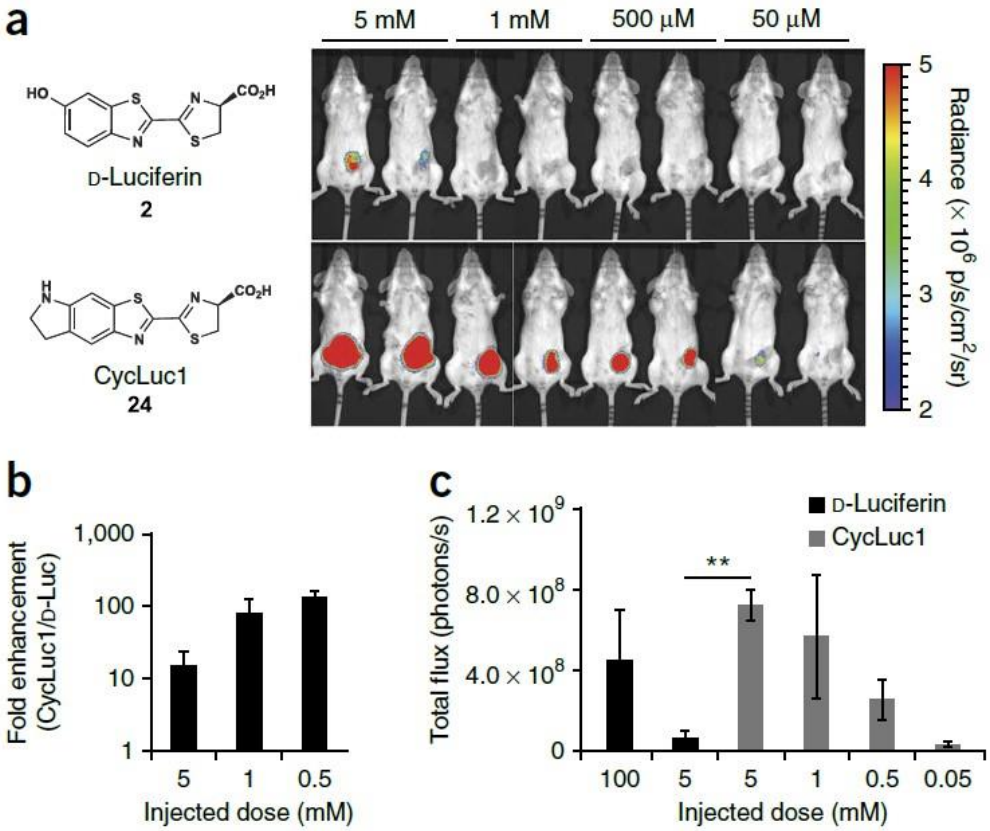

Scheme 6: Comparison between bioluminescence imaging with D-Luciferin and CycLuc1

Other chromophore modifications on firefly luciferin have also been reported. The *(S)*-carboxylic acid group was found to be necessary for interacting with firefly luciferase and it was usually kept unchanged. A major modification was performed by changing the heteroatoms of the thiazoline ring. Substitution of the thiazoline for an imidazole ring in 2012 showed that bioluminescence of synthetic firefly luciferin **26** was not observed[35] (**scheme 7**). In 2016, Ioka *et al* made an oxazoline-based firefly luciferin **27**, but again, no bioluminescence was observed when treated with firefly luciferase. [36] They also synthesized a dihydropyrrole-based luciferin **28**. Surprisingly, molecule **28** gave a blue-shifted bioluminescence (547nm) and had a higher binding efficiency than original D-luciferin.

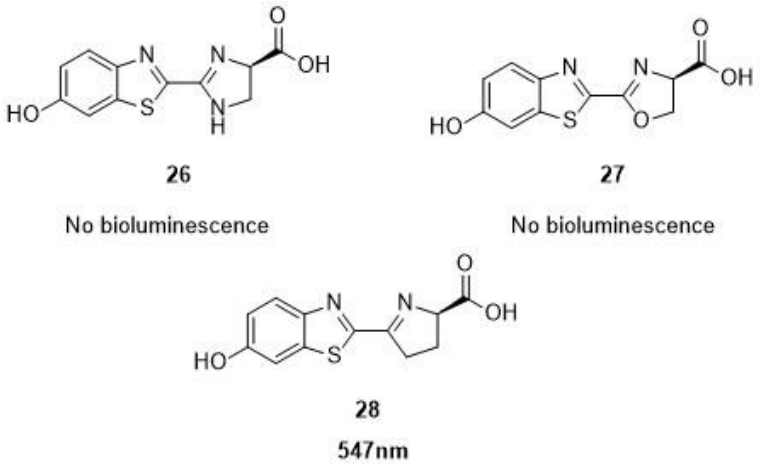

Scheme 7: Synthetic firefly luciferin by chromophore modification

1.2.2 Synthesis of firefly luciferins

Past syntheses have developed three major synthetic routes to produce D-luciferin and its derivatives. Most of the previous examples were generated from one of these synthetic routes. The earliest route was developed by White *et al* in 1963 (**scheme 8**).[30]

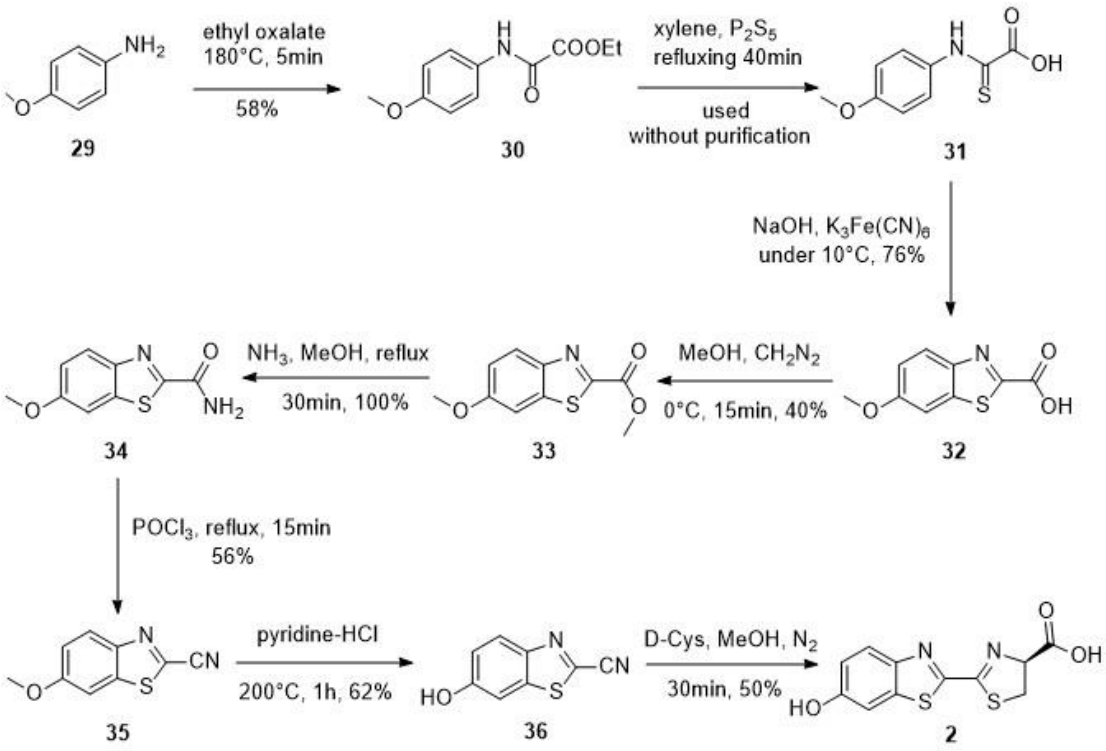

Scheme 8: D-luciferin synthetic route reported by White *et al*.

The synthesis began with simple molecule **29**. Condensation with ethyl oxalate led to amide **30** and sulfonation with P_2S_5 gave thioamide **31**. Jacobson synthesis generated benzothiazole **32**.[37] Esterification followed by condensation with ammonia yielded the intermediate amide **34**. Cyclization with $POCl_3$ formed the desired 6-methoxybenzo[d]thiazole-2-carbonitrile (**35**). The methyl ether was then deprotected by pyridine-HCl and condensation of cysteine with the nitrile formed the thiazoline and the final D-luciferin **2** as a single enantiomer. The condensation of cysteine with the nitrile is the same step that is used in nature.

Within this synthesis, the mechanism of Jacobson synthesis is still unclear. There are two reasonable explanations to this step (**scheme 9** and **10**).

Metzger and Planck proposed one pathway which initiated by formation of sulfur electrophile.[38] Molecule **31** firstly tautomerized into form **37** and the thiol attacked nitrile on $Fe(III)(CN)_6^{3-}$. After elimination of $Fe(II)(CN)_6^{4-}$, thioimidic cation **39** was generated and self-cyclization generated the desired benzothiazole **32**.

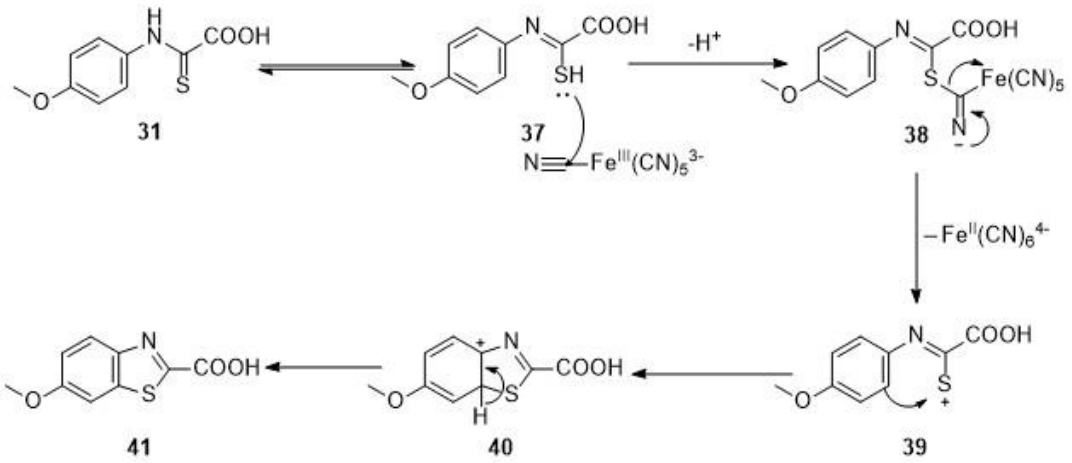

Scheme 9: Proposed Jacobson synthesis mechanism A

An alternative radical mechanism was proposed by Stevens *et al*. Molecule **31** was deprotonated under basic condition and tautomerized into imidothiolate **41**.[39] Then, electron transfer with $Fe(III)(CN)_6$ generated radical intermediate **42**. A radical cyclization with aromatic ring lead the benzothiazole **32**.

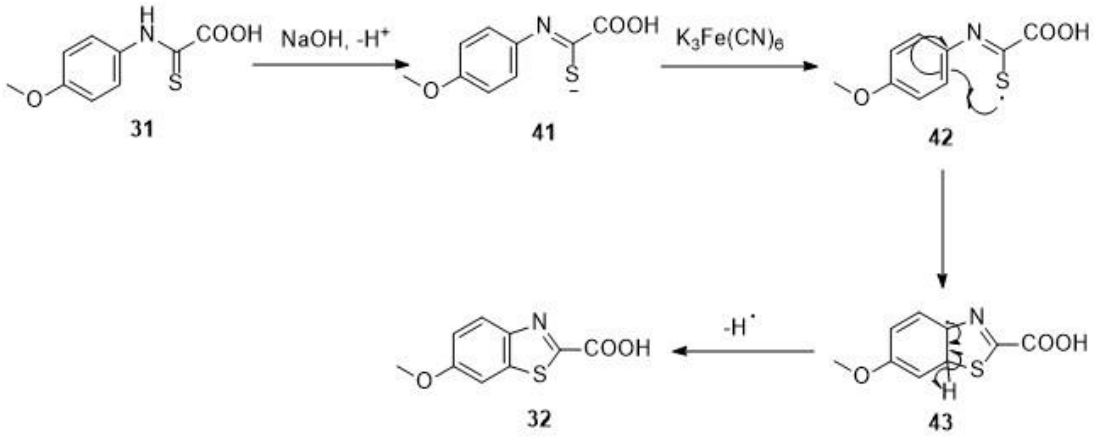

Scheme 10: Proposed Jacobson synthesis mechanism B

The improved method was based on diazotization of 6-methoxybenzo[d]thiazol-2-amine **44** (**scheme 11**). [40] Substitution of N_2^+ with CuCl generated chlorobenzothiazole **45**. The nitrile **36** was generated directly by substitution with KCN on the deprotected material and the thiazoline was formed by the biomimetic condensation reaction as described above. The yield reported in the original paper was not high but it was improved significantly (45% increase in overall efficiency) in later papers. [41,42,43]

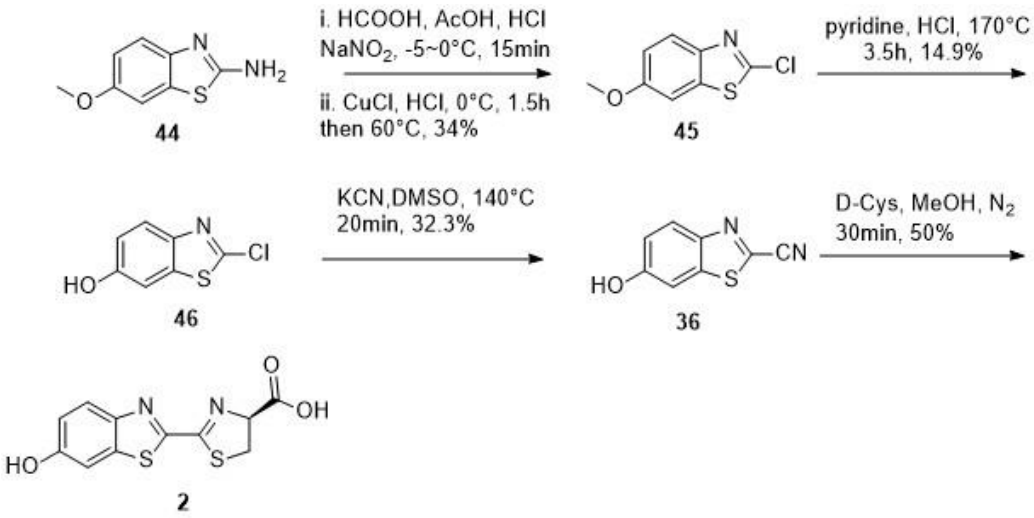

Scheme 11: D-luciferin synthetic route based on diazotization chemistry.

The third method utilized Appel's salt to shorten the pathway of generating nitrile **36** (**scheme 12**).[44] An intermediate **47** was made by treatment of **29** with Appel's salt. Fragmentation of **47** with DBU lead to **48** which was cyclized using palladium catalysis to give the desired nitrile **35**. Deprotection with pyridine HCl led the **36** and reaction with D-cystine led to the final D-luciferin **2** as usual.

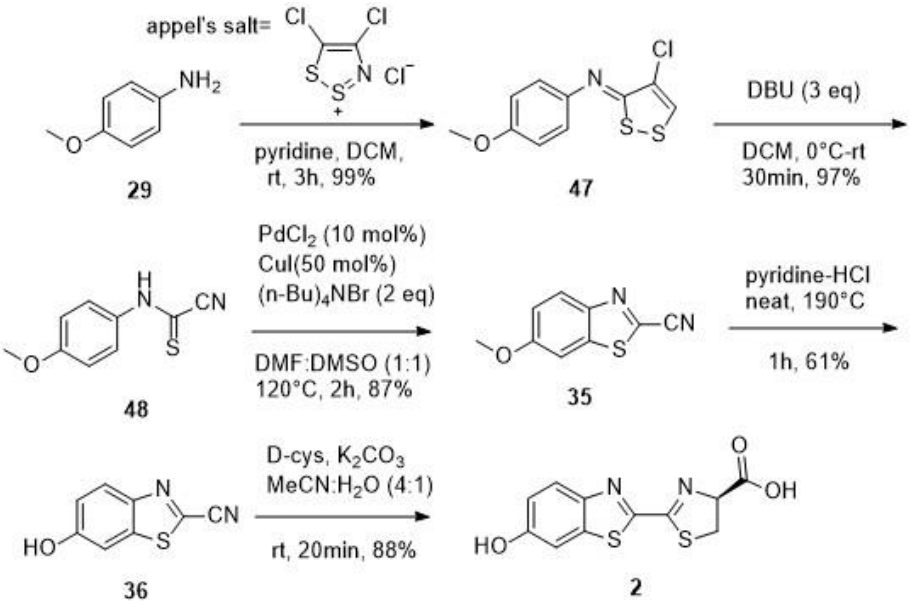

Scheme 12: D-luciferin synthetic route based on Appel's salt chemistry.

For modified D-luciferins with extended conjugation, Wittig methodology was frequently applied to build the *trans*-alkene structure (**scheme 13**).[45] For example, the synthesis of **19** began with aldehyde **49**. Reaction between **49** and stabilized Wittig reagent lead *trans*-alkene **50** in high yield. The product was then condensed with a suitable amino acid derivative and cyclized with Hendrick's reagent, lead the desired product **52**. The detailed mechanism of cyclization is shown in **scheme 14**. Deprotection of the benzyl ether and methyl ester of **52** gave the final *trans*-D-luciferin **19**. [43]

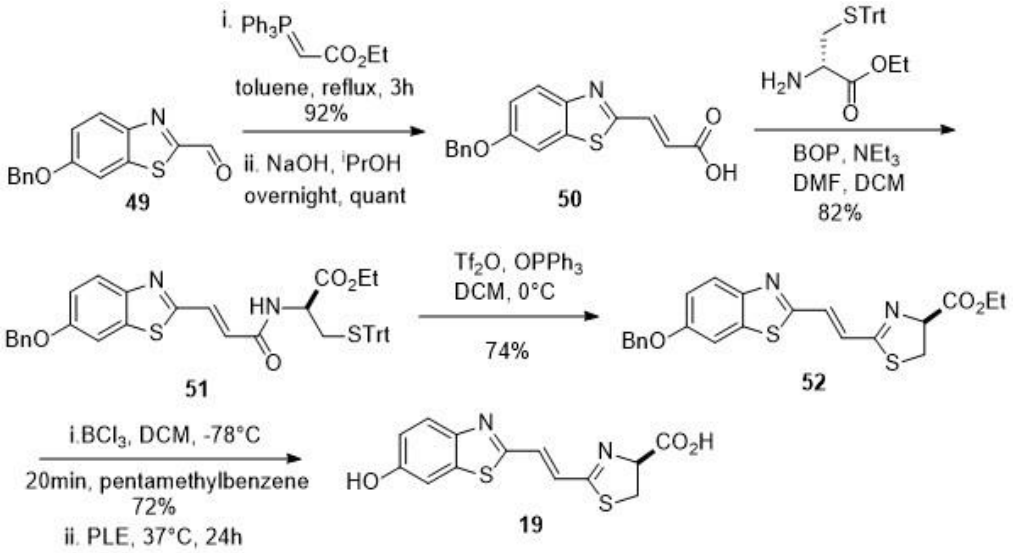

Scheme 13: *Trans*-D-luciferin **19** synthesis by Wittig reagent.

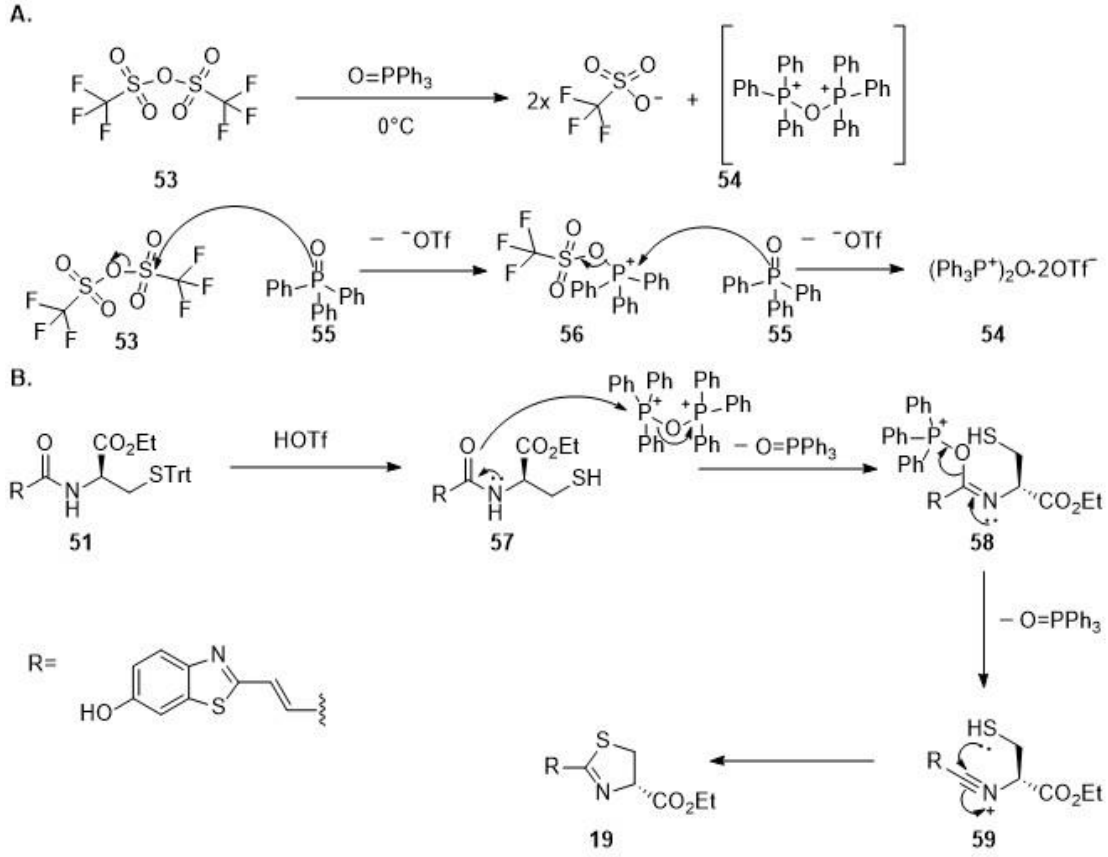

Scheme 14: **A**. Formation of Hendrick's reagent **B**. Mechanism of **51** cyclization.

Hendrick's reagent is an ionic compound with formula $(^{+}PPh_3)_2O.2OTf^{-}$, generated *in situ* by mixing $O{=}PPh_3$ and Tf_2O at 0°C (**scheme 14 A**). [143,144] The resultant oxy phosphonium salt is highly electrophilic and acts as a good dehydrating agent. The S-Trt group in molecule **51** was firstly deprotected with HOTf to give amide **57**. The oxygen in the amide group was then eliminated by the oxy phosphonium salt to form the nitrilium ion **59**. The naked thiol in **59** initiated a *5-endo-dig* cyclization and formed 5-membered ring **19** (**scheme 14 B**).

1.3 Fungal bioluminescence and synthetic fungal luciferins

1.3.1 Introduction

Fungal bioluminescence widely exists as a green-yellow light emission (~530nm) process. The mechanistic study of this process began in the early 20th century and whether it included a luciferase-luciferin system was frequently argued. Many researchers tried to regenerate fungal bioluminescence *via* the classic luciferase-luciferin test, which a hot extract of the proposed luciferin molecule was mixed with cold extract of luciferase enzyme. Airth and McElory reported that nicotinamide adenine dinucleotide (NADH or NADPH) extended the duration of fungal bioluminescence light emission when mixed with luminous fungal extract. [46] Later in 1966, Kuwabara and Wassink found that an enzyme was necessary for fungal bioluminescence and reported a method to isolate crude luciferin.[47] They also found the crude luciferin mixture gave a 524nm chemiluminescence under the addition of hydrogen peroxide. However, detailed data of the luciferin was not given, and their work was not continued. A successful luciferase-luciferin test by combing hot extract of luciferin and cold extract of enzyme was carried out in 2009.[48, 141] Hot and cold extractions of *G. viridilucens* mycelium were prepared and cross reaction between the two extraction solutions generated light (For similar seminal studies see page 10 bioluminescent clam experiment). This experiment finally confirmed fungal bioluminescence was a luciferase-luciferin based system. The isolation of pure fungal luciferin, 3-hydroxyhispidin, was completed until Konstantin *et al* in 2015.[26] In their research, NADPH was found to be necessary for the generation of the fungal luciferin molecule. They suggested all the luminous fungi shared one common precursor molecule, hispidin, and that this was converted to a common luciferin molecule, 3-hydroxyhispidin. The detailed mechanistic study was carried out by Kaskova's group in 2017.[50] They reported the complete mechanism of fungal bioluminescence pathway and discovered the structure of the corresponding fungal oxyluciferin. In 2018, a genetic study of luminous fungi was carried out by Alexey's group.[12] The group found three major genes, *luz*, *h3h* and *hisps* were involved in all luminous fungi. Two additional genes, *cpy450* and *cph* were only contained in a few luminous fungal systems. After the classification of luminous fungal gene tree, four bioluminescent fungal genes, *cph*, *luz*, *h3h* and *hisps* were encoded into tobacco plants and created

self-glowing tobacco.[52] The biopathway of fungal bioluminescence was non-toxic to the tobacco plant and the plant showed bioluminescent properties in all growth stages. After that, Khakhar's group produced more auto-luminescent plants, including tomato (*Solanum lycopersicum*), dahlia (*Dahlia pinnata*), rose (*Rosa rubiginosa*), periwinkle (*Catharanthus roseus*) and petunia (*Petunia hybrida*).[53] In these transient plant studies, fungal bioluminescence showed a major advantage in its non-toxic biopathway and short luminous gene expression. On the other hand, fungal bioluminescence in animal experiments is still developing, more research is being carried out on improving the fungal bioluminescence quality and fungal bioluminescence has a high potential in future imaging applications.

1.3.2 Bioluminescent fungal gene tree

Nature develops diverse living species which can be subdivided into Animalia, Plantae, Fungi, Protista, Archaea and Bacteria. Fungi plays an important role in the bottom of food chain as well as Plantae and Bacteria.[54] Until 2020, more than 2.2 million of fungi species were recorded and 109 bioluminescent fungi species were discovered.[55, 56] These bioluminescent fungi can be divided into four molecular lineages: *Omphalotus* lineage (12 species), *Armillaria* Lineage (10 species), *Mycenoid* lineage (85 species) and *Lucentipes* lineage (2 species). [55, 57]

Armillaria lineage is the most classic bioluminescent fungal lineage and probably responsible for "glowing wood" in ancient records. There are more than 40 species in genus *Armillaria* and 10 of them are bioluminescent fungi.[58] Most of the *Armillaria* fungi are saprotrophs and tree root pathogens. They obtain nutrition from the root of plants and release long term bioluminescence (up to 10 weeks) when forming complete mycelium.[59]

Omphalotus lineage is also well recorded in past research of bioluminescent fungi. The lineage is known for large mushrooms such as *N. gardneri* and *N. nambi*.[60] Different from *Armillaria* lineage, *Omphalotus* lineage generates bioluminescence from fruit bodies not mycelium.[61] A cold and hot extract experiment was performed on *Armillaria* lineage and *Omphalotus* lineage separately. Cold and hot extracts were prepared from mycelium and fruit bodies of each lineage. For *Armillaria* lineage, there was no significant change in bioluminescence when the cold extract of fruit bodies met the hot extract of fruit bodies. However, a greater bioluminescence was

regenerated when the cold extract of mycelium met the hot extract of mycelium. The author concluded that hot water denatured enzymes necessary for bioluminescence, but retained the substrate. While the cold water kept the enzyme and consumed all the substrate. When the hot and cold extract of mycelium were combined, the enzyme (luciferase) and substrate (luciferin) met again, and bioluminescence was reproduced. An inversed result was observed in *Omphalotus* lineage. The result suggested luciferase was contained within mycelium of *Armillaria* lineage and fruit body of *Omphalotus* lineage. Therefore, *Armillaria* lineage utilizes mycelium for bioluminescence and *Omphalotus* lineage utilizes fruit body for bioluminescence. *Mycenoid* lineage contains a wide range of species (more than 600) which have significant differences in colour, shape, habitat, and nutritional modes. 85 of these *Mycenoid* species are bioluminescent and their bioluminescence properties are diverse.[55,57,62] In some fungi such as *Mycena jingyinga*, bioluminescence can only be observed in mycelium while in other fungi such as *Mycena luxarboricola*, bioluminescence can be observed in both mycelium and fruit body. Because there is such a big difference in each individual species of *Mycenoid* lineage, the ancestor of this lineage is still a question and several hypotheses such as endophytic ancestors are waiting to be proved.

The last two bioluminescent fungi belong to *Lucentipes* lineage which is an unnamed family. Due to the limitation in molecular sequence study, these two species are much less well-known compared to previous lineages. [55]

Early genome research of bioluminescent fungi focused on tracing three major genes, *luz*, *h3h* and *hisps*, which were necessary for bioluminescence. A phylogeny tree of *Agaricales* species was mapped out based on these genes (**figure 3**). [12] The *luz* gene which codes for Luz luciferase was widely found throughout the *Agaricales* order. Interestingly, there seems to be a strong link between the *luz*, *h3h* and *hisps* gene and they usually sit close to each other in a cluster (**figure 2**). Only four species with the *luz* gene are not relevant to *h3h* or *hisps* gene. Within the *h3h* and *hisps* branch, a large number of species which code *hisps* is non-bioluminescent. The same situation is also observed in *h3h* homologs and many of them are non-bioluminescent due to a lack of ketoreductase and dehydratase. The rest of the bioluminescent fungi were divided into four lineages as stated before, but the *Marasmiaceae* lineage was changed into the *Lucentipes* lineage during years of study. There is a duplication of the *h3h* and *hisps* genes in evolution of *Agaricales* with the luz gene as a base

separating throughout the whole *Agaricales* species. This pattern suggests bioluminescent fungi might have a common ancestor. Other interesting patterns of evolution, such as some bioluminescent fungi (*Armillaria* lineage) are sister groups of non-bioluminescent fungi (*Physalacriaceae* lineage) require more complicated explanations: [55]

1. There was a common ancestor for all bioluminescent fungi but some bioluminescent genes were lost during evolution.
2. Several convergent evolutions took place in different ancestors of bioluminescent fungi.

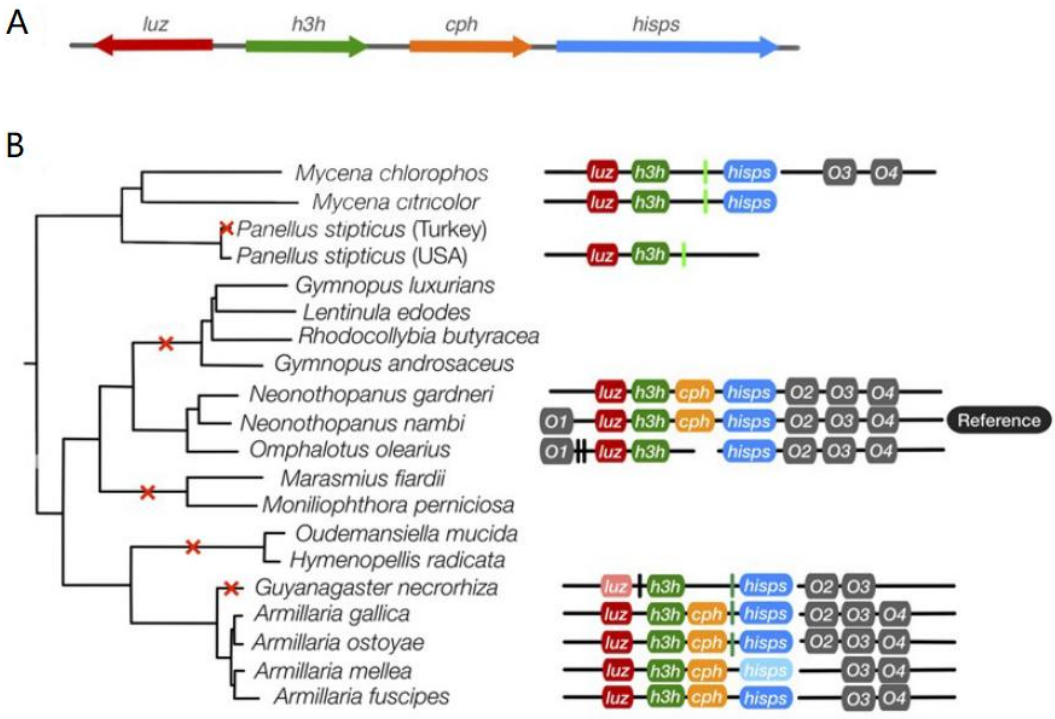

Figure 2: A. Classic order of bioluminescent related gene in *N.nambi*.
B. Gene cluster of some fungi clade. A red cross means the species have no bioluminescence ability. A green tick means cytochrome P450 like gene and black tick indicates other gene. Grey O1~O4 represent for gene relates to the cluster.

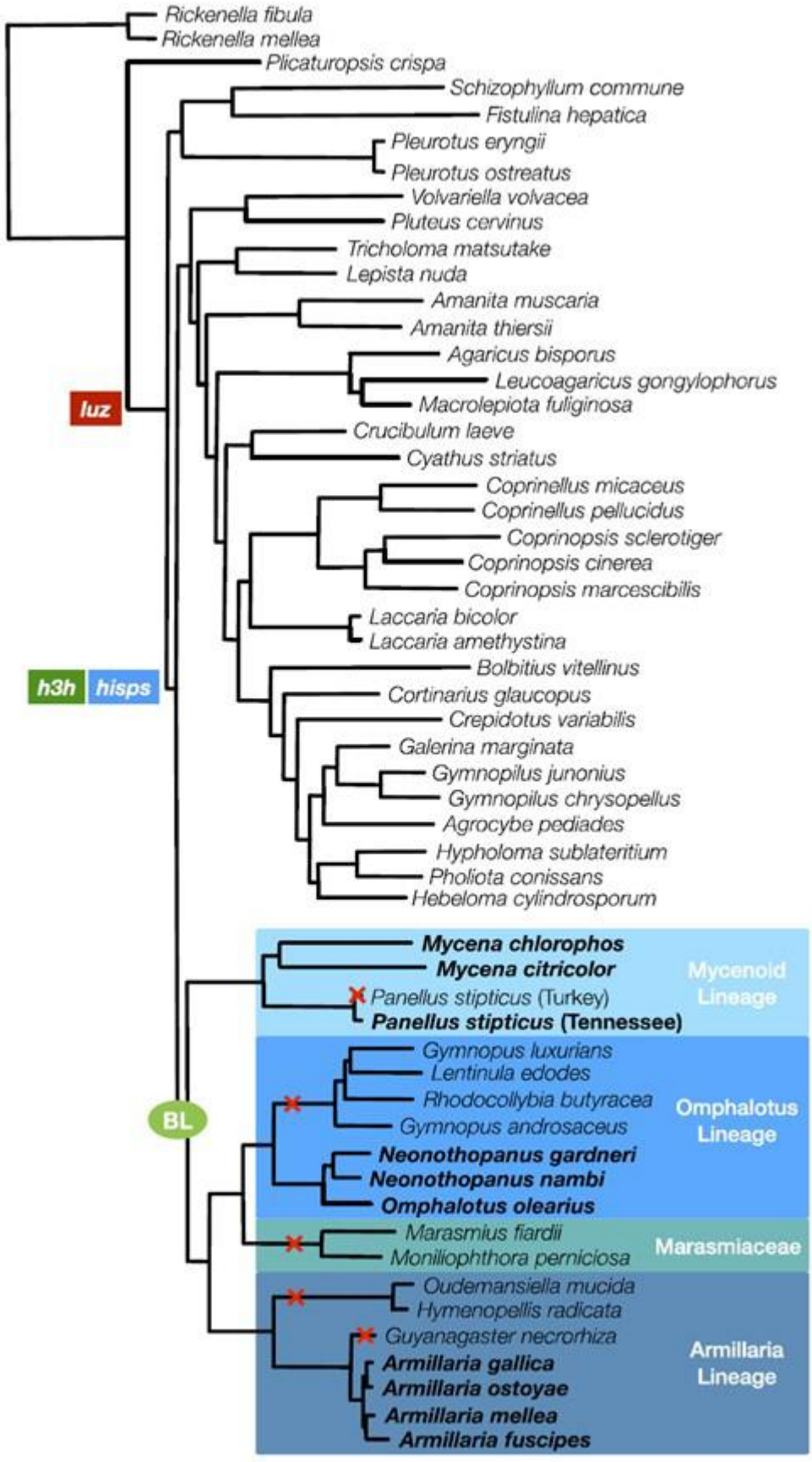

Figure 3: Gene tree of *Agaricales* species based on *luz*, *h3h* and *hisps* gene. [12]

1.3.3 Fungal bioluminescence pathway

Caffeic acid is the first precursor molecule of fungal luciferin. It is a product from common metabolites such as phenylalanine and tyrosine (**Scheme 15**).[63] The generation pathway of caffeic acid is usually two to three steps long. Elimination of the primary amine by PAL converts phenylalanine into cinnamic acid. The two hydroxyl groups on benzene are introduced by C4H and C3H hydroxylase with NADPH and oxygen. The production pathway from tyrosine follows the same route. Elimination of primary amine with TAL generates *p*-coumaric acid and the same hydroxylation with C3H converts *p*-coumaric acid into caffeic acid.

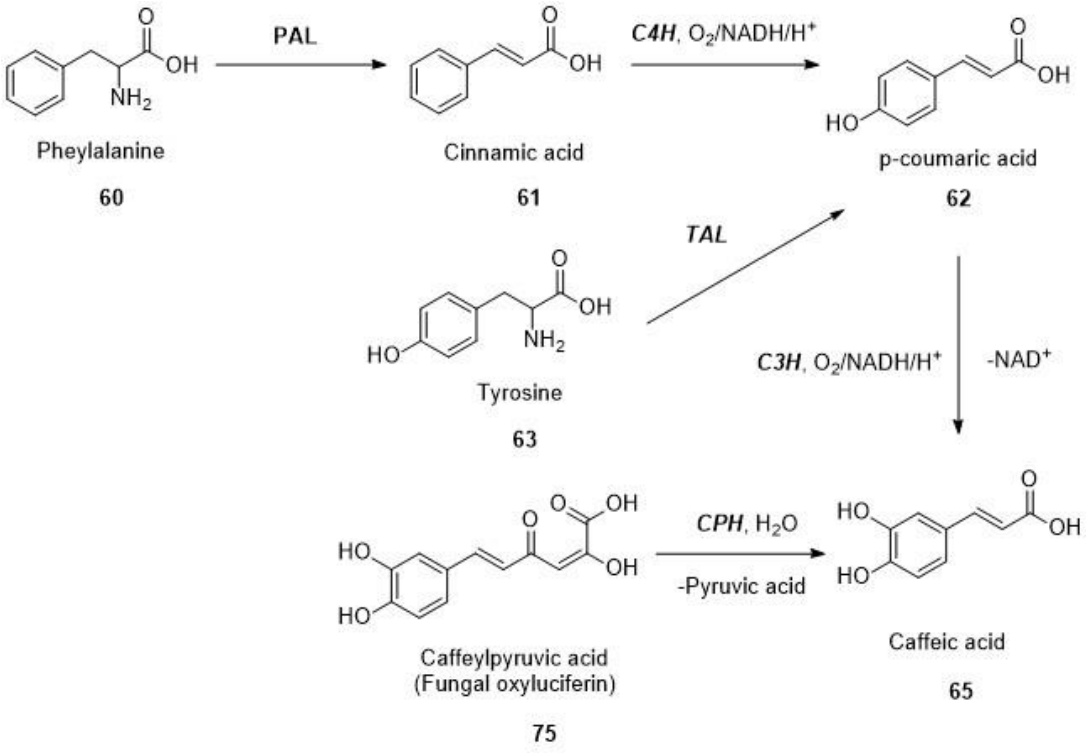

Scheme 15: Source of caffeic acid in fungal

The fungal bioluminescence pathway also recycles the oxyluciferin to produce caffeic acid. Caffeylpyruvate hydrolase (CPH) catalyses the decomposition of the final metabolite (caffeylpyruvic acid) of fungal bioluminescence with water, forming one unit of pyruvic acid and caffeic acid[12].

Hispidin is the second precursor molecule of fungal luciferin from caffeic acid. Past research proved its production was catalyzed by *hisps*, a member of the polyketide synthase family (**scheme 16**). [12] The function of polyketide synthase (PKS) usually relates to carbon chain length increase by addition of malonyl moieties.[49] The extra four carbon difference between hispidin and caffeic acid suggests hispidin may be synthesized by two malonyl unit additions to caffeic acid, followed by a self-lactonization. An enzyme cofactor, CoASH, is firstly attached to caffeic acid under PKS catalysis. Then, molecule **67** is attached to PKS after substitution of CoASH. The carbon chain increases by two after the first addition of a malonyl group, and one more malonyl addition gives the complete carbon skeleton structure **69** before cyclization. The enol form of **69** cyclizes to generate hispidin **73** *via* self-lactonization.

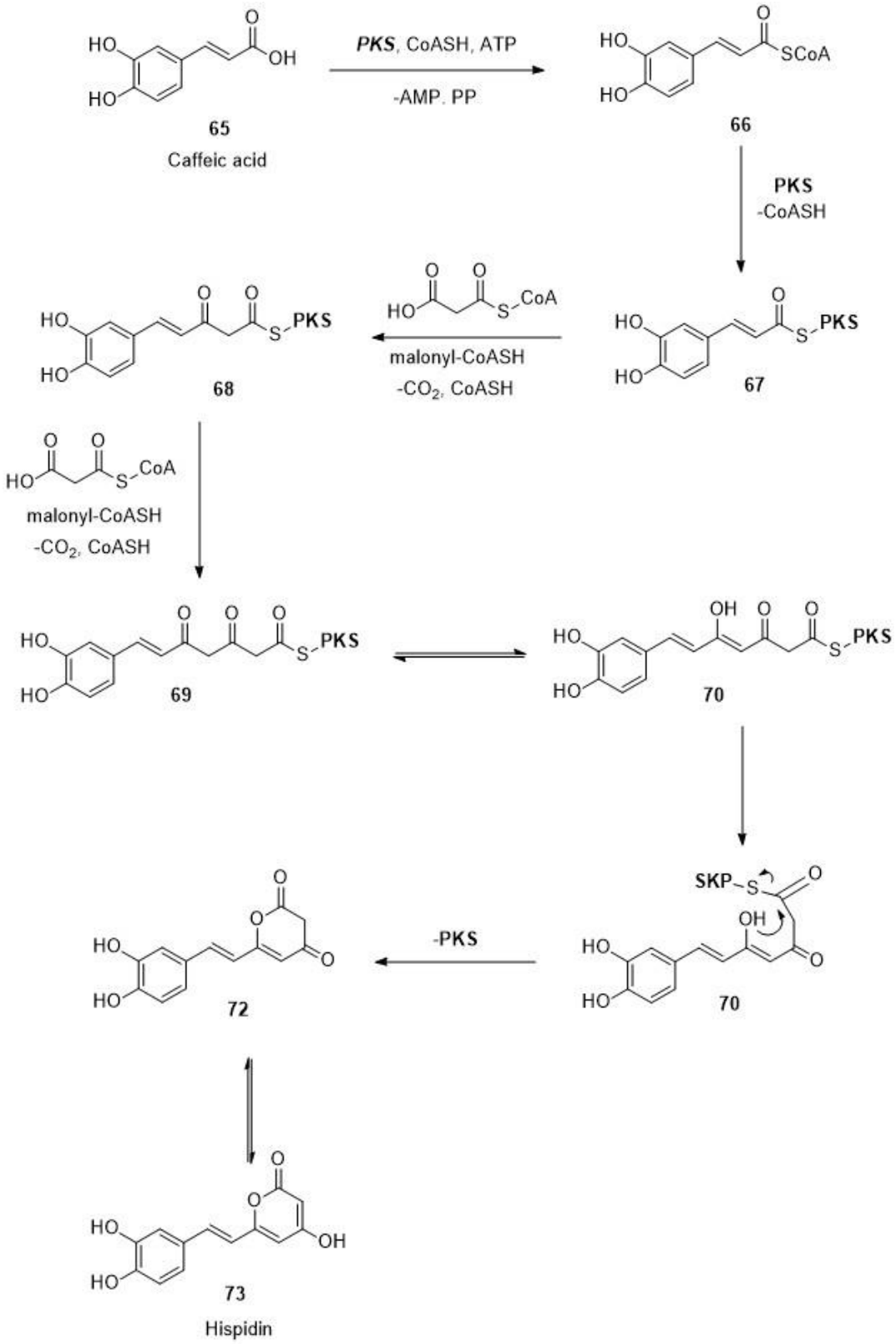

Scheme 16: Proposed hispidin synthesis mechanism from caffeic acid in fungi. [12]

The formal fungal luciferin, 3-hydroxyhispidin, has a similar bridged heterocyclic ring structure as firefly luciferin (**scheme 17**). They both contain an electron-donating aromatic ring and an oxygen based light activating part which can be oxidized by corresponding luciferase. The 3-hydroxyhispidin is generated from hispidin by hispidin-3-hydroxylase (H3H).[51] The hydroxyl group on C3 position is introduced by H3H hydroxylation with oxygen and NADPH.

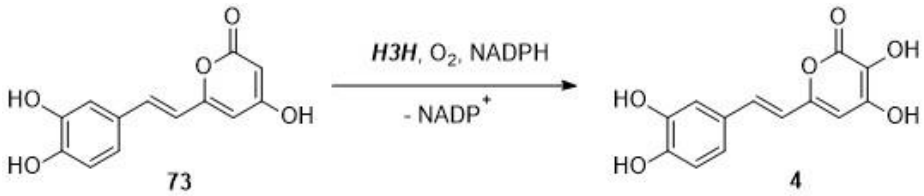

Scheme 17: Hydroxylation of hispidin by H3H.

The 4,5-dihydroxy-2H-pyran-2-one part is its light activating part and the 1,2-benzenediol ring donates electron density to this part. To generate bioluminescence, the fungal luciferase (Luz) firstly oxidises the light activating part by adding an

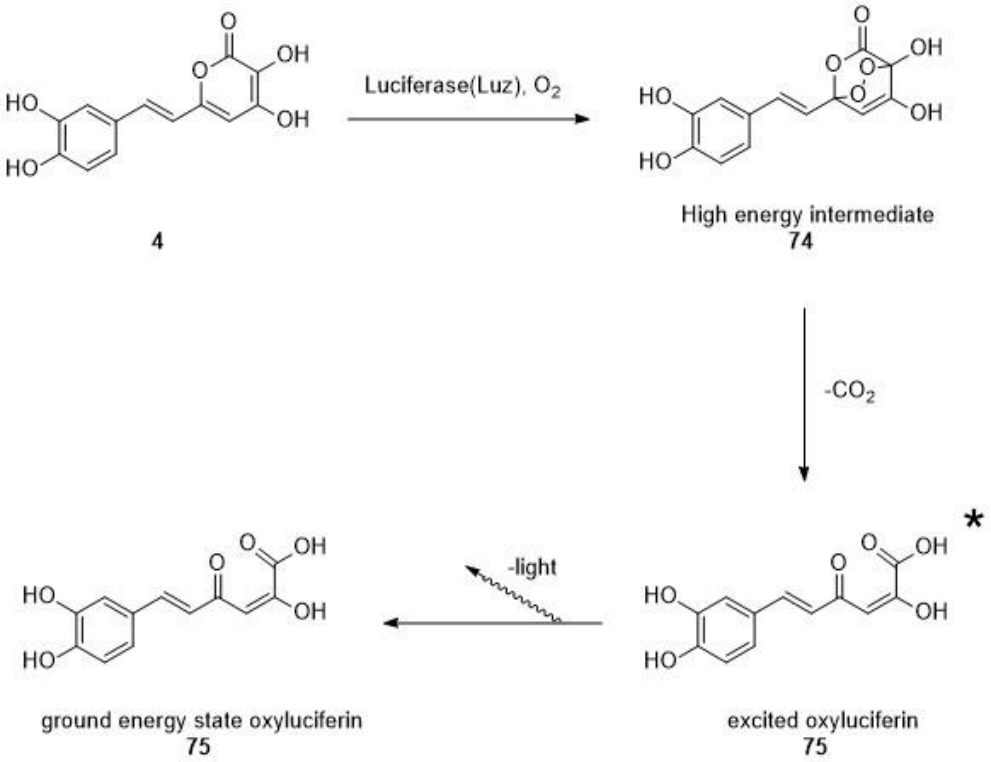

Scheme 18: Fungal bioluminescence pathway from fungal luciferin 3-hydroxyhispidin.

oxygen molecule (**scheme 18**). The resulting endoperoxide is an unstable high energy intermediate. It decomposes to form the excited oxyluciferin, which generates light when it relaxes back to its ground energy level. [50]

In past research of endoperoxide chemiluminescence, this type of decomposition usually breaks two σ-bonds of dioxetane and forms an excited carbonyl π-bond. The bond cleavage process has many different mechanisms based on the substituents beside the dioxetane. Unimolecular biradical cleavage is one of the most favoured mechanisms for simple hydrocarbons. Gary B. Schuster has reported thermolysis of 1-(4,4-dimethyl-1,2-dioxetan-3-yl)ethan-1-one as a unimolecular biradical cleavage (**scheme 19**). [63]

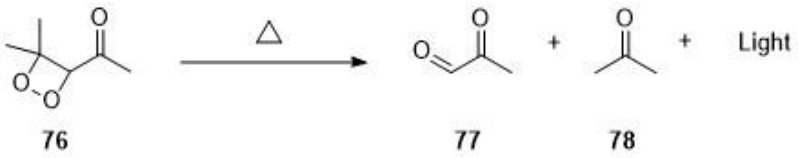

Scheme 19: Thermolysis of 1-(4,4-dimethyl-1,2-dioxetan-3-yl)ethan-1-one

Other mechanisms of dioxetane cleavages can involve elimination of gas molecules. Luminol **79** (**scheme 20**) is frequently used as a chemiluminescence dye in medicinal experiments.

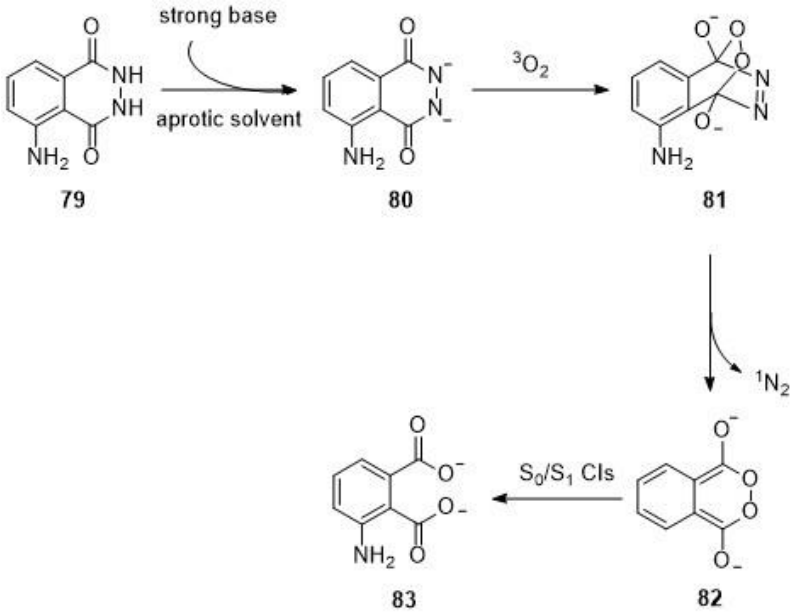

Scheme 20: Luminol chemiluminescence in aprotic solvent.

The molecule gives strong chemiluminescence when mixed with oxidizing agents, such as H_2O_2, O_2 or hemoglobin. In aprotic solvent such as DMSO, only a strong base and molecular oxygen are required to generate chemiluminescence.[64, 65] Computational modelling suggested the reaction was initiated by deprotonation of **79** under strong base. Concerted addition of triplet oxygen to the luminol dianion yielded endoperoxide **81**. Then, concerted elimination of N_2 gas yield peroxide **82** and decomposition of peroxide ring *via* two conical intersections yield the final chemiluminescent molecule **83**.

Thermal decomposition of **119** has a similar mechanism to the high energy intermediate decomposition in fungal bioluminescence pathway (**scheme 21**). Endoperoxide **84** is made by oxidation of **119** with singlet oxygen. Carbon dioxide is eliminated under thermal 4n+2 six electron decarboxylation, leading intermediate peroxide **85**.[66] Chemiluminescence is generated by chemically initiated electron exchange luminescence (CIEEL) between **85** and side-product **86**.

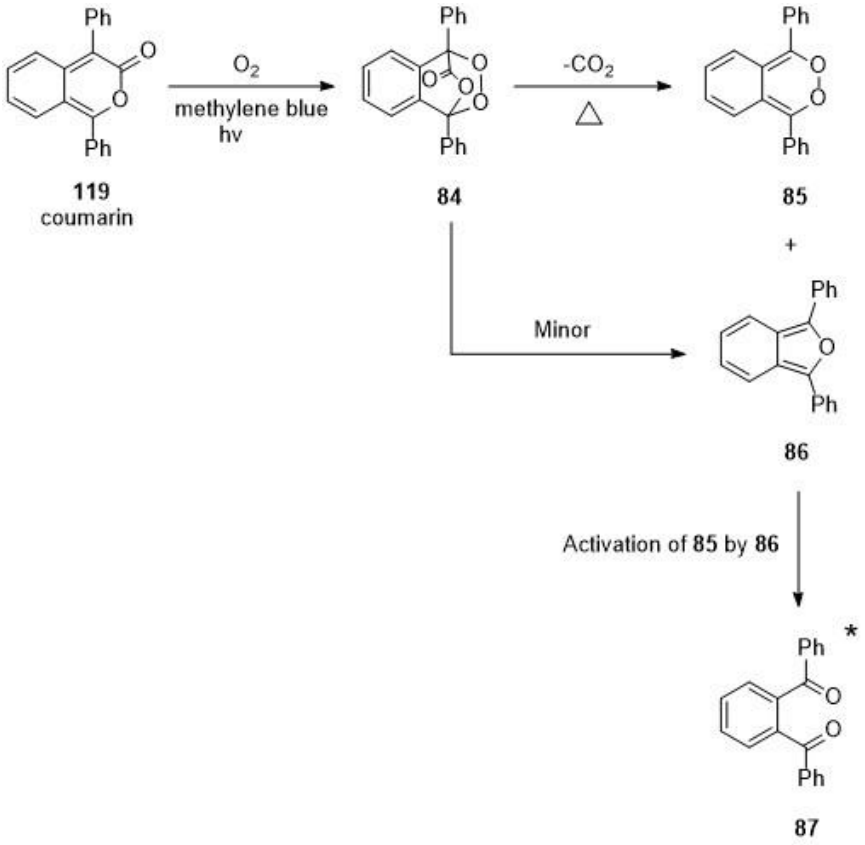

Scheme 21: Chemiluminescence of coumarin.

The pyrone ring 3-hydroxyhispidin **4** has a high electron density due to the two hydroxyl substituents. Kaskova *et al* found the hydroxyl group on C-3 was essential for the formation of high energy endoperoxide **74** (**scheme 18**). They performed enzymatic oxidation on hispidin **73** and did not observe light emission. Later, they found 3-hydroxyhispidin **4** only had half the reversible oxidation potential (211mV versus Ag/AgCl) than hispidin **73** (428mV versus Ag/AgCl). The group carried out an enzymatic oxidation experiment of a similar molecule **88** under $^{18}O_2$ and the mass spectrum of the resulting residue confirmed formation of the excited oxyluciferin **90** with [O^{18}] labelled (**scheme 22**).[50]

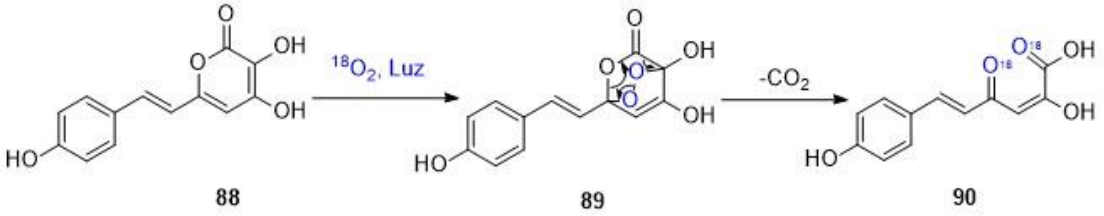

Scheme 22: Bioluminescence of **88** with O^{18} labelling

A similar oxidation experiment was performed with singlet oxygen generated by $DMNO_2$ (**scheme 23**).[50, 67] The reaction resulted in chemiluminescence and the same oxyluciferin. However, the high energy intermediate **91** was not observed from mass spec analysis.

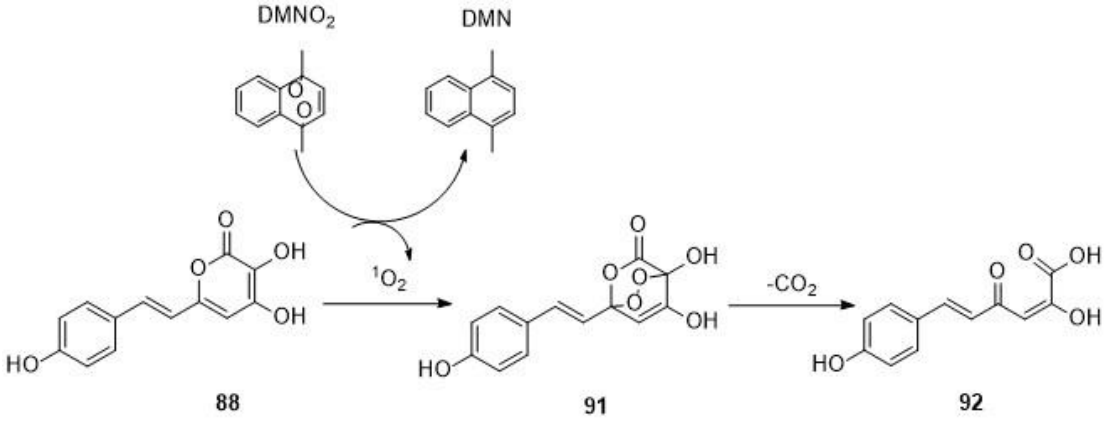

Scheme 23: Oxidation of **88** by singlet oxygen *via* plausible intermediate **91**.

Although [O^{18}] labelled endoperoxide **89** was not observed directly. The result suggested [O^{18}] in **90** was introduced by [4+2] cycloadduct between **88** and singlet $^{18}O_2$ and decarboxylation of **93** generated the [O^{18}] labelled molecule **94** (**scheme 24**).

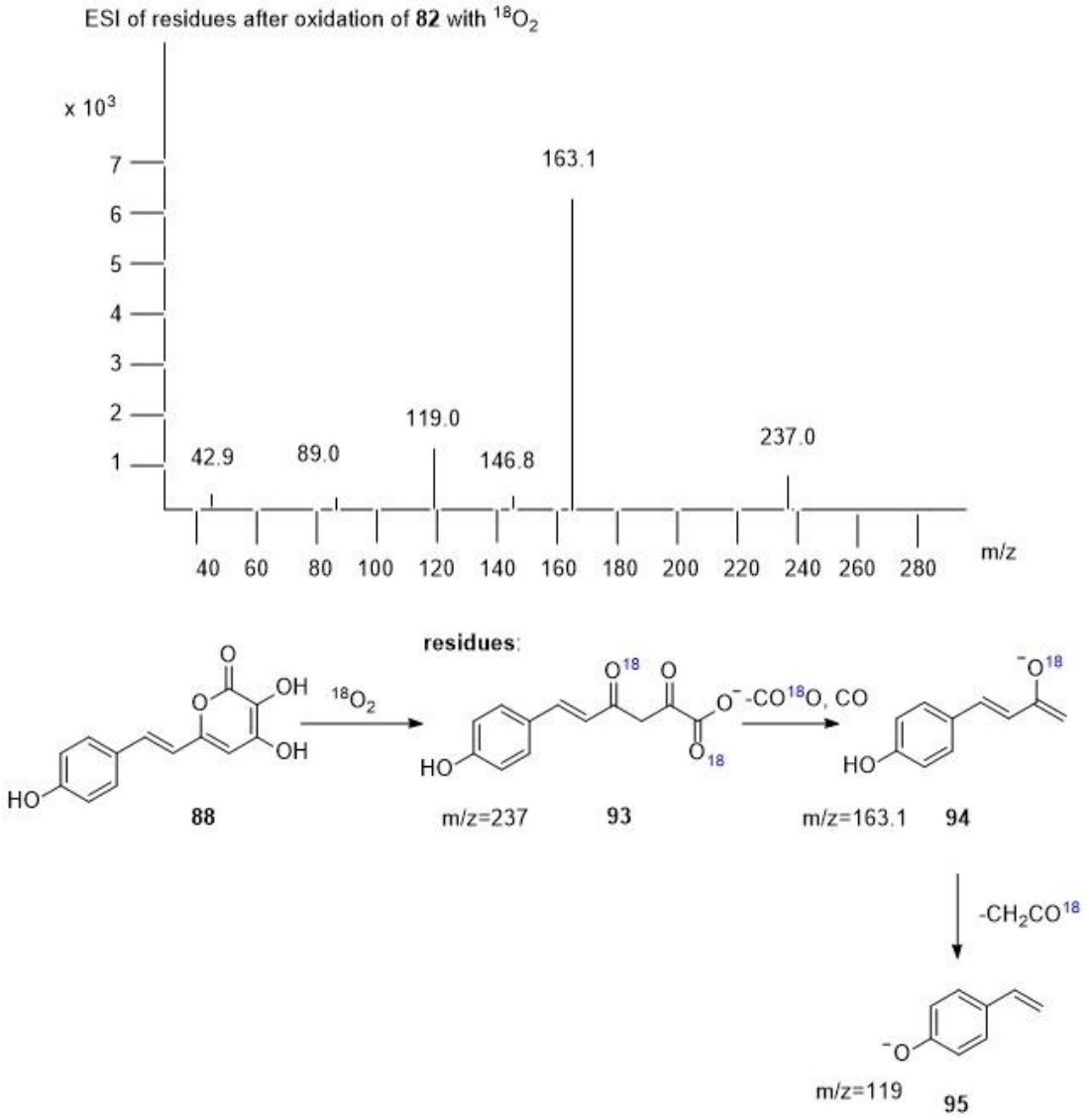

Scheme 24: Proposed mechanism based on O^{18} labelling and ESI.

Computational modelling study by Ming-Yu's group suggested a slightly different mechanism (**scheme 25**). By calculating transition state Gibbs free energy using DFT method, the first oxygen addition step was found to have a lower activation energy under basic catalysis and might have an even lower activation energy by fungal luciferase. The C-3 hydroxyl group might donate electrons into the conjugated π system of the pyrone and form the C-Oxygen bond.[68] Although there was a high energy barrier for this step, it might be possible under luciferase catalysis. The peroxide $O\text{-}O^-$ then attacked the carbonyl group to generate the high energy intermediate **74**. The group also suggested a two-step thermal decarboxylation mechanism should have a lower energy barrier than one step decarboxylation. The C_6-O_1 bond cleaved to form the zwitterion **97** and decarboxylation of **97** lead to the formation of excited intermediate **75**. The calculated emission energy of **98** had a strong accordance with maximum emission wavelength of fungal bioluminescence (530nm) and there was only a small energy gap (20.3kcal/mol) between **75** and **98**. It was suggested **75** was converted to **98** first, relaxed to its minima excited state and de-excited to ground energy level S_0 with light emission. Although the paper did not calculate the mechanism inside the binding site of fungal luciferase, it still gave another possible mechanism of fungal bioluminescence.

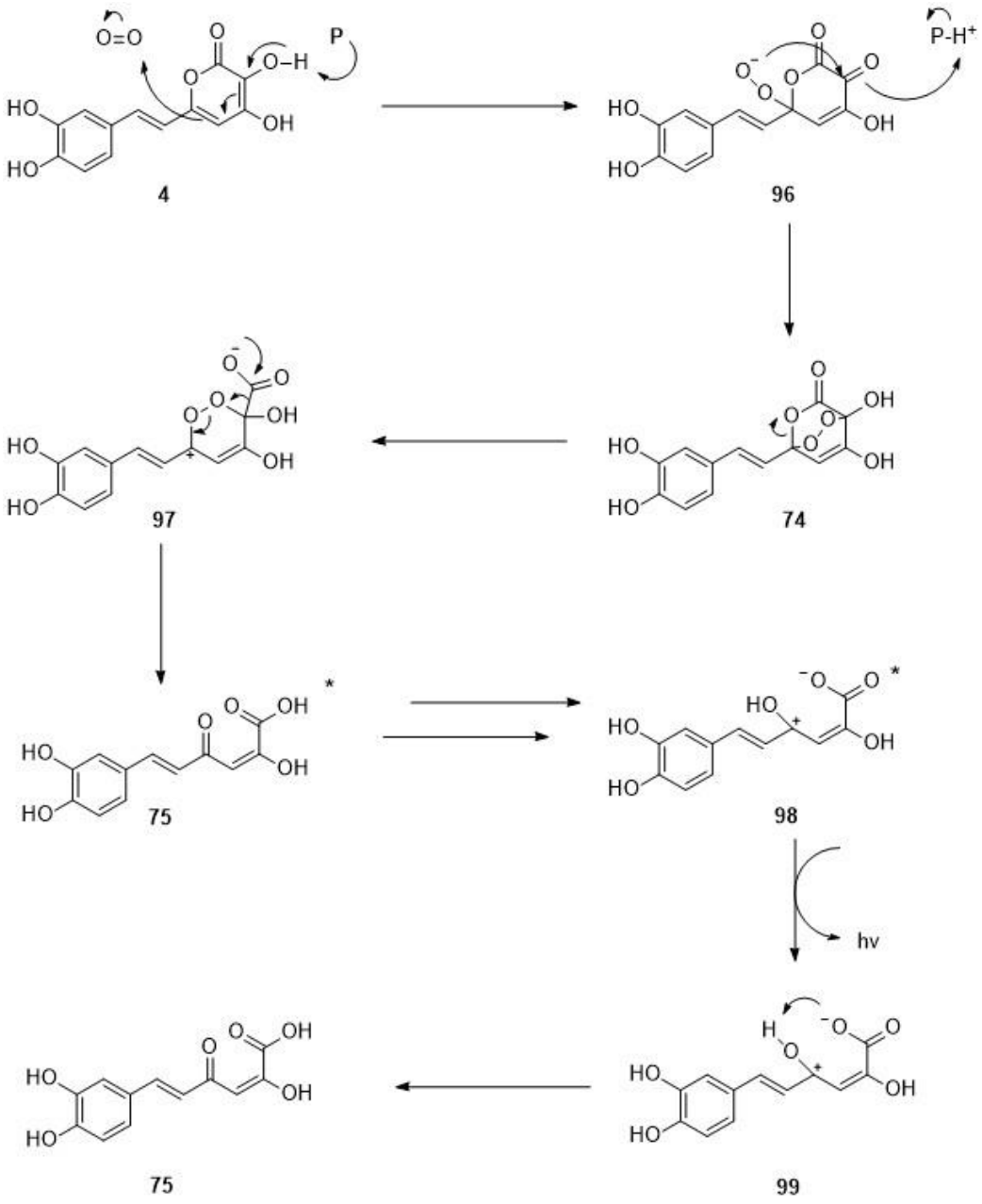

Scheme 25: Theoretical mechanism of fungal luciferin bioluminescence pathway based on Gibbs free energy study. P meant a proton acceptor and it was imidazole in the modelling experiment.

Beside the above mechanistic argument, the state of the oxygen molecule during luciferase oxidation remains unanswered. Normal oxygen in air exists in the form of diradical (triplet oxygen), which does not undergo [4+2] cycloadduct reactions or the addition of nucleophiles. The singlet oxygen could be generated at the binding site of fungal luciferase, which could then react with diene to form the expected endoperoxide, but how could that occur? Photosensitization is one of the most common reactions to produce singlet oxygen in the laboratory. However, a stable light source is required during photosensitization. Fungi perform bioluminescence in a dark environment and so it is unlikely to involve a mechanism requiring initiation by light. Other sources of singlet oxygen can originate from oxidized metabolites within the cell. Ingenbosch *et al* has reported one [4+2] cycloaddition of cyclohexadiene by heme peroxidase and oxygenase.[69] The singlet oxygen was generated from common metabolite, hydrogen peroxide, by iron(III)$^{+}$ at the center of heme peroxidase and oxygenase. A [4+2] cycloaddition then took place immediately and formed the desired endoperoxide (**scheme 26**).

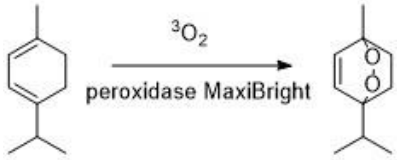

Scheme 26: [4+2] Cycloadduct between oxygen and diene **100** with peroxidase catalyst

Based on previous understanding of oxidative bioluminescence,[27] our group also suggests another possible mechanism of fungal bioluminescence (**scheme 27**).

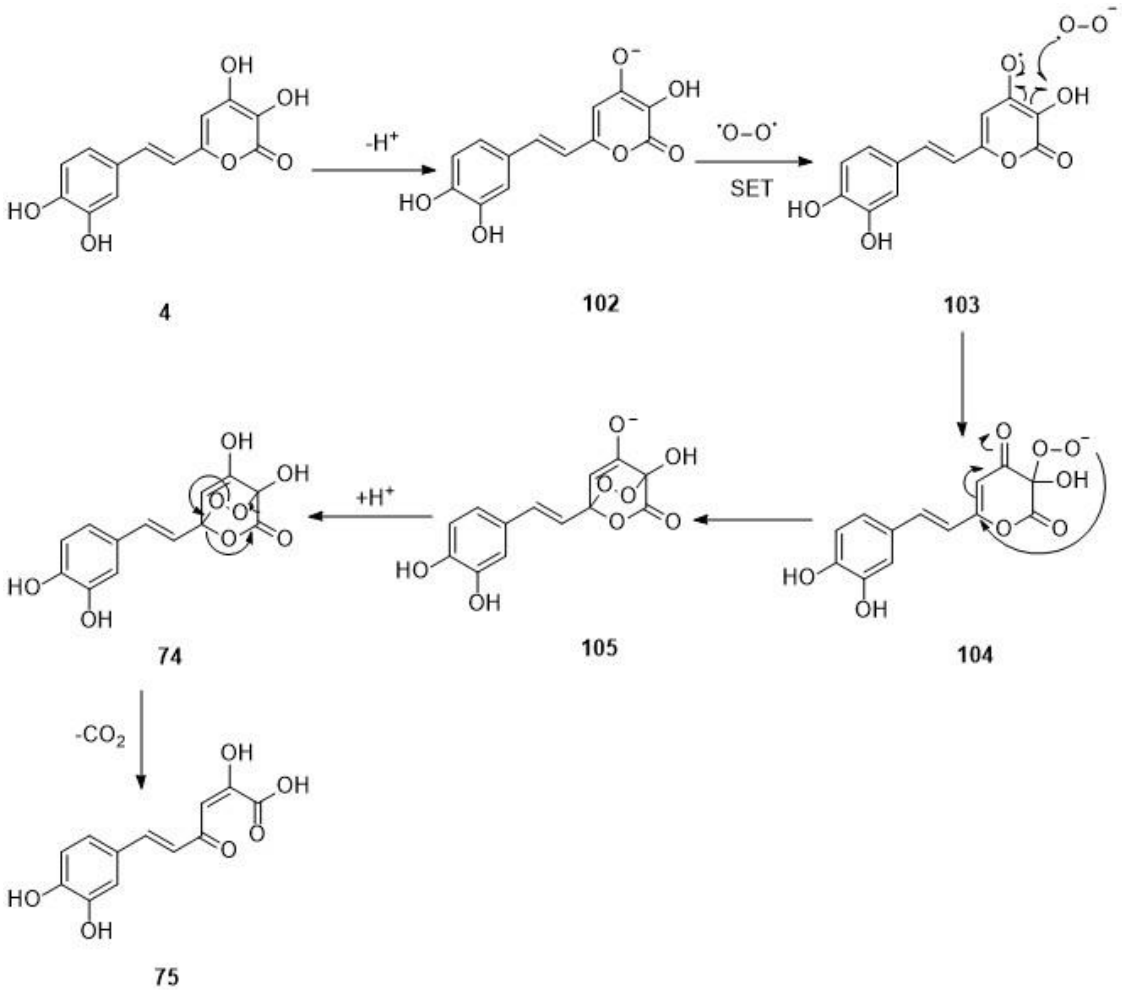

Scheme 27: Proposed fungal bioluminescence mechanism by JCA group.

The first few steps of mechanism are based on single electron transfer of triplet oxygen, similar to the accepted SET mechanism in firefly bioluminescence. The diradical oxygen has very low reactivity towards alkene. The SET adds an electron to oxygen from **102** and improves the reactivity of the oxygen radical. After addition of oxygen, the oxygen anion adds to the C-6 carbon *via* a conjugate addition. Then, the cleavage of CO_2 by a concerted process may yield the desired oxyluciferin **75**. Although the existence of radical pair of **103** and $^{\cdot}O\text{-}O^{-}$ is still waiting to be proved, the rest of reaction pathway is reasonable based on previous computational modelling.

1.22 Synthetic fungal luciferins

The synthesis of fungal luciferin 3-hydroxyhispidin was first achieved by Purtov *et al* in 2015.[26] It was uncommon to see 3,4-dihydroxyl pyrone structure as a building block and the group introduced one of the hydroxyl groups by enzyme catalysis. The synthetic route was four steps long including the enzyme catalyzed hydroxylation of hispidin (**scheme 28**).

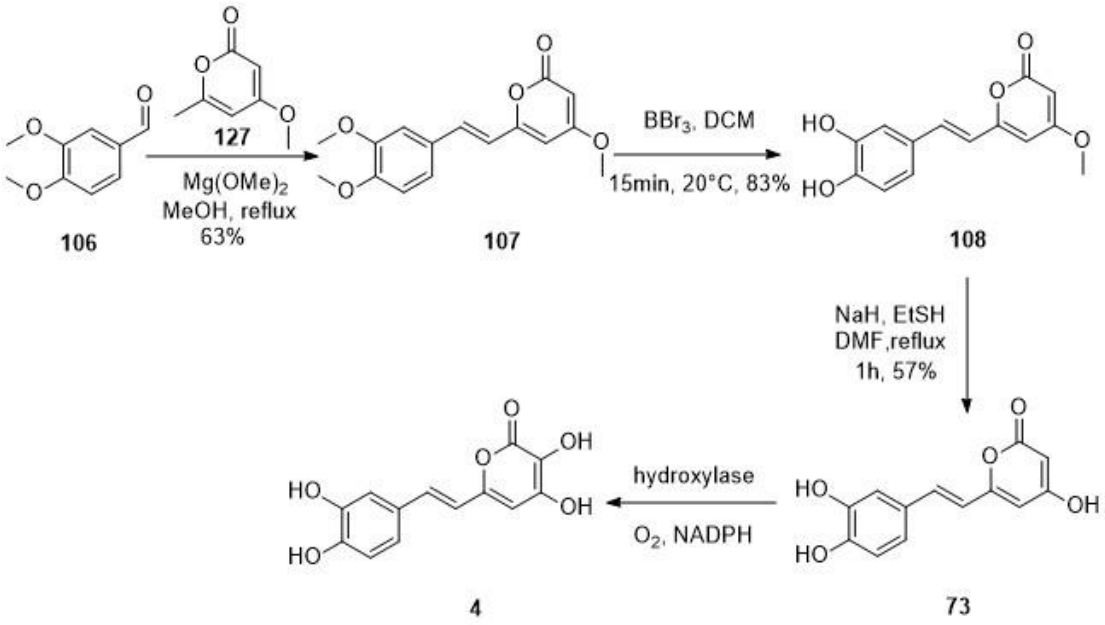

Scheme 28: Synthetic route of 3-hydroxyhispidin by Purtov *et al* in 2015.

Commercially available reagent **106** was chosen as the starting material for synthesis. Magnesium methoxide was used as a mild base for the condensation reaction between pyrone and benzaldehyde, giving the thermodynamically *trans*-linked product **107**. The methoxy groups were deprotected with BBr_3 and NaH/EtSH. The final hydroxylation was catalyzed by hispidin-3-hydroxylase to generate the C-3 hydroxyl group.

The route had a major advantage in the time taken to complete the synthesis. Although the procedure was only four steps long, the overall yield was not high due to the relatively low yields of the condensation reaction (~30% yield) and the sulfur deprotection (~50% yield) steps. The enzymatic hydroxylation was also a major problem for repeating the synthesis because hispidin-3-hydroxylase is not a commercially available reagent.

Later, in 2017, Kaskova's group reported a total chemical synthesis route of 3-hydroxyhispidin with an eight-step-procedure (**scheme 29**). [50]A hypervalent iodine reagent was used instead of enzymatic catalysis to generate the C-3 hydroxyl group.

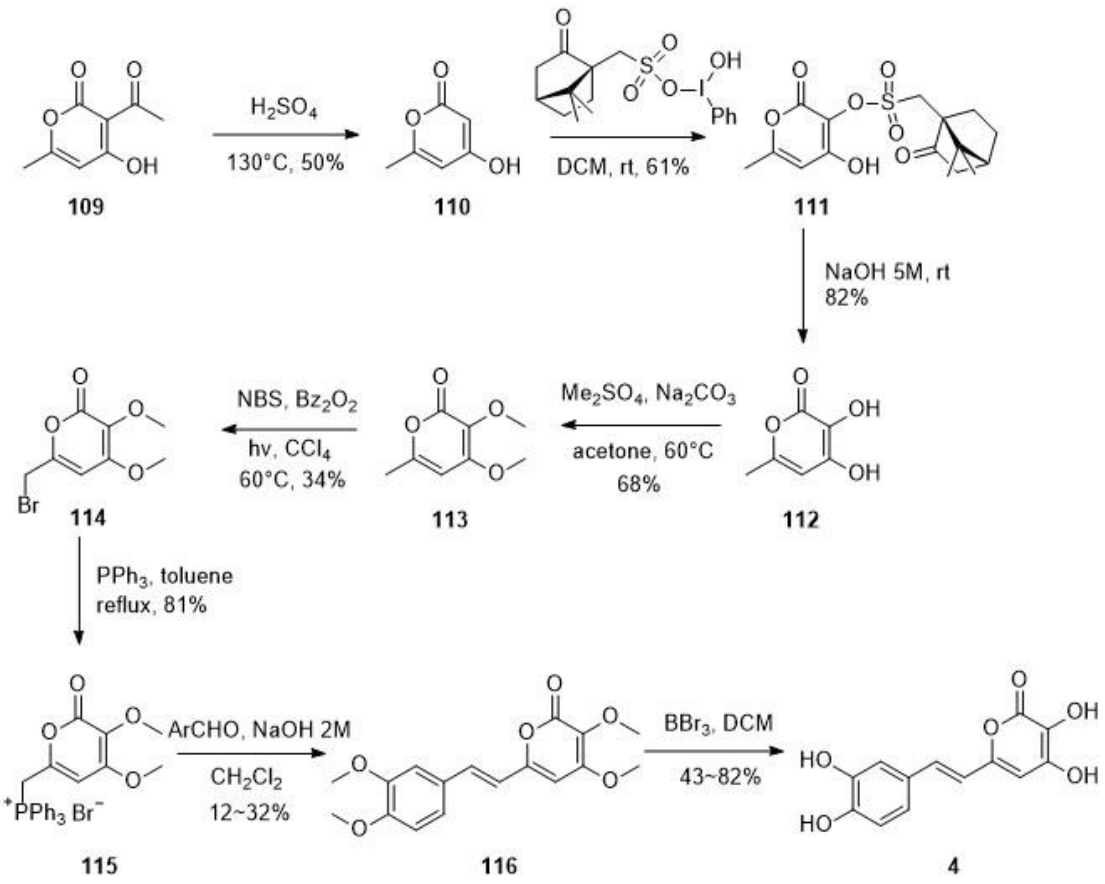

Scheme 29: Total chemical synthesis of 3-hydroxyhispidin by Kaskova's group in 2017.

The synthesis began with commercially available reagent **109**. The extra carbonyl group was cleaved by strong acid and a hypervalent iodine reagent was used to introduce the C-3 hydroxyl group.

The mechanism of carbonyl cleavage results in the formation of acetic acid (**scheme 30).**

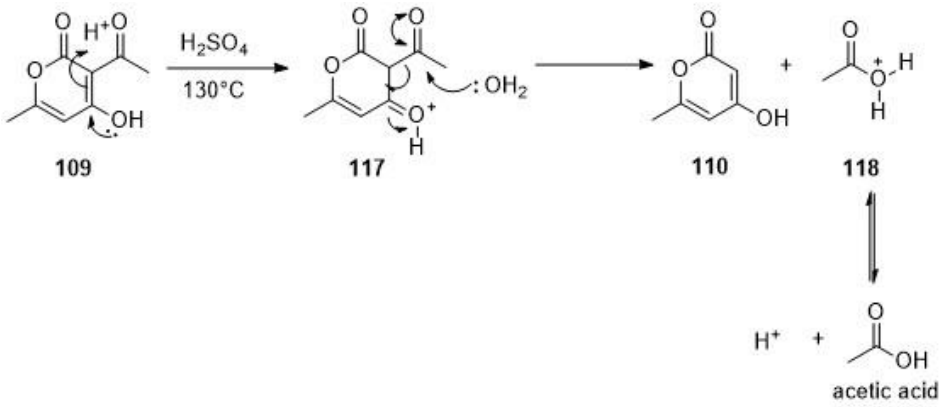

Scheme 30: Carbonyl cleavage mechanism of **109**.

The C-3 carbon of **109** is protonated due to lone pair donation of the C-4 hydroxyl group. Water will then attack the acetyl group and cleave it off in the form of acetic acid.

The mechanism of hypervalent iodine oxidation is still under discussion. The original paper stated that **110** could attack the hypervalent iodine directly to generate **120** (**scheme 31**).[70] After elimination of water, the iodonium ion $^{+}$IPh formed is a good leaving group and the sulfonate group is inserted into **122** *via* a substitution mechanism.

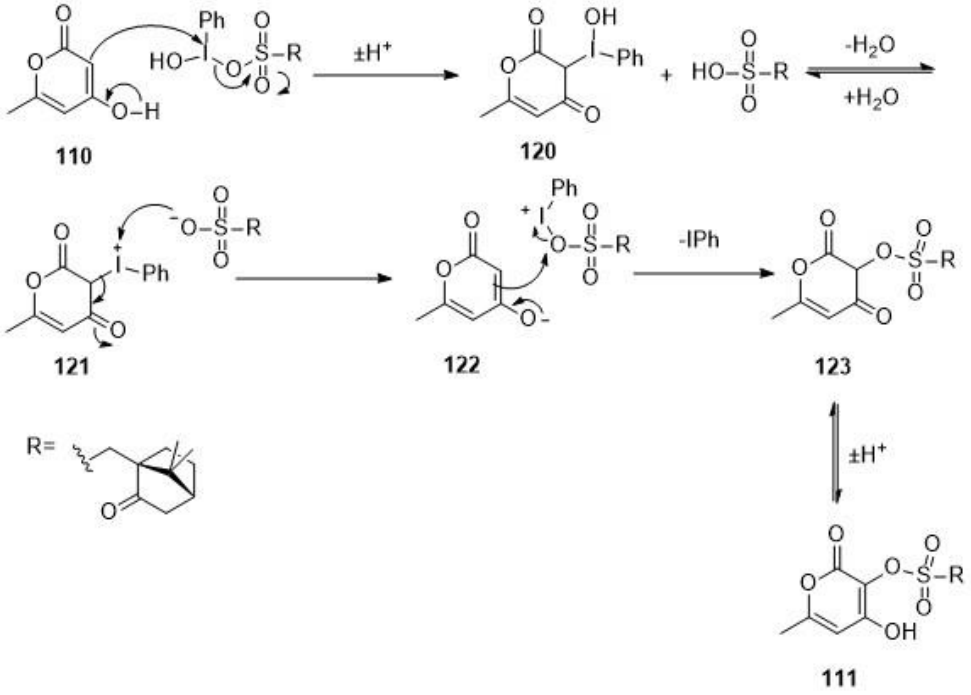

Scheme 31: Hypervalent iodine reagent mechanism suggested in original paper.

Alternatively, it is conceivable that the OH of the enol could attack the hypervalent iodine reagent and substitute the sulfonate leaving group (**scheme 32**). After elimination of water from the hypervalent iodine, the leaving group $^{+}$IPh of intermediate **125** can be displaced by conjugate substitution by the sulfonate group.

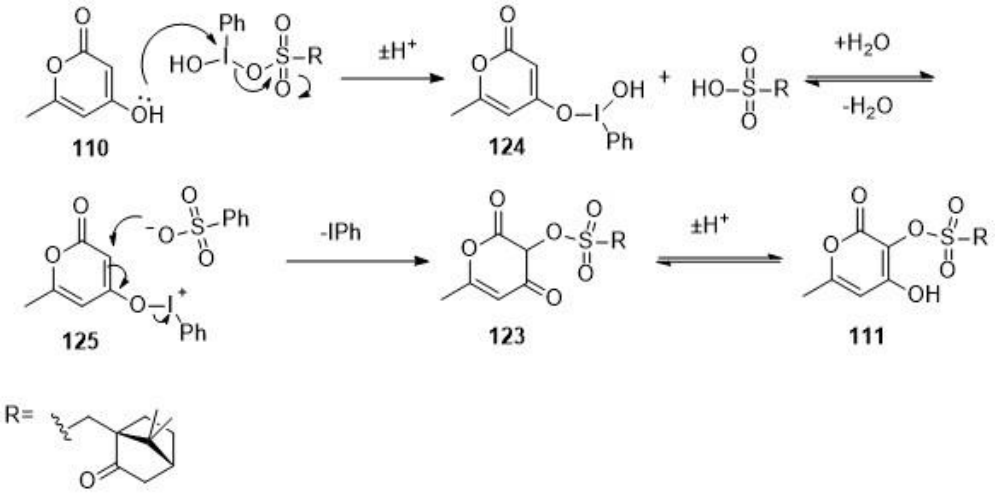

Scheme 32: Alternative hypervalent iodine reagent mechanism.

Hydrolysis of **111** with aqueous NaOH gave dihydroxyl pyrone **112** (**scheme 29**). To avoid any side reactions during the Wittig reaction, both hydroxyl groups were protected as their methyl ethers before the bromination of **113**. The radical bromination did not give good selectivity and past experiments on similar molecules such as **127** showed di- or tri- brominated products were common (**scheme 33)**.[71] The phosphonium salt was synthesized by displacement with triphenylphosphine. Deprotonation with NaOH gave the ylide and reaction with benzaldehyde gave the *trans*-alkene **116**. Global deprotection of the methoxy groups with BBr_3 yielded the desired product 3-hydroxyhispidin **4** (**scheme 29**). Although this route used more common and uses commercially available reagents, it still had disadvantages in the overall yield and number of steps.

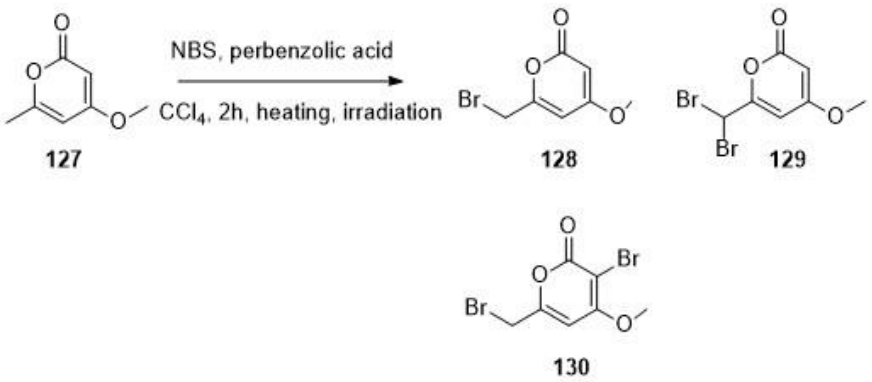

Scheme 33: Radical bromination of 4-methoxy-6-methyl-2H-pyran-2-one

The group also synthesized a series of synthetic fungal luciferin analogues with different aromatic ring structures **73** and **131 ~135** using this route and chemiluminescence tests were carried on these synthetic luciferins.

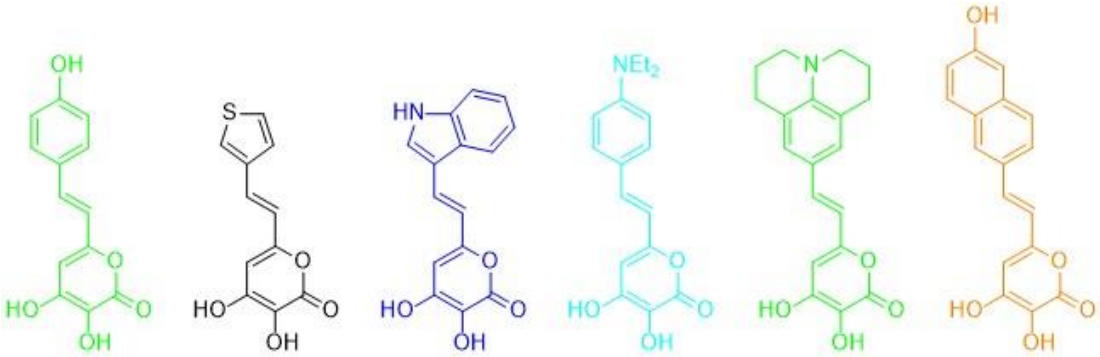

Compound	CL, λ max (nm)	CL, λ max comparing to molecule **4**	Abs, λ max (nm)	Exc, λ max (nm)	FL, λ max (nm)	relative Φ CL
73	520	Blue shift	372	367	458	0.6
131	-	-	376	350	430	-
132	480	Blue shift	386	351	431	0.003
133	504	Blue shift	366	370	430	3
134	534	No change	424	450	574	0.004
135	564	Red shift	380	350	430	1

Figure 4: Maximum chemiluminescence wavelength/ Maximum absorption wavelength/ Maximum excitation wavelength/ Maximum fluorescence wavelength/ Relative quantum yield of chemiluminescence of compound **73** and **131~135**.

The maximum chemiluminescence wavelength and maximum fluorescence wavelength would predict an increase or decrease in bioluminescence wavelength.

The relative quantum yields of chemiluminescence of the compounds was also important as they were directly related to the amounts of bioluminescence light emission. Above synthetic luciferins had a general decrease in maximum chemiluminescence wavelength. Only synthetic luciferin **135** had a red-shifted maximum chemiluminescence wavelength but it did not give a good quantum yield. The overall data shown in **figure 4** suggested more factors, including electron density and conjugation level were required to be considered for designing a better synthetic luciferin.

After the total synthesis of fungal luciferin, Bubyrev's group reported an optimized route in 2018 (**Scheme 34**).[72] The first three steps to prepare **4** were the same as Kaskova's method. Pyrone **113** was then deprotonated with LDA at -78°C and added to benzaldehyde to give alcohol **136**. Elimination reaction with MsCl and NEt_3 formed the *trans*-alkene **116**. The molecule was then globally deprotected as before with BBr_3 to yield the target compound **4**. Comparing to the one step magnesiummethoxide promoted condensation (32% yield) in previous route, the two-step reaction with LDA had a much higher yield (72%).

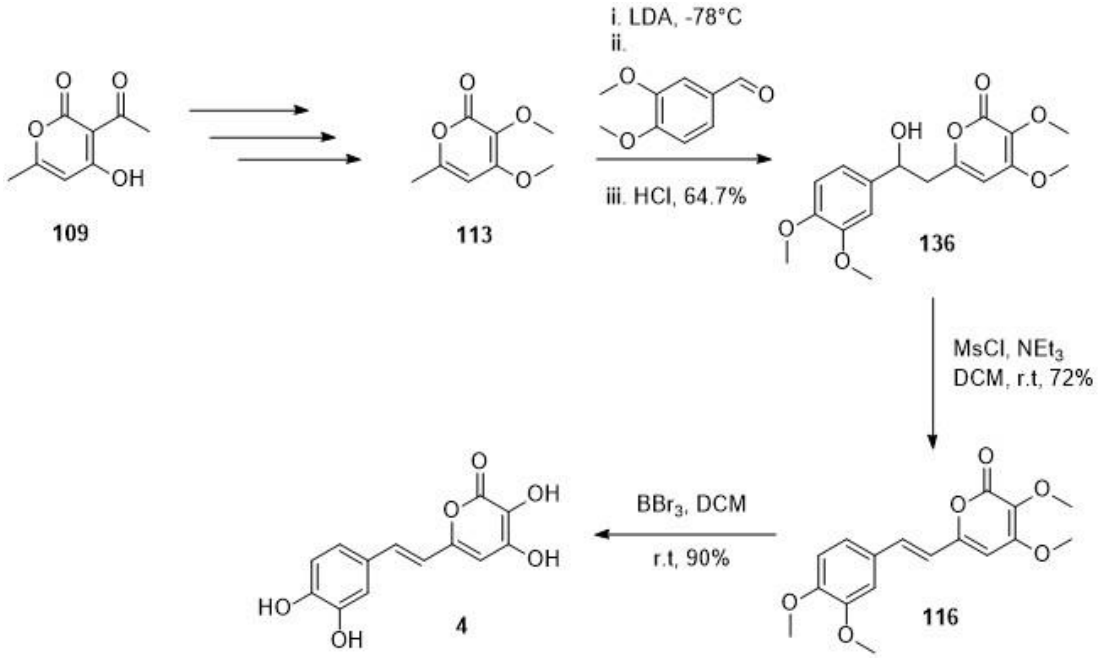

Scheme 34: Bubyrev's optimized route to fungal luciferin.

Chemiluminescence data of synthetic oxyluciferins can be a useful indicator of the bioluminescence quality for the corresponding luciferins. Garcia-Iriepa's group reported a synthetic route to fungal oxyluciferin in 2020 (**Scheme 35**).[73]

Commercially available reagent **137** was firstly treated with LiHMDS (1M) to generate the enolate and treated with oxalyl chloride to give the protected oxyluciferin **138**. Deprotection of the phenolic methyl ethers with BBr_3 and hydrolysis of the ester with aq. HCl formed the oxyluciferin **75**.

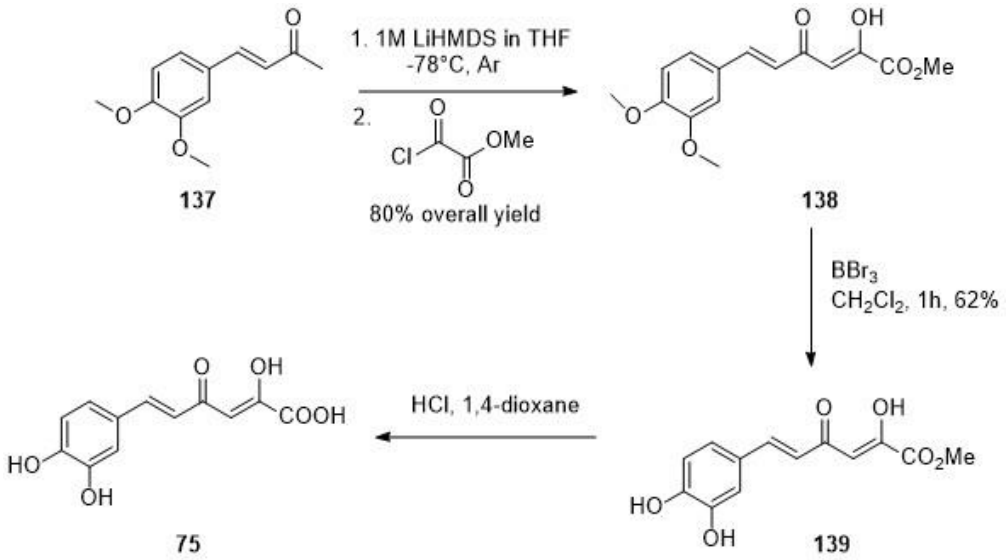

Scheme 35: Synthetic route to fungal oxyluciferin **75**

A computational study of oxyluciferin **75** suggested that the (3*Z*)-4-hydroxy-2-oxo form was stable in both ground state S_0 and first excited state S_1 and it was the light emission form during fungal bioluminescence (**table 1**). Fluorescence experiments in water (pH=5-5.5) showed that the emission spectrum of synthetic oxyluciferin **75** only had small difference from the natural oxyluciferin (**figure 5**). The pH value of water solution was found to be a significant factor influencing emission density of oxyluciferin. By varying the pH from 5 to 9, the oxyluciferin showed some red shifting in fluorescence wavelength, and a constant decrease in emission density was observed for both natural oxyluciferin and synthetic oxyluciferin.

compound	state	(2*Z*)-2-hydroxy-4-oxo	(3*Z*)-4-hydroxy-2-oxo
138	S_0	2.5	0.0
	S_1		64.3
139	S_0	0.25	0.0
	S_1	69.2	63.7
75	S_0	0.2	0.0
	S_1	69.9	65.6

Table 1: Relative Electronic Energies (in kcal/mol) for the *(2Z)*-2-Hydroxy-4-oxo and *(3Z)*-4-Hydroxy-2-oxo, computed with CAM-B3LYP/6-31+g(d,p) Method Considering Water as an Implicit Solvent

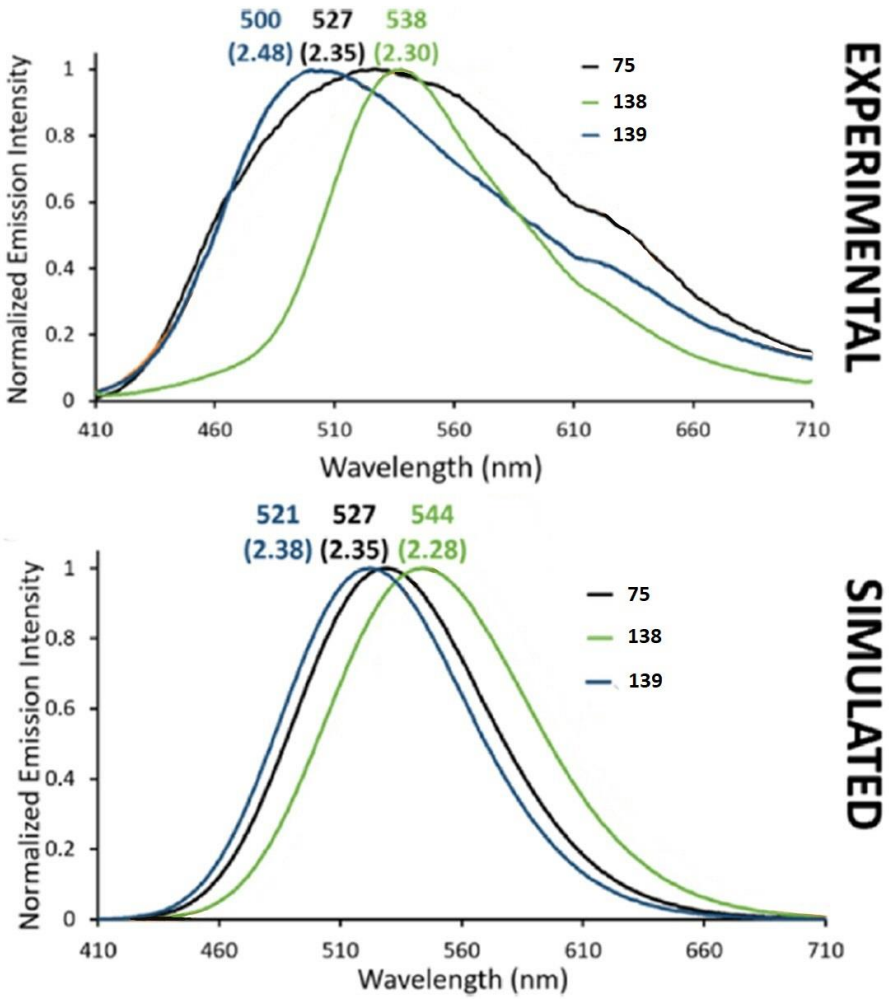

Figure 5: Experimental and simulated emission spectra of **138**, **139** and **75**.

1.3.4 Application of fungal bioluminescence

Compared to other bioluminescence systems, the fungal bioluminescent pathway includes three major enzymes, *luz*, *h3h* and *hisps*, to generate excited oxyluciferin. Two extra enzymes, *cpy450* and *cph* are found in a few bioluminescent fungi and are responsible for fungal luciferin recycling. Most of these enzymes take part in the 3-hydroxyhispidin synthesis pathway and only *luz* is involved in oxidation of 3-hydroxyhispidin.[12,50] A series of interesting *in vitro* experiments were performed to prove the importance of each enzyme and fungal bioluminescence system were built into different species based on the results of these experiments.

In the early stage of fungal bioluminescence *in vitro* experiments, nnluz mRNA sequence was introduced into the *Xenopus laevis* embryo by microinjection, and the embryo showed bioluminescence after injection of fungal luciferin, 3-hydroxyhispidin (**figure 6**). The experiment was performed without *h3h* and *hisps* and proved the *luz* enzyme was responsible for oxidation of fungal luciferin. When *luz*, *h3h* and *hisps* were introduced in yeast *Pichia pastoris* cells, only precursor of luciferin, caffeic acid, was required to generate fungal bioluminescence. The result showed each enzyme plays an independent role in fungal bioluminescence pathway and starting metabolites can be varied based on different enzyme taking part in the pathway. To build a complete biopathway of fungal bioluminescence in non-bioluminescent species, additional genes related to the biosynthesis of caffeic acid were necessary to

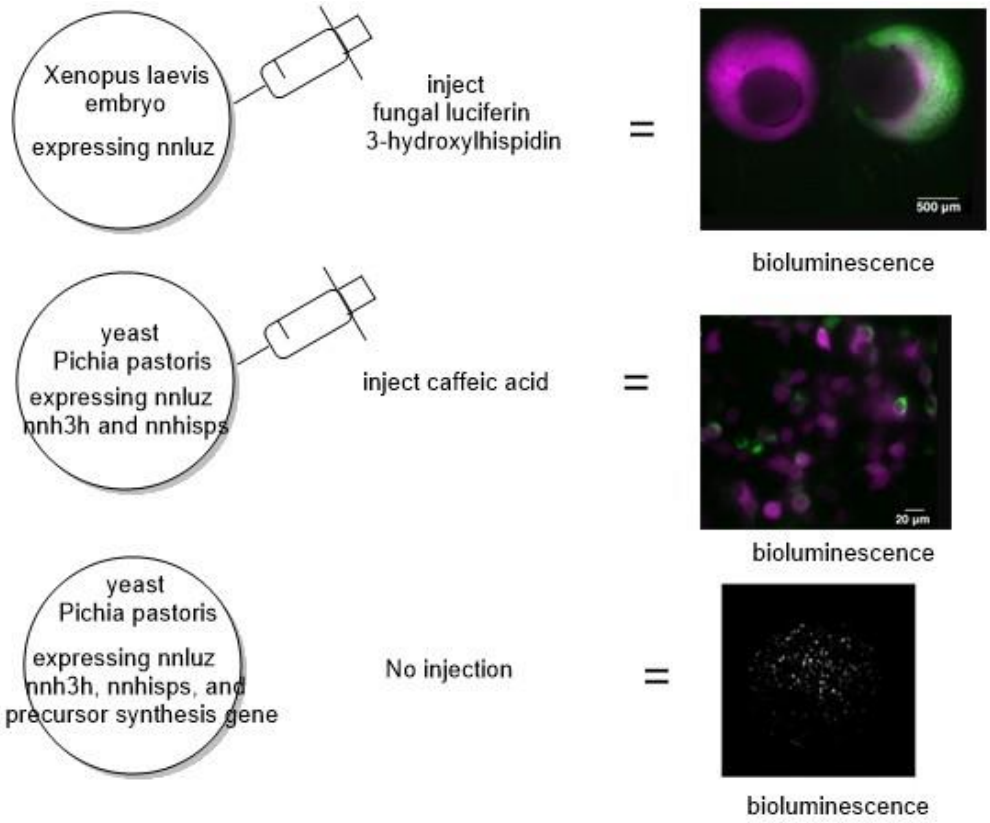

Figure 6: Different combination of luminous fungal gene sequences and substrate.[18]

give a stable supply of luciferin precursor molecules. When tyrosine, Rhodobacter capsulatus tyrosine ammonia lyase and two *E. coli* 4-hydroxyphenylacetate 3-monooxygenase components were expressed in yeast *Pichia pastoris* cell with *npgA*, *hisps*, *h3h*, and *luz* gene sequences, a complete luciferin precursor pathway and oxidation pathway were contained in the yeast, and the yeast gave an autonomic bioluminescence without injection of extra substances.

Until 2023, it was very rare to see fungal bioluminescence imaging in mammals and one of the representative experiments was performed by Alexey *et al* (**figure 7**). Fungal bioluminescence gene *nnluz* was firstly introduced into murine carcinoma cells CT26. The tumor cells were then injected into a mouse followed by injection of 3-hyroxyhispidin. The resulting bioluminescence was measured and the distribution of the tumor cell was shown by bioluminescence intensity.

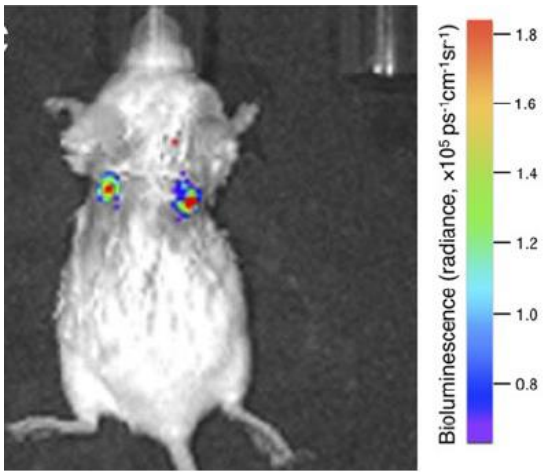

Figure 7: Tumor cell mapping *via* fungal bioluminescence itensity.[18]

In addition to these previous experiments, fungal bioluminescence has been applied in plant experiments. In 2019, Mitiouchkina's group introduced four fungal enzymes: luciferase Luz, hispidin synthase HispS, hispidin-3-hydroxylase H3H, and putative oxyluciferin recycling enzyme CPH into tobacco plants and engineered self-glowing tobacco (**figure 8**).[52] Because caffeic acid is a common metabolite in vascular plants,

the gene related to caffeic acid synthesis was not considered. In early stages of growth, the root and stem part of the plants had a higher bioluminescence intensity than other parts. In the flowering stage, the bioluminescence intensity of the flower grew stronger, and the older part of the shoot dimmed slowly. The bioluminescence strength of different parts reflected the availability of caffeic acid, which depended on expression pattern of phenylalanine ammonia-lyase.

Figure 8: Self-glowing tobacco plants by introduction of fungal Luz, HispS, H3H and CPH enzyme[19].

Later in 2020, Khakhar's group produced more auto-luminescent plants by Agrobacterium infiltration.[53] H3H, Hisps and Luz gene were firstly transferred into T-DNA of Agrobacterium and introduced into plants *via* bacterium infection. The plant N. benthamiana showed auto-luminescent property throughout the whole plant after Agrobacterium infiltration. The technique was restricted by caffeic acid concentration inside different parts of plant and the leaf part of *N. benthamiana* had a relatively low

bioluminescence. To solve this limitation, the group introduced an extra caffeic acid biopathway by building T-DNA with Rhodobacter capsulatus tyrosine ammonia lyase and two Escherichia coli 4-hydroxyphenylacetate 3-monooxygenase components. The extra biopathway could convert the common metabolite tyrosine into caffeic acid and the plant showed a significant increase in bioluminescence intensity after T-DNA transfer. The auto-luminescence was also tested in common plants with high caffeic

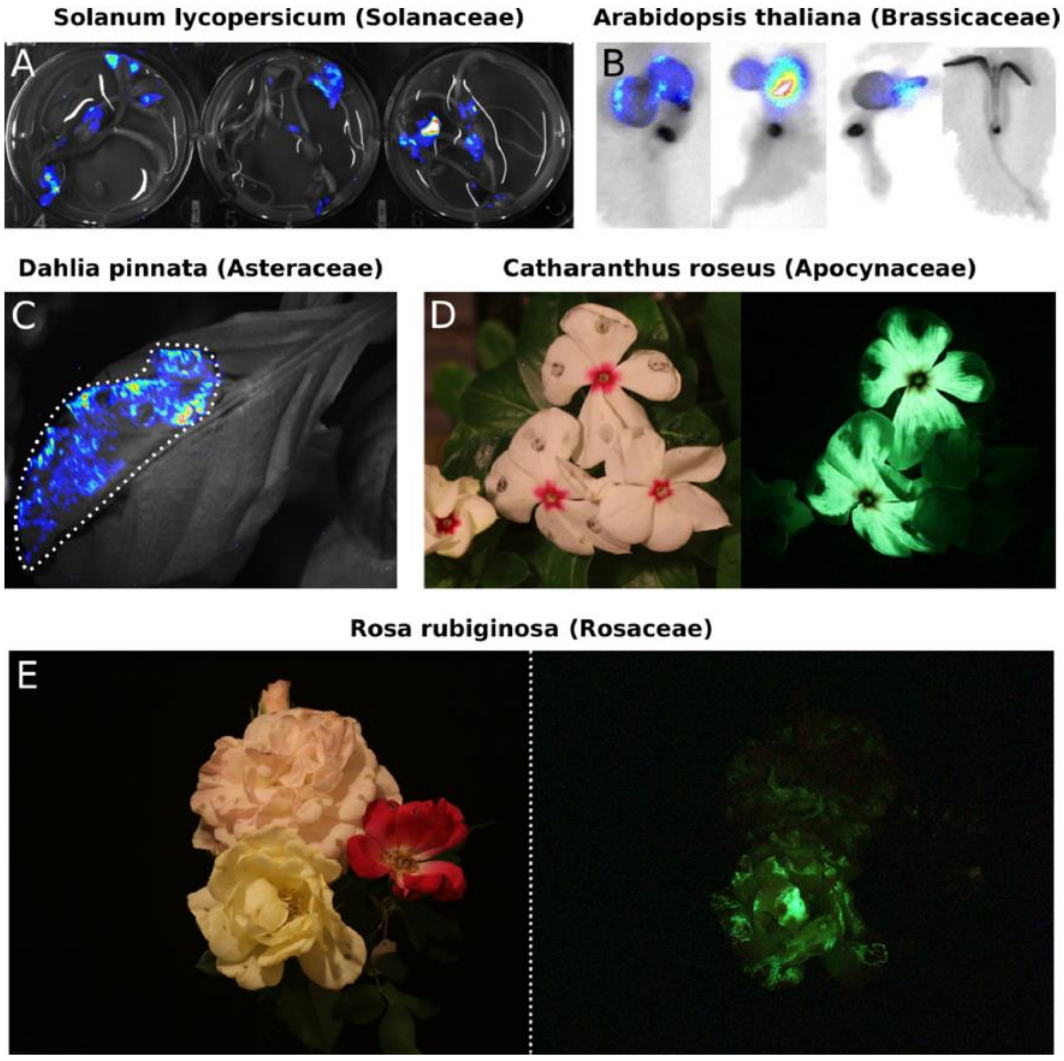

Figure 9: Fungal bioluminescence in **A.** *Solanum lycopersium*, **B.** *Arabidopsis thaliana*, **C.** *Dahlia pinnata*, **D.** *Catharanthus roseus* and **E.** *Rosa rubiginosa*

acid concentration such as *Solanum lycopersium* (tomato), *Arabidopsis thaliana*, *Dahlia pinnata*, *Catharanthus roseus* and *Rosa rubiginosa* (Rose) (**figure 9**). The result showed that all these plants were capable for bioluminescence and luminescence strength strongly related to tissue caffeic acid concentration. The group aimed to make the bioluminescence system commercially available with self-assembled DSLR-based imaging platform and open-source software. The overall cost of these components was below $2500 and fungal bioluminescence is developing towards a low-cost and long-term imaging system.

2.Result and Discussion

2.1.Research propose

Bioluminescence has been widely used for *in vitro* and *in vivo* imaging experiments. Compared to fluorescence imaging, the cold light generated by bioluminescence has no background noise and produces a clear signal with high accuracy.[74] In past research, tissue penetration and emission intensity were found to be the biggest barriers for bioluminescence imaging applications. Natural bioluminescence usually has a wavelength of emission similar to the skin absorption band and therefore gives weak signals for certain *in vivo* experiments. Red shifting the bioluminescent light has become a popular strategy to allow more penetrant light through tissue and blood as it is less absorbed by those media. Researchers have developed several methods of achieving better imaging, such as mutating luciferases, better optical probes and artificial luciferins to have the overall effect of improving the bioluminescence imaging quality. [18,19,75, 76] Firefly bioluminescence is one of the most popular imaging techniques. The light is generated by firefly luciferase and its corresponding substrate, D-luciferin. Among all the imaging quality improving methods, artificial luciferins have provided the best improvement in firefly bioluminescence quality. Many factors, such as wavelength, quantum yield, binding efficiency, cell permeability and pharmacokinetic properties were considered during firefly luciferin modification. Past research has synthesized numerous modified D-luciferins and a small molecular library was built for artificial D-luciferins. Based on the library, researchers tried to synthesize artificial luciferins with infra-red bioluminescence, which avoided tissue absorption. The most successful cases were the CycLuc and AkaLumine (**Scheme 36**)[77, 78] types and many clear *in vivo* images have been recorded.[34] The

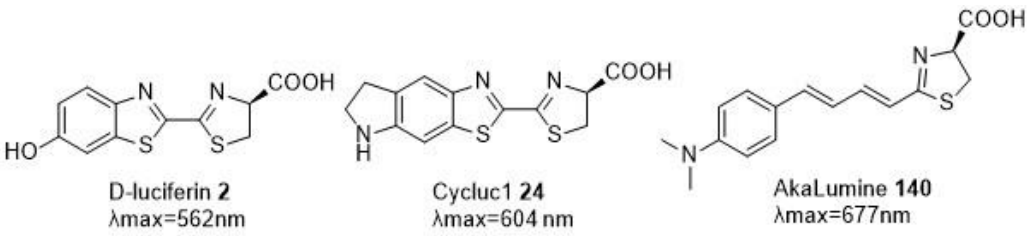

Scheme 36: Bioluminescence maximum wavelength of CycLuc and AkaLumine.

exploration of other artificial D-luciferins has slowed down since 2022, possibly due to past research exhausting the available permutations for new modified luciferins. More analogues are desirable to continue the improvement of imaging techniques and therefore more modification strategies are required to give wider choices in the design of new luciferins.

Mixing functional groups from different chemiluminescent molecules is a common strategy in synthesizing new chemiluminescent molecules. The production of new chemiluminescent dioxetanes from related phenoxy enolethers is a classic example of

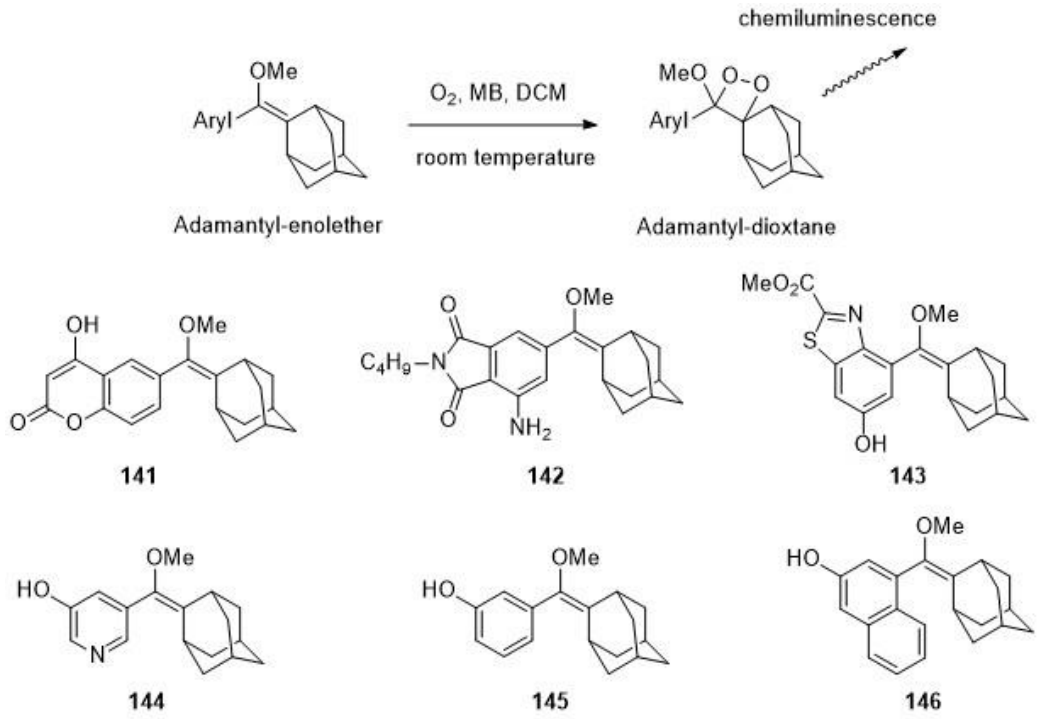

Scheme 37: Phenoxy adamantyl-enolethers generated by varying functional groups from different chemiluminescent compounds.

such a strategy (**scheme 37**).[79] By mixing the luminophore of adamantyl-enolether and a substituted phenoxy group from other chemiluminescent compounds, new types of adamantyl-enolethers were obtained and dioxetanes with higher quantum yield were generated.

The project aims to apply a new strategy, which different parts of natural luciferins are combined to generate a chimeric luciferin and test whether chimeric luciferin could generate bioluminescence or not. Molecules **147** and **150** were designed by linking the electron donating structure of D-luciferin and the luminophore of fungal luciferin (**scheme 38**). An investigation into the heteroatoms of the benzothiazole portion was proposed with structures **148** and **149**. By increasing the conjugation level of electron donating groups, artificial fungal luciferin molecules **147**-**150** should exhibit a red-shifted bioluminescence which is required in modern applications of bioluminescence imaging.

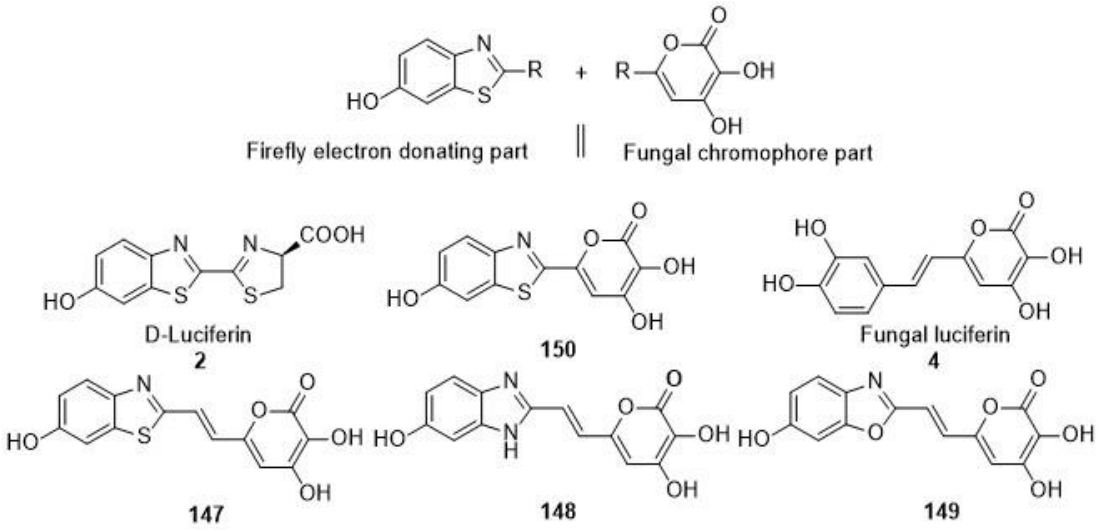

Scheme 38 Research target compounds **147~150**

The structures **151** and **152** (**scheme 39**) were designed to test the variability of fungal chromophore structures, with the natural electron donating group of fungal luciferin left unchanged. The analogue **151** was conceived by converting the *trans* double bond into a thiazole ring, and it aimed to have an increase in conjugation, electron density and rigidity. Rigidity may be important in reducing the degrees of freedom in the excited state and minimising radiationless decay.[32] The analogue **152** was conceived

by substituting the oxygen heteroatom in the pyrone ring with a nitrogen atom, and it aimed to have an increase in electron density.

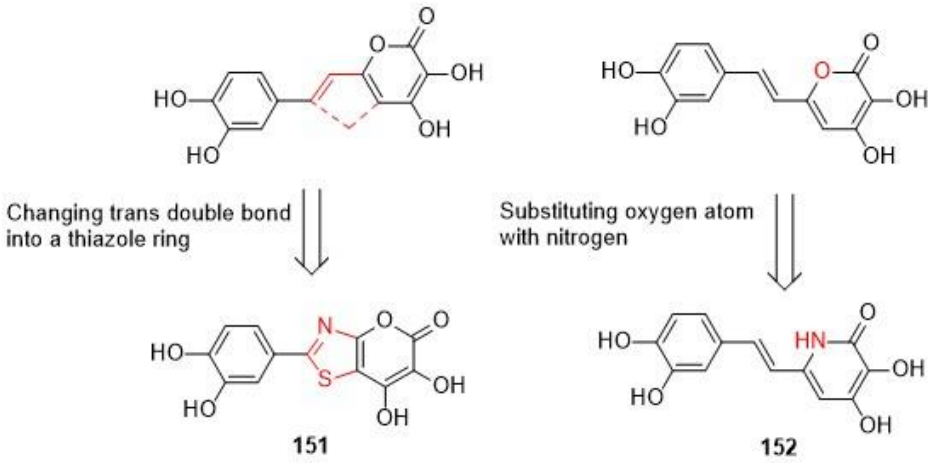

Scheme 39: Research target compound **151** and **152**

The project set out to investigate a multi-directional modification of artificial fungal luciferins, including electron density, conjugation level and rigidity. By comparing the final bioluminescence data of the chimeric fungal luciferins, more knowledge of fungal luciferin modification could be gained, and a better concept of artificial luciferin synthesis could be formed. The overall research is beneficial to select future artificial fungal luciferins and help fungal bioluminescence applications *in vivo*.

3. Synthesis of (*E*)-4-(2-(6-hydroxybenzo [d]thiazol-2-yl)vinyl)benzene-1,2-diol (147)

3.1 Retrosynthesis

The *trans*-heterocycle **147** consists of two heterocycles connected by a *trans* double bond. Past synthesis has provided several convenient strategies to achieve the bridged heterocyclic structure *via* disconnection from the *trans* double bond (**Scheme 40**).

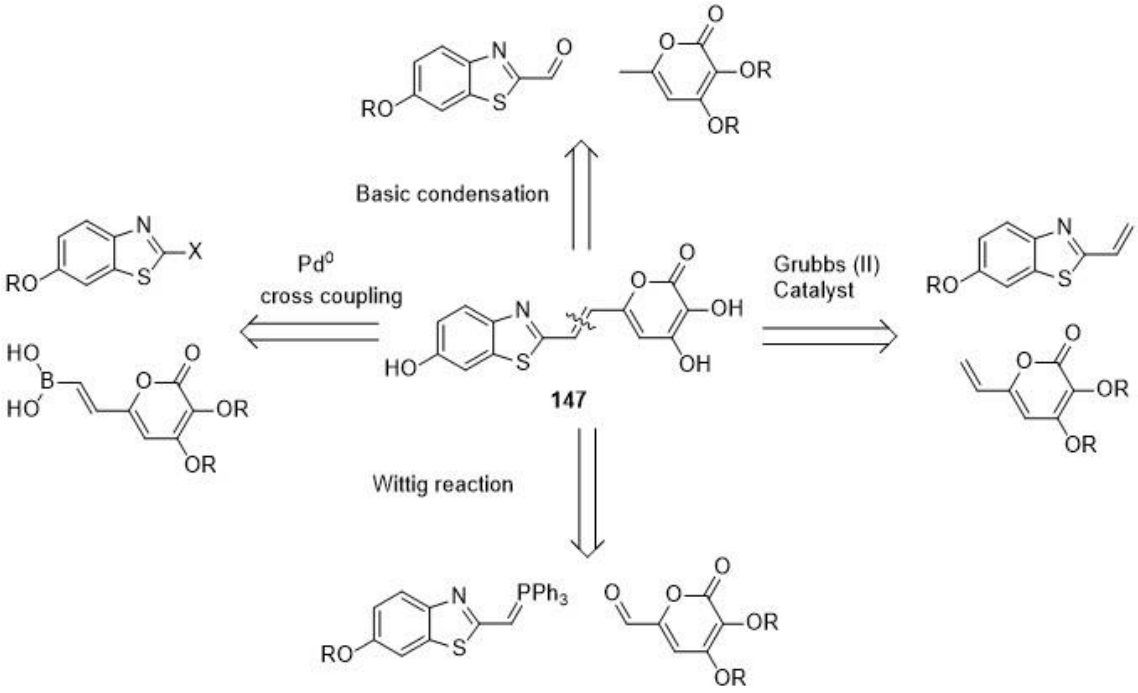

Scheme 40: Disconnection strategies *via* trans double bond in **147**

Basic condensation between pyrone and aldehyde was widely recorded in previous research (**scheme 28** and **scheme 34**).[26, 72] Liu's group reported a series of condensation reactions between 4-methoxy-6-methyl-2H-pyran-2-one and a range of different aldehydes (**scheme 41**).[81] The reactions were performed in methanol and a mild base $Mg(OMe)_2$ was used to deprotonate the C-6 methyl group. The resulting

carbanion was stabilized by conjugation with the pyrone ring and nucleophilic addition to the aldehyde generated the alcohol intermediate. The elimination of alcohol intermediate occurred *in situ* under the mildly basic reaction conditions and gave the pure *trans* products in 30%~50% yield.

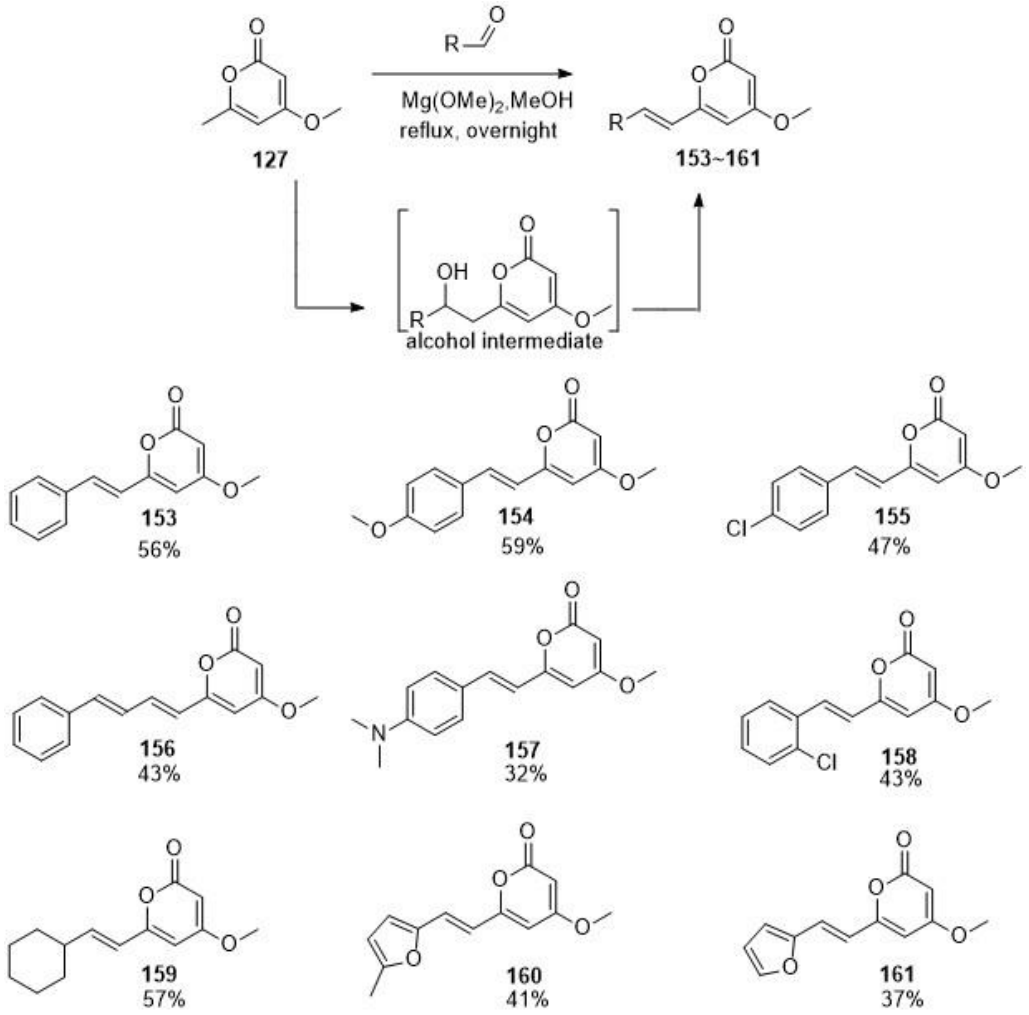

Scheme 41: Condensation between 4-methoxy-6-methyl-2H-pyran-2-one and aldehyde under mild basic condition.

The *trans* geometry was generated from the elimination step (**scheme 42**).[81] As the elimination took place under basic condition and the hydroxyl group was not a good leaving group, the mechanism of elimination was considered as an E2 elimination. The most reactive conformation was when there was an *anti*-periplanar arrangement between the H and OH leaving group and the substituents were on either side of the newly formed π-bond, leading to the thermodynamic *trans* product.

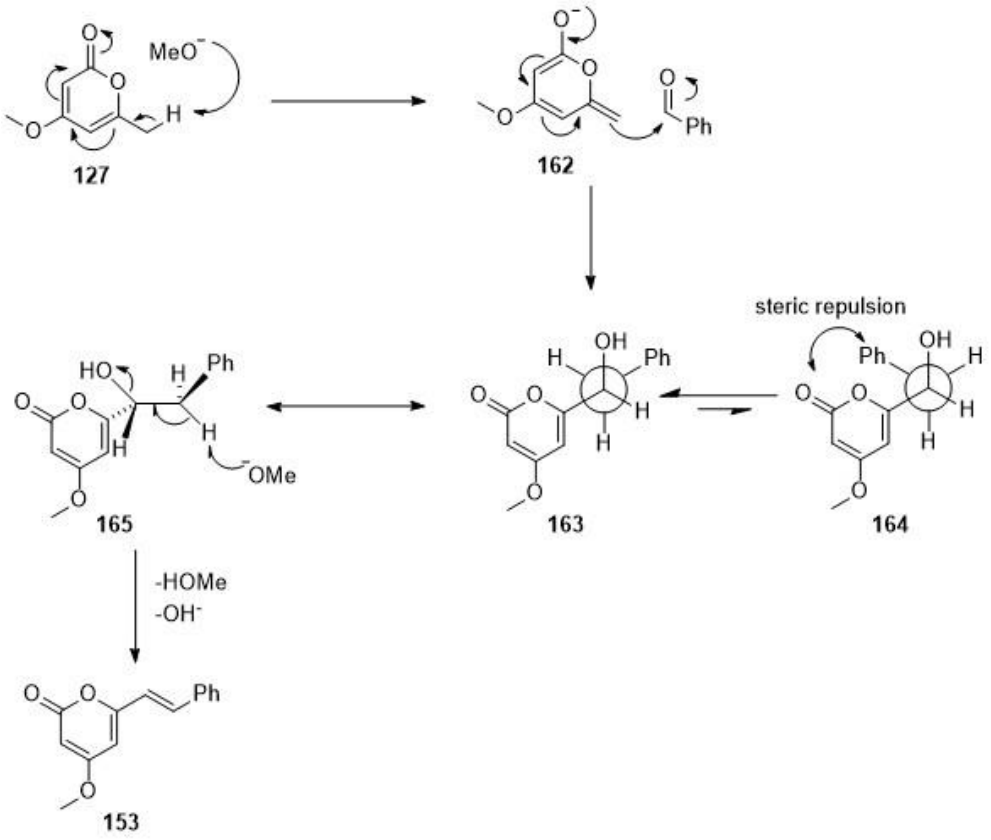

Scheme 42: Mechanism of $Mg(OMe)_2$ condensation.

Wittig methodology is also a widely used method for preparing *trans* alkenes. In 2011, Riberio's group published a method of building *trans*-heterocyclic compounds by Wittig methodology (**scheme 43**).[82] In the study, a series of Wittig reagents were produced from halogenated methyl benzothiazole, methyl benzoxazole and methyl benzoimidazole with triphenylphosphine. The group then treated Wittig reagents with benzaldehyde to generate the corresponding alkenes. The unstabilized Wittig reagent produced a mixture of *E/Z* products in good yield (21%).

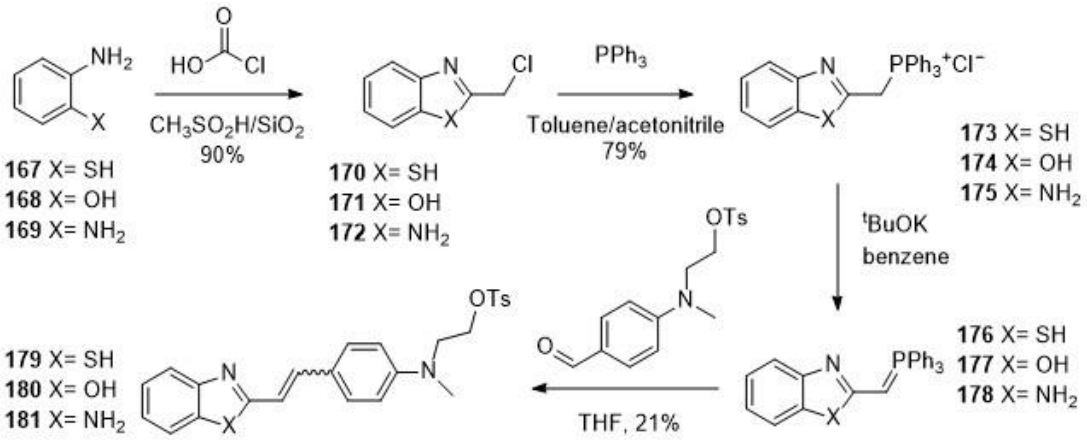

Scheme 43: Examples of the synthesis of *trans*-heterocyclic compounds by Wittig methodology

An alternative solution was developed by using stabilized ylides to build the *trans*-alkenes (**scheme 44 A**). The benzaldehyde **182** was treated with the stabilized Wittig reagent ethyl (triphenylphosphoranylidene)acetate. The reaction was under thermodynamic control and the thermodynamically stable product **183** was generated as single alkene isomer (**scheme 44 B**).[83] Acid hydrolysis of the ester followed by displacement of the tosylate with fluoride ion, gave carboxylic acid **184**. Cyclization of **184** with PPA produced the desired benzoimidazole **181**. The overall yield of this route was very low (10%) but the product was pure *E*-**181**.

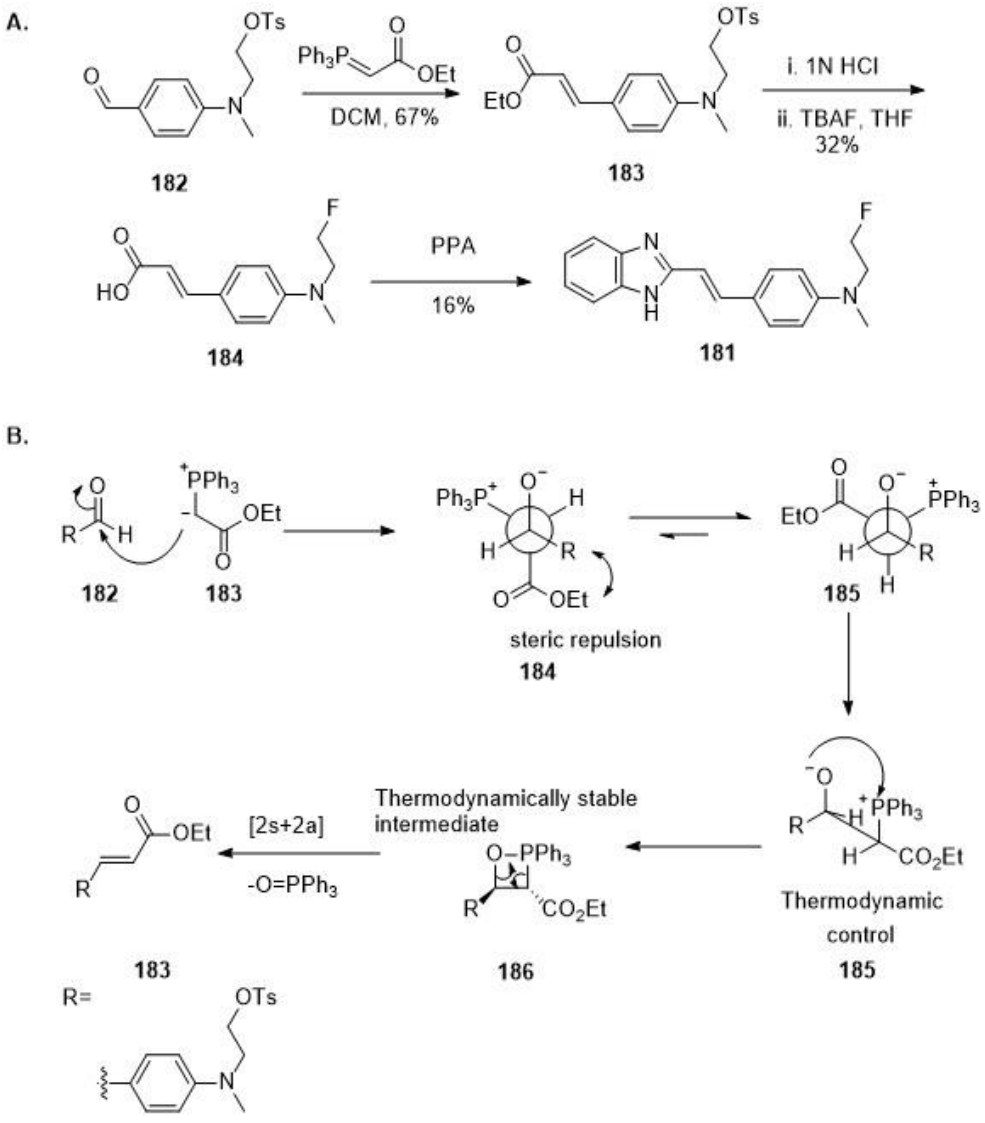

Scheme 44: **A**. Synthesis of **181** *via* stabilized ylide. **B**. Explanation for *E*-selective Wittig reaction

3.2 Attempt Synthesis of 147

The attempted synthesis of **147** began with the route based upon the base promoted condensation. We decided to test the condensation reaction on a simpler structure **127** as its synthesis is shorter. The methylpyrone **127** was prepared based on a method reported by Cheng's group (**scheme 45**).[90]

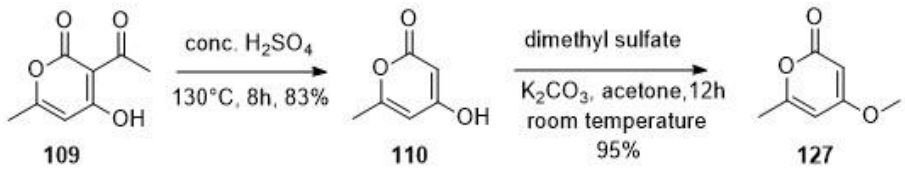

Scheme 45: Preparation of **127** based on Cheng group's method.

The aldehyde **188** was prepared *via* a modified method from the literature (**scheme 46**).[84] Previous research had formed an anion of **187** by halogen-lithium exchange with nBuLi, followed by carbonylation with DMF to give the corresponding aldehyde **188**. We found that the bromo-substituent was not necessary and nBuLi could deprotonate **190** directly to generate an organolithium nucleophile. Preparation of **188** followed the method reported in literature. Diazotisation of amino benzothiazole **44** followed by transfer of an electron from excess *in situ* NO to the diazonium salt generates a carbon radical that abstracts hydrogen from the solvent THF to give the reduced product **190** in 81% yield (literature yield 95%).[123, 146, 147, 148]Aldehyde **188** was prepared from **190** by deprotonation and addition of anhydrous DMF to give aldehyde **188** in 32% yield.[123]

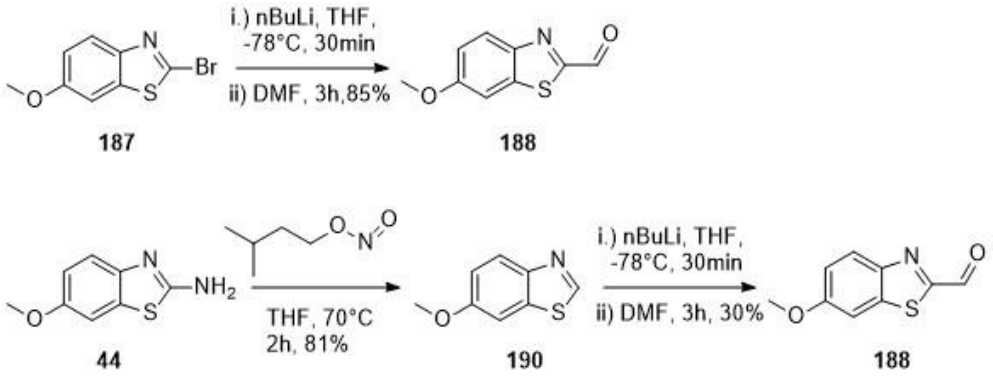

Scheme 46: Preparation of aldehyde **188**.

The base promoted condensation followed the same method as reported in the literature. [85] The $Mg(OMe)_2$ was freshly prepared by refluxing Mg foil in MeOH. Compounds **188** and **127** were then added and refluxed with the magnesium methoxide in methanol (**scheme 47**). After the complete disappearance of **188** by TLC, about 80% of **127** was unreacted and a complicated mixture of unknown compounds with an abundance of aromatic signals was observed under proton NMR. The experiment was repeated with commercial $Mg(OMe)_2$, however, no desired product was isolated.

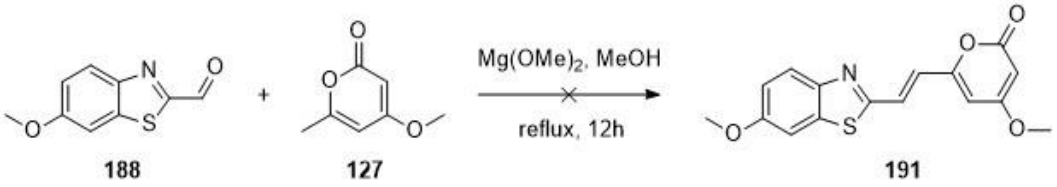

Scheme 47: Basic condensation between **188** and **127**

The literature condition was verified by repeating the reaction between **106** and aldehyde **127** (**scheme 48).** The reaction was successful with an isolated yield of 72% (literature yield 63%[26]). It appeared that **188** was unstable to the $Mg(OMe)_2$ conditions.

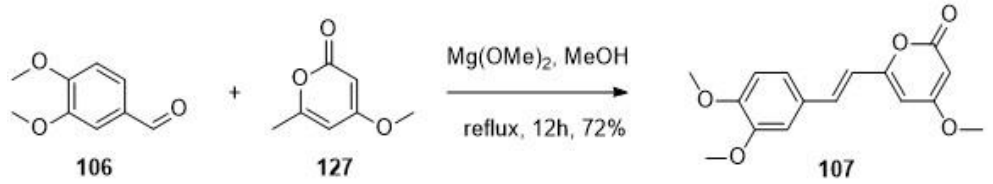

Scheme 48: Basic condensation between **106** and **127**.

The condensation between **188** and **127** was then repeated with bases ^{t}BuOK, NaOAc, piperidine and DBU, but none of them yielded the desired product. The results suggested a different reactivity of aldehyde **188**. Thus, the Wittig disconnection became a more favorable proposition and we sought to use the route of Kaskova's group who had prepared some fungal luciferin analogues. The route would require a Wittig reagent to be prepared from a benzothiazole and combined with the known pyrone aldehyde. A test version of an unsubstituted benzothiazole Wittig reagent was investigated to test the viability of this route.

The benzothiazole Wittig reagent required halogenated 2-methylbenzothiazole as the starting material. Radical chlorination of 2-methylbenzothiazole (**192**) is a convenient method to synthesize 2-(chloromethyl)benzo[d]thiazole (**170**). The literature method reported by Michael *et al* refluxed trichloroisocyanuric acid in chloroform and gave the **170** in ~50% yield (**scheme 49**).[86] However, the usage of trichloroisocyanuric acid was restricted in the lab and the route was not recommended.

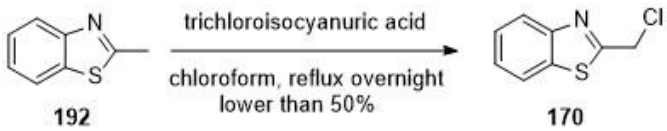

Scheme 49: Radical chlorination of 2-methylbenzothiazole.

Hydroxyl substitution is also one of the most frequently used methods to prepare halogenated benzothiazole. The method reported in past literature refluxed **194** in PPh_3 and CCl_4 (**scheme 50**).[87] The yield of reaction (92%) was higher than radical chlorination but it required one more extra steps to generate the benzo[d]thiazol-2-ylmethanol.

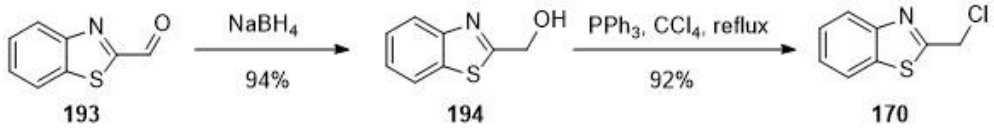

Scheme 50: Hydroxyl substitution of benzo[d]thiazol-2-ylmethanol.

Cyclization between 2-aminobenzenethiol and chloroacetyl chloride provides chlorinated benzothiazole directly. The method reported by Peprah *et al* refluxed 2-aminobenzenethiol and 2-chloroacetyl chloride in and produced 2-(chloromethyl)benzo[d]thiazole (**170**) in high yield (**scheme 51**).[88] As the route has a high yield and short synthesis time, this method was chose to generate the starting material for Wittig reagent.

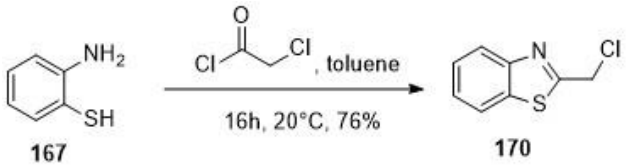

Scheme 51: Synthesis of **170** *via* acetyl cyclization.

Molecule **170** was synthesized following the traditional cyclization of benzothiazole (yield 85%, literature yield 76%[88]) (**scheme 52**). The chlorinated methyl benzothiazole was treated with PPh_3 followed with ^tBuOK to generate the target ylide **196** (yield 95% and literature yield 85%). [87, 97]

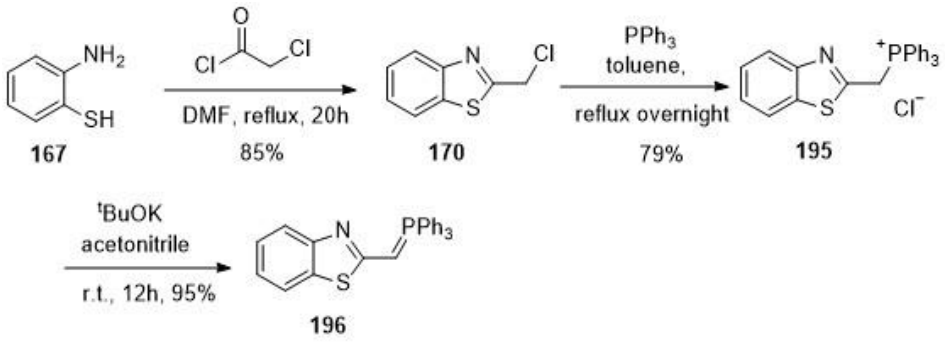

Scheme 52: Preparation of ylide **196**

Riley oxidation of **127** had been reported in the literature and it was chosen to generate pyrone aldehyde **197** (yield 43% and literature yield 91%[89, 90]) (**scheme 53**). The aldehyde was produced by SeO_2 oxidation of **127** under microwave heating or by heating in a sealed tube.[89, 124] The yield of the Riley reaction was somewhat lower than reference. The experiment was repeated several times and it was found that dimethyl sulfate residue from the previous step decreased the yield significantly. Optimisation of the solvent by anhydrous 1,4-dioxane also gave a higher yield (63%) than 1,4-dioxane from the stock bottle (43%).

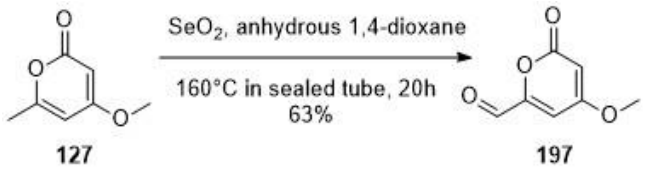

Scheme 53: SeO_2 oxidation of **197** *via* sealed tube method

During Riley oxidation, SeO_2 reacts with **127** in an ene reaction and is then transferred to the methyl group by a [2,3]-sigmatropic rearrangement (**scheme 54**).[91] The corresponding intermediate **199**, can then undergo direct hydrolysis to form **201** or undergo an oxidation step to form aldehyde **197**. Extra water can lead to more hydrolysis and generate **201** as the major product.[92, 93] The mechanism for the yield decrease caused by dimethyl sulfate is unclear. One hypothesis is that dimethyl sulfate could methylate any of the Se-OH species **202** and block the rearrangement. Then, hydrolysis will still take place and lead to **201** as a major byproduct.

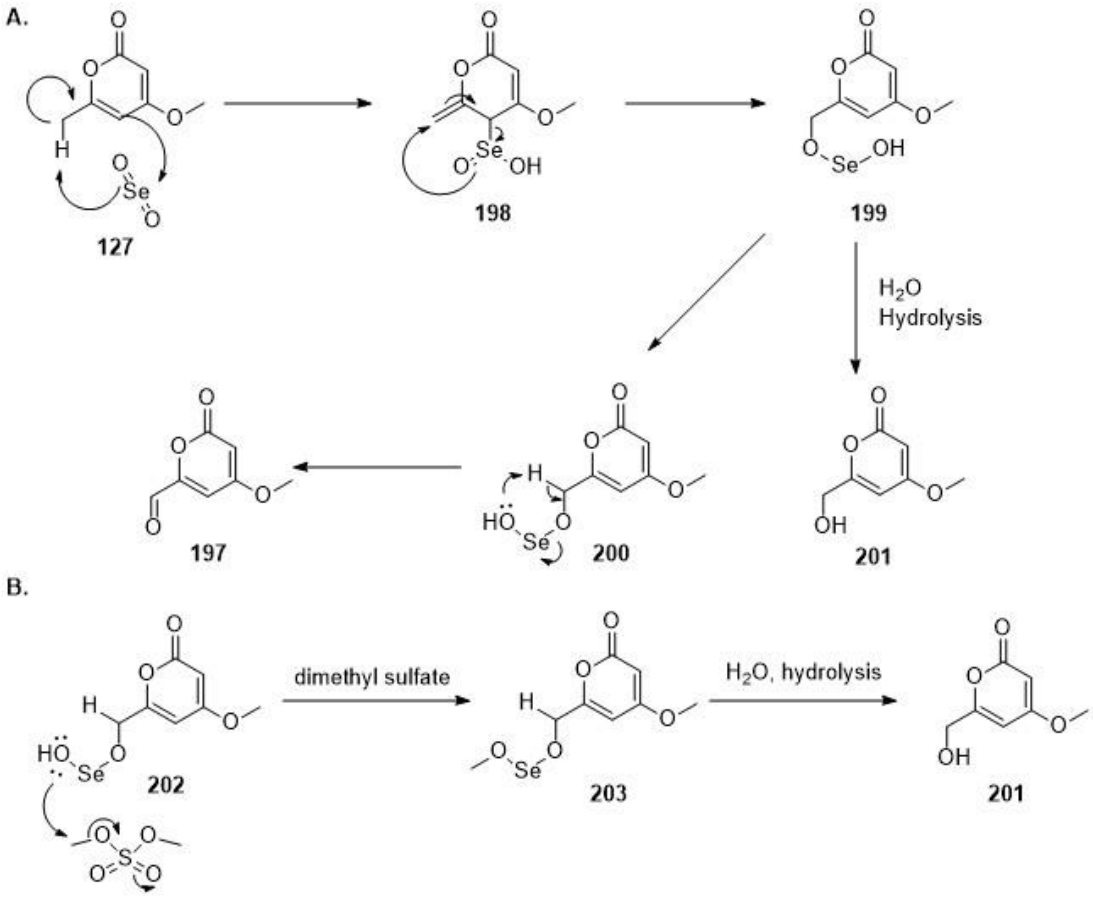

Scheme 54: Riley oxidation mechanism of **127**.

The wittig reaction between **196** and **197** was successful but the product **204** was a *E/Z* isomer mixture (83% and 4:1 *E/Z* ratio) (**scheme 55**). Because there exist several methods to potentially isolate the *trans* isomer or interconvert the *cis* isomer into the *trans*[94], the synthesis was contiuned with the *E/Z* isomeric mixture.

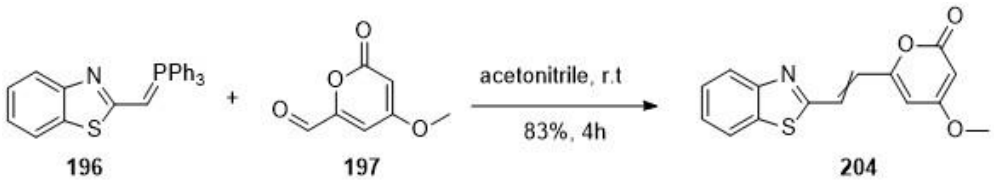

Scheme.55: Wittig reaction between **196** and **197**

Due to the success of the model system, the final retrosynthesis of **147** was based on the Wittig reaction (**scheme 56**). The molecule **147** was firstly protected by methyl groups to prevent side reactions giving **245**. Disconnection of the *trans* double bond gave ylide **207** and aldehyde **244**. The extra C-3 oxygen and aldehyde group in **244** could be introduced by hypervalent iodine reagent[70] and Riley oxidation reported by Fang. [89] The rest of the synthesis of **112** followed the same route as previously described for the model compound. The ylide **207** followed traditional route of preparing Wittig reagent and was prepared by refluxing **206** with PPh_3. The halogenated benzothiazole **206** was generated by cyclization between **205** and

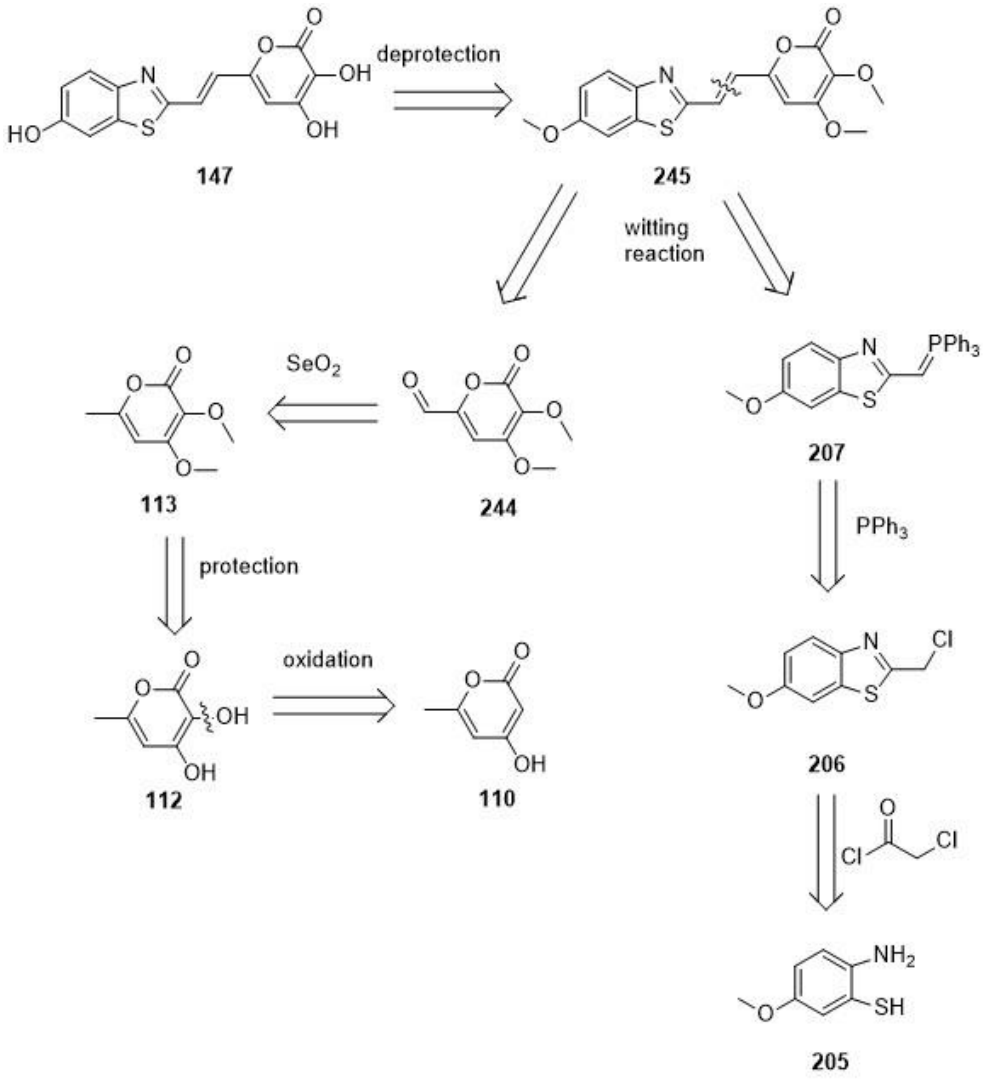

Scheme 56: Retrosynthesis of **147** based on Wittig reaction.

chloroacetyl chloride. [95]The aminobenzenehiol **205** could be prepared by hydrolysis of many common methoxy benzothiazoles.

Commercially available reagent **44** was chosen as the staring material as it was readily available in the lab. Hydrolysis of **44** yielded aminobenzenehiol **205** (62%) and cyclization of **205** with chloroacetyl chloride yielded chlorinated benzothiazole **206** (**scheme 57**).[95] However, the yield of cyclization was low (20%) with an orange solid remaining at the end of the reaction that was similar by mass balance to the starting material.

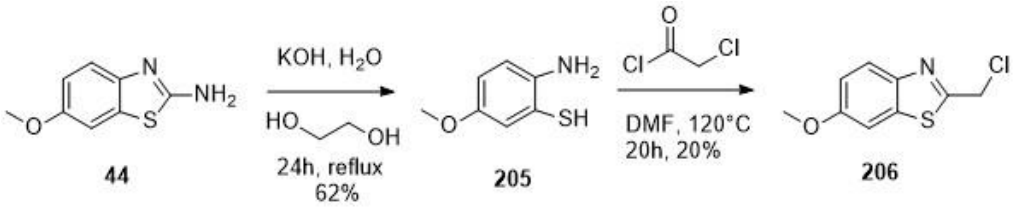

Scheme 57: Synthesis of **206** *via* cyclization

Both steps were checked several times and another compound with a very similar NMR was found in compound **205**. According to the literature molecule **205** could be readily oxidized in air to form the bridged sulfur compound **208** (**scheme 58**).[96]

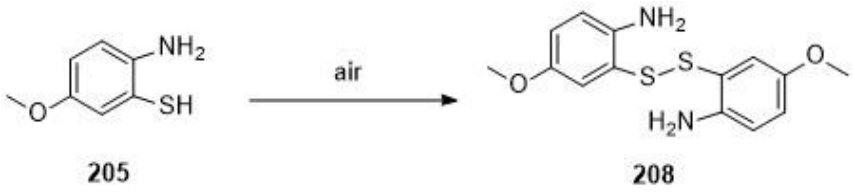

Scheme 58: Oxidation of **205** in air

The disulfide compound could not cyclize with chloroacetyl chloride and was responsible for the low yield of cyclization. Similar reaction was viewed in literature (**scheme 59**). Treatment of **208** with chloracetyl chloride gave an orange solid which was identical to that produced previously.[145]

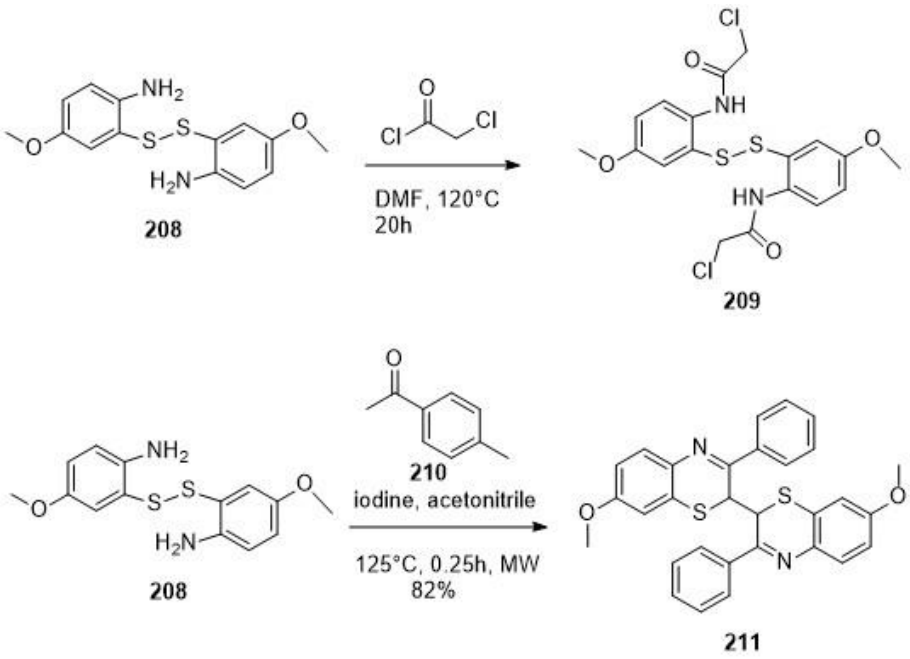

Scheme 59: Formation of intermediate **209** and similar formation of **211** reported in literature.

In past references, a sulfur reductant was added into reaction mixture to improve the yield by reducing the disulfide bond of **208** *in situ* (**scheme 60**). [97]

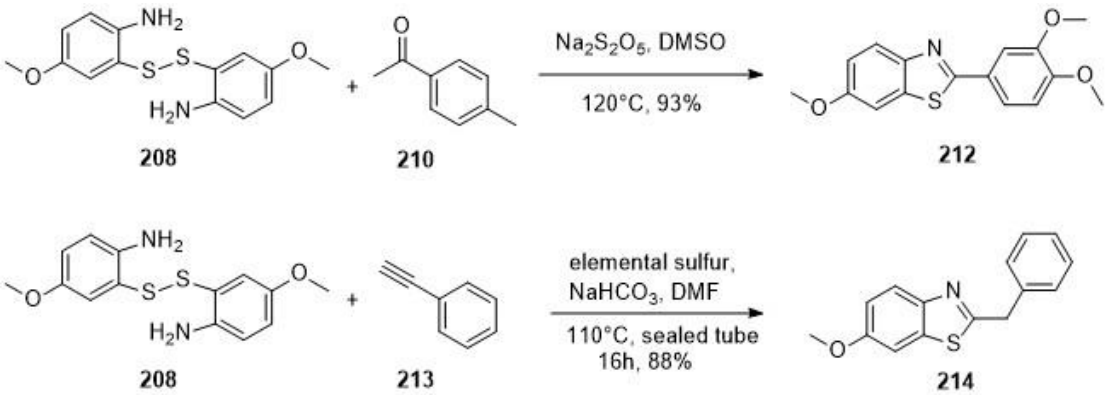

Scheme 60: Cyclization of **208** with a reductant gave **212** and **214**

The yield of cyclization was doubled by adding one equivalent of Na_2S, but extra amount of Na_2S didn't lead any yield increase (**scheme 61**).

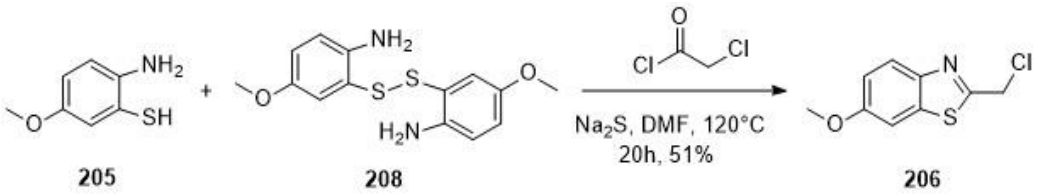

Scheme 61: Improved cyclization by adding Na_2S.

Refluxing **206** with triphenylphosphine gave the phosphonium salt **215** and deprotonation with ^{t}BuOk generated the corresponding ylide **207** in 53% overall yield (**scheme 62**). [87, 98]

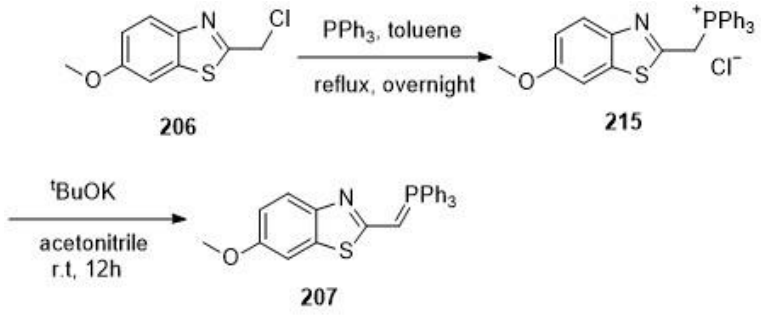

Scheme 62: Synthesis of ylide **207**.

3.3 Functionalization of C-3 carbon in 4-methoxy-6-methyl-2H-pyran-2-one (110)

The reactivity of 2-pyrone has been studied and the electronic property of each position is documented. [99, 100] As both alkenes are in conjugation with the C-2 carbonyl group, nucleophiles can attack the two electrophilic positions *via* conjugate addition (**Equation A, scheme 63**). The C-1 oxygen can donate a lone pair into the alkenes and render the C-3 and C-5 position nucleophilic (**Equation B, scheme 63**).

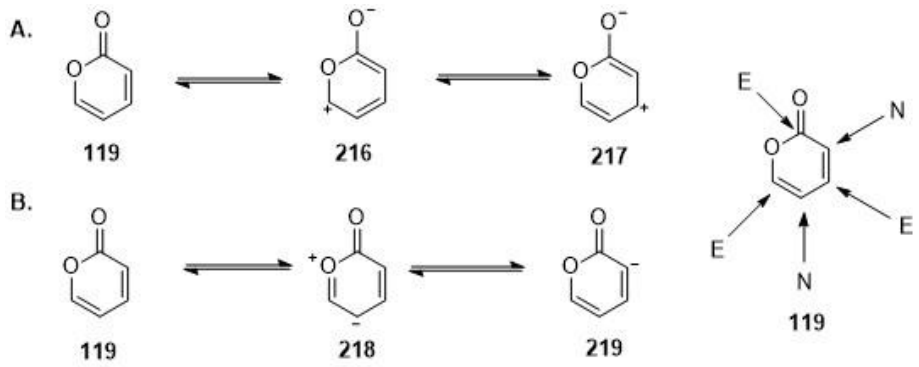

Scheme 63 Reactivity of each position on **119**. E means electrophilic and N means nucleophilic.

The molecule **110** has a similar reactivity as **119**. The C-2 and C-6 positions are electrophilic and the C-3 and C-5 are nucleophilic (**Equation B, scheme 64**).[101, 102] The methyl group has no obvious reactivity as no functional group is conjugate to it. Under basic condition, the C-4 hydroxyl group will be deprotonated first and the methyl group will still be unreactive.

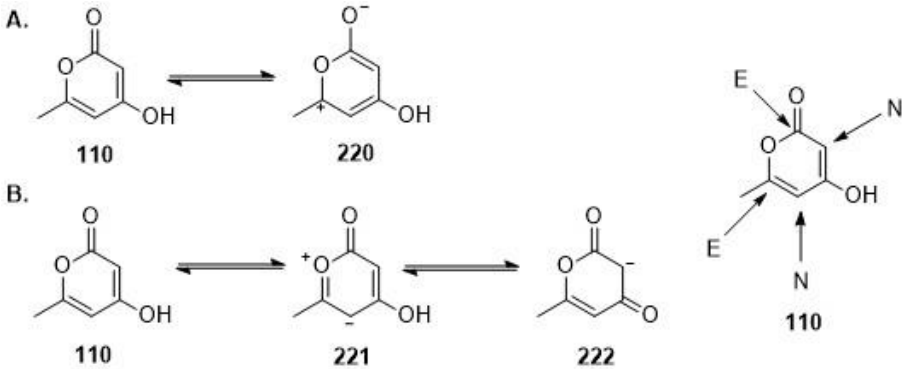

Scheme 64: Reactivity of each position on **110**. E means electrophilic and N means nucleophilic.

The hydroxyl functionalization of the C-3 position began with diazonium substitution. The 'enol' like C-3 carbon could add to electrophiles such as diazonium salts and a hydrazine could be generated by such method. From the literature, hydrolysis of hydrazine could be performed under acidic condition and the reaction lead the target carbonyl compound (**scheme 65**). [103]

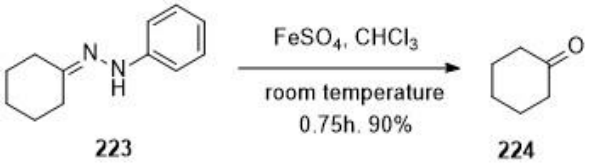

Scheme 65: Hydrolysis of hydrazone under acidic condition.

Amino benzene was treated with $NaNO_2$ and HBF_4 to generate diazonium salt **226** (yield 85% and literature yield 60%) (**scheme 66**).[104] Molecule **226** was treated with **110** at 0°C to afford hydrazine **227** (91%). The product was confirmed by MS, but isolation of pure **227** *via* flash column was unsuccessful. Investigation of the procedure was stopped and hydrolysis of **227** was not achieved.

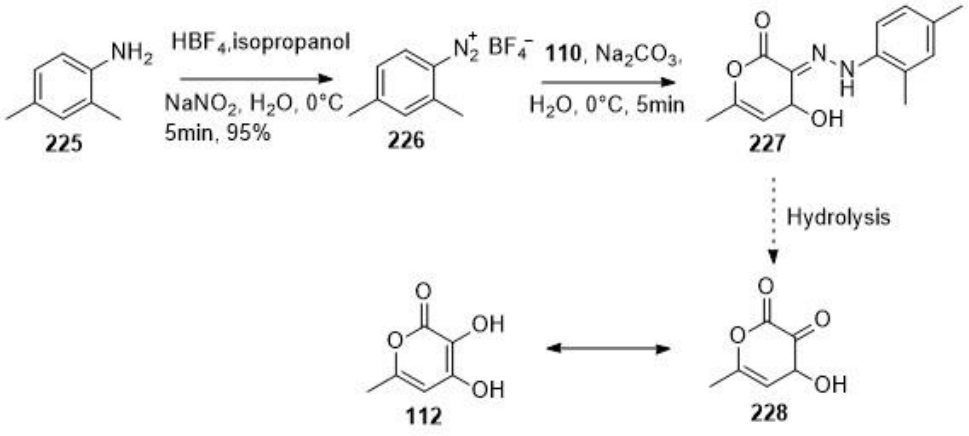

Scheme 66: Attempt synthesis of **112** *via* hydrazine formation.

The second attempt was based on electrophilic nitration. Hydroxyl group could be generated from direct hydrolysis of diazonium salt. This strategy has been widely applied in hydroxylation of complicated molecules (**scheme 67**). [105]

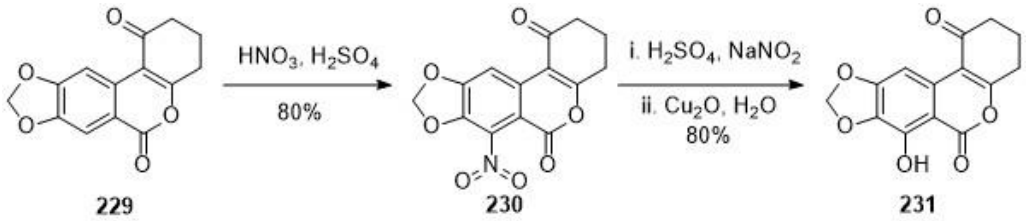

Scheme 67: Literature example of hydroxyl group generation from diazonium salt. [105]

Molecule **110** was treated with nitrating mixture HNO_3 and H_2SO_4 to afford **232** (yield 90% and literature yield 79%[127]) and reduced by H_2/ Pd-C to produce the corresponding amine **233** (yield 82% and literature yield 80%) (**scheme 68**). Conversion of **234** to **112** *via* diazonium chemistry,[106] was unsuccessful. All of the starting materials were consumed, and a mixture of unknown compound was isolated at the end of the reaction.

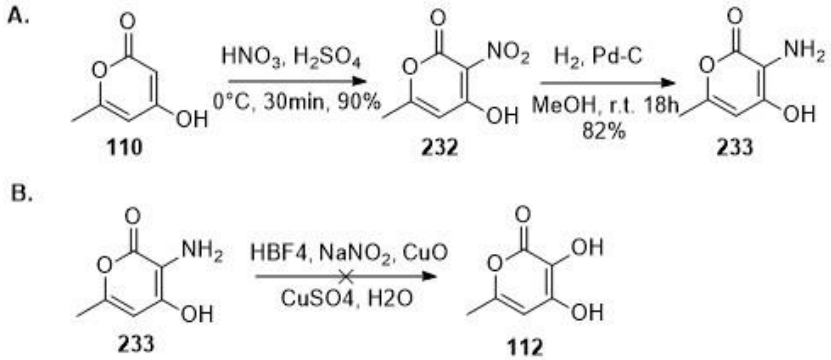

Scheme 68: Diazonium route towards **112**.

A third attempt was based upon the hydrolysis of an iodonium ion. The phenyl iodonium compound **235** was reported by Kappe *et al* and it could easily be functionalized under several mild conditions. [107]

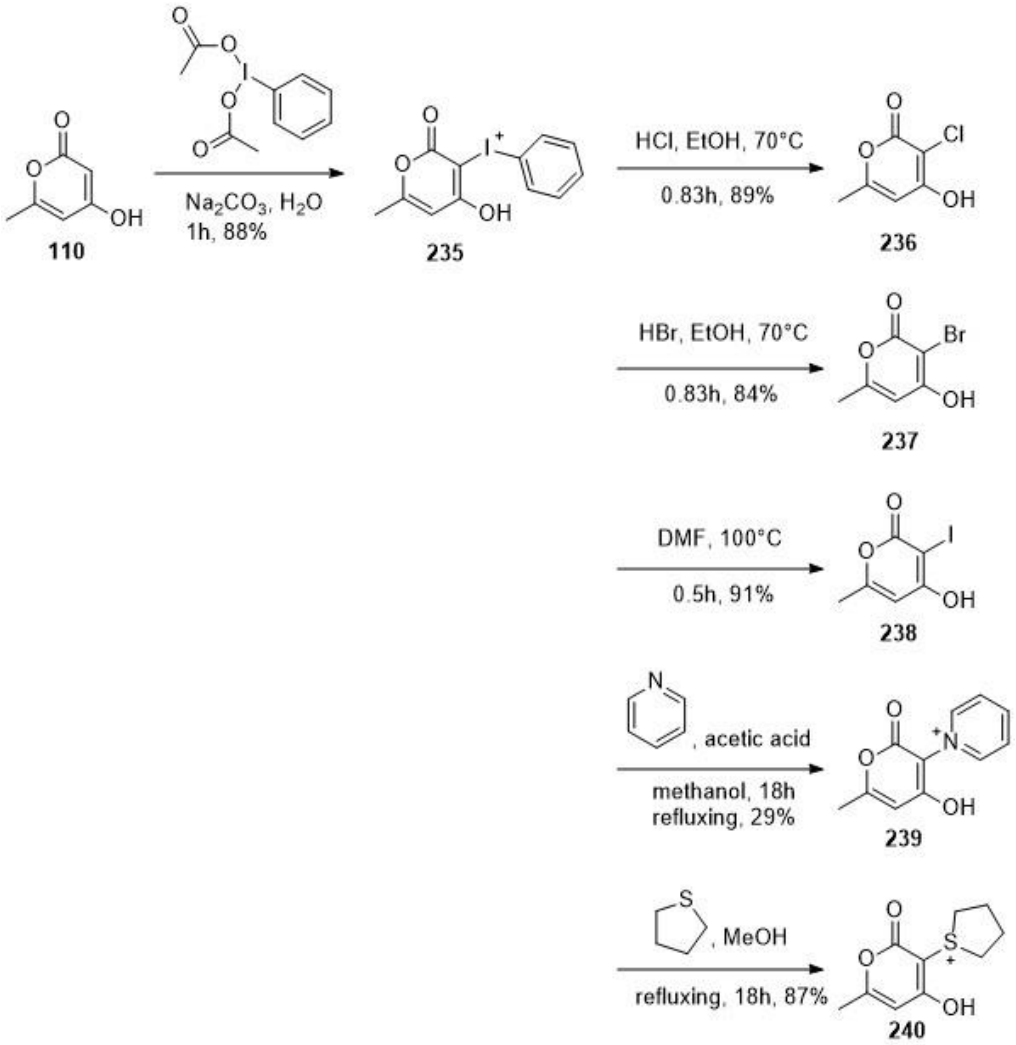

Scheme 69: Functionalization of **110** *via* phenyl iodonium method

Molecule **110** was treated with iodosylbenzene under weakly basic condition to generate **235** (84%) (**scheme 70**). The hydrolysis of **235** was unsuccessful and the route was stopped.

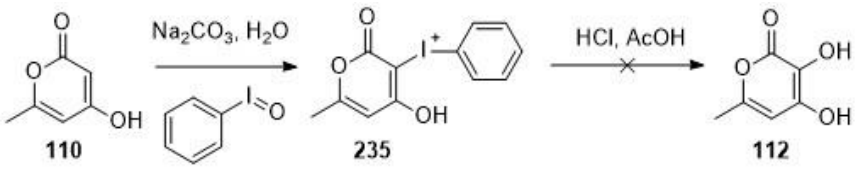

Scheme 70: Attempt synthesis of **112** *via* hydrolysis of iodonium species **235**.

A fourth attempt used a hypervalent iodine reagent based on the method reported by Evangelia *et al* (**scheme 71**).[70] Reagent **243** was synthesized by standard means and then added to **110** to generate sulfate **111** (yield 73% and literature yield 42%). The mechanism of reaction remains unclear. Although the paper said it was a radical reaction, other mechanisms such as direct nucleophilic attack could also be considered (**scheme 31 and 32**).

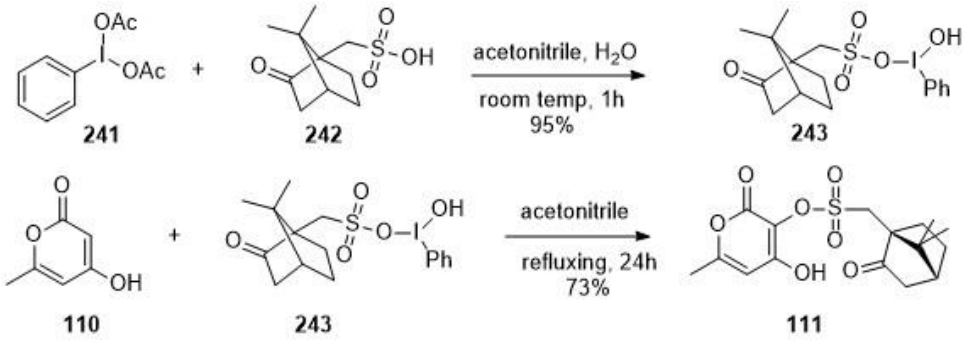

Scheme 71: Introduction of C-3 oxygen by hypervalent iodine reaction.

Basic hydrolysis of **111** gave the desired diol **112** (yield 90% and literature yield 82%). The rest of synthesis followed the same procedure reported by Kaskova *et al* (**scheme 72**). The diol was firstly protected with methyl groups and oxidation with SeO_2 lead the aldehyde **244** (55%). [50]

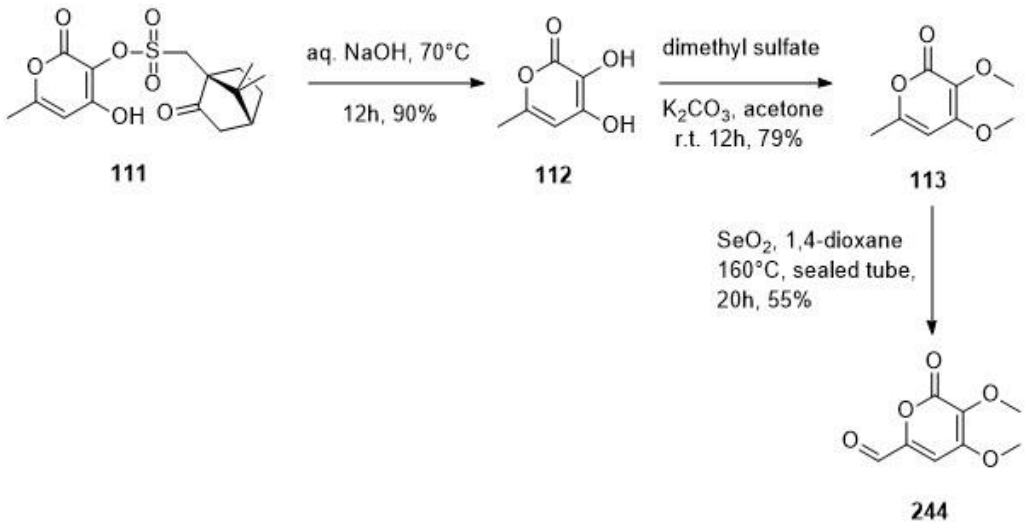

Scheme 72: Synthesis of aldehyde **244.**

The Wittig reaction between ylide **207** and aldehyde **244** gave the desired alkene **245** (84%) (**scheme 73**). Surprisingly, the reaction only formed a small amount (~8%) of the *cis* product as an inseparable mixture with the major *trans* isomer. After a week, a second NMR analysis showed only the pure *trans* product. Photoracemisation, or acidic catalysis from trace HCl in the deuterated chloroform, could have been responsible for the *cis* to *trans* isomerisation.

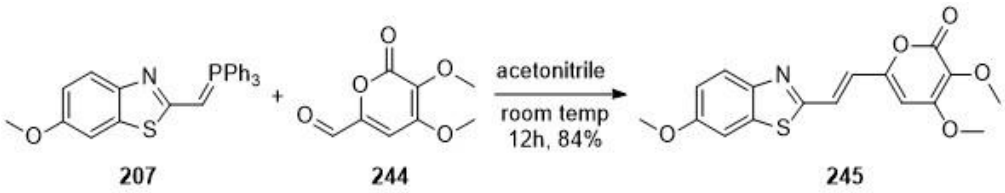

Scheme 73: Wittig reaction between ylide **207** and aldehyde **244**.

The deprotection of **245** was performed with NaH/EtSH and then BBr_3.[26] The molecule was firstly treated with NaH/EtSH to generate a singly deprotected product (71%). The C-4 carbon was considered to be cleaved and tentative structure **246** was thought to be the deprotection product. (**scheme 74**). Nucleophilic EtS^- could attack

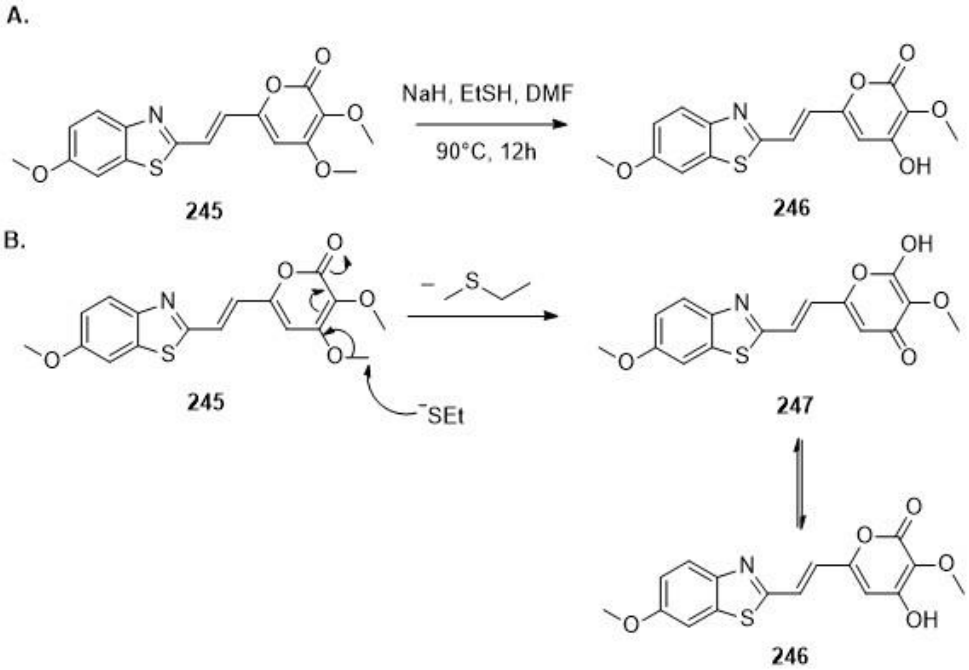

Scheme 74: A. Deprotection of **245** by NaH/EtSH. **B.** Mechanism of deprotections the basis for the tentative assignment of **246**.

the most reactive C-4 methoxy group by conjugate substitution. Product **246~247** were arguably the most stable leaving group and the two other methoxy groups were unchanged under NaH/EtSH condition. For the remaining deprotections, the procedure followed the method used by Kaskova for the synthesis of **4**.[50] However, cleavage of both methoxy groups were unsuccessful. When **246** was treated with 2 equivalents of BBr_3, only one of the remaining two methoxy groups was deprotected to give what we think was **248** (**scheme 75**). When **246** was treated with 10 equivalents of BBr_3, the molecule decomposed, and no desired product could be isolated. The overall yield of **248** from **245** was around 43% by two-step NaH/EtSH and BBr_3 deprotection.

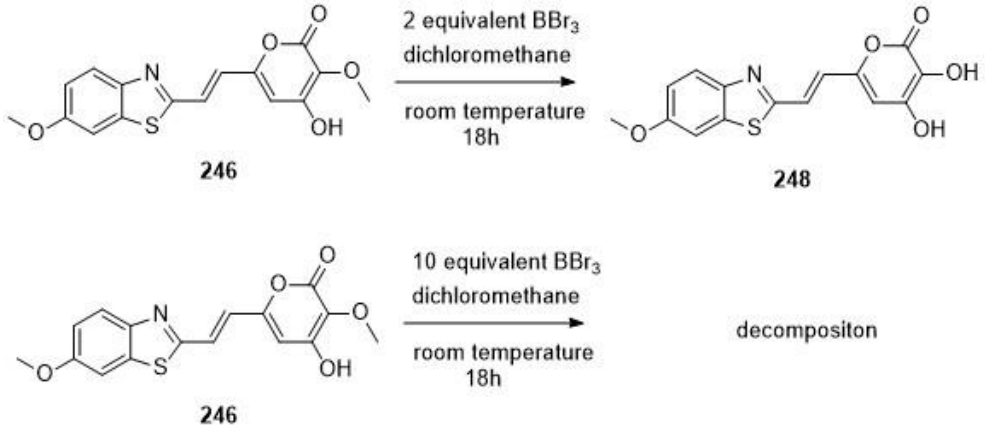

Scheme 75: Deprotection on **246** with BBr_3

Our tentative assignment of **248** is based upon the likely mechanism of BBr_3 deprotection (**scheme 76**). The intermediate **249** might chelate to BBr_3 *via* hydroxyl group. [108]

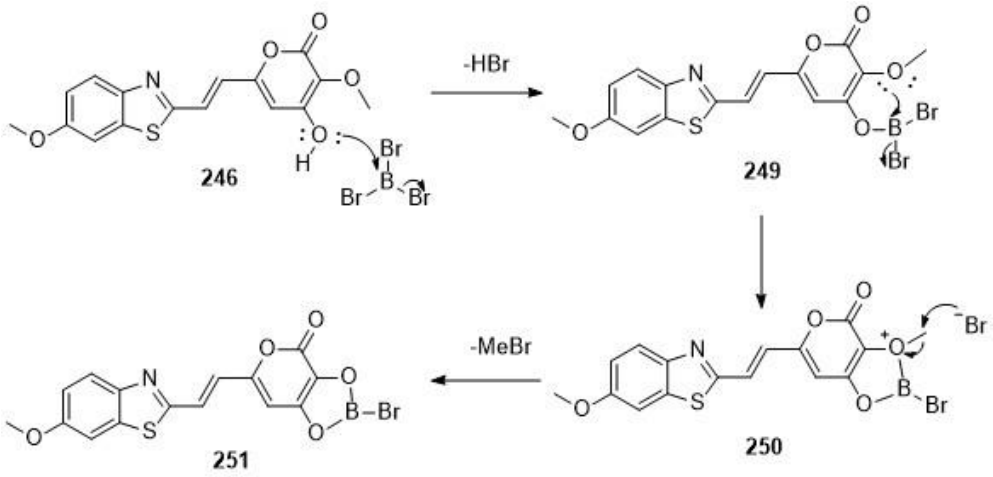

Scheme 76: Mechanism of **246** deprotection *via* BBr_3

The same deprotection procedure was repeated on pyrone **127**, **113** and benzothiazole **253**. The C-4 methoxy group on **127** was cleavable under NaH/EtSH and both methoxy groups on **113** were cleavable by NaH/EtSH followed by BBr_3 (**scheme 77**). The methoxy group on **253** had the highest stability among all three methoxy groups. It was uncleavable with NaH/EtSH and slightly deprotected (less than 10%) by BBr_3.

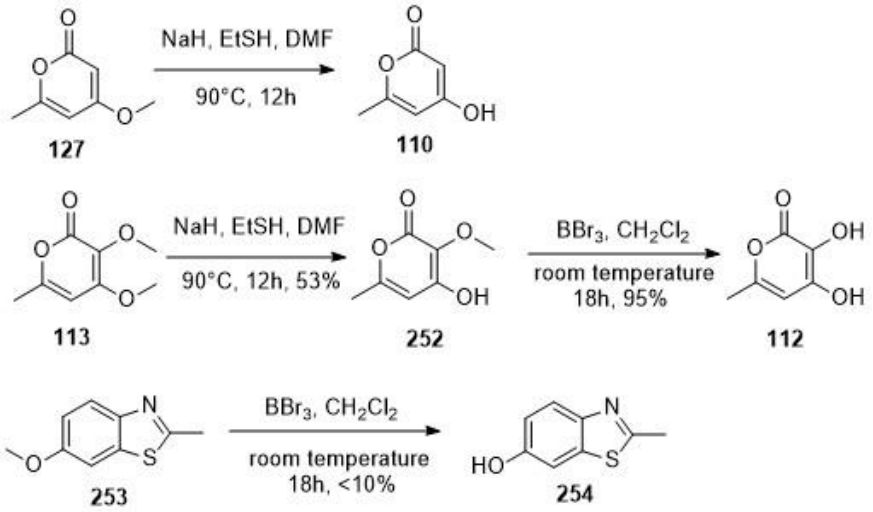

Scheme 77: Methoxy groups deprotection test on **127**,**113** and **253**.

Demethylation with pyridine/HCl has been reported for many similar molecules (**scheme 78**). In this mechanism the methoxy group is first protonated to generate a better leaving group for Cl^- to substitute. [109]

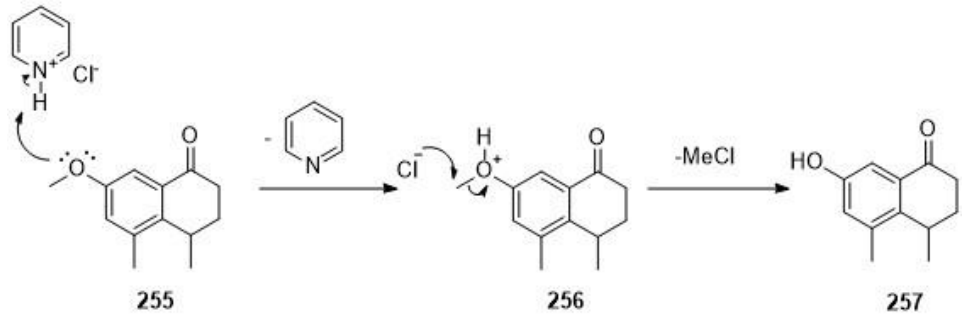

Scheme 78: Demethylation of **255** *via* pyridine/HCl

Molecule **255** was treated with neat pyridine/HCl at 160°C. However, the reaction mixture quickly became a black residue and no product could be isolated. At this stage, the methoxy group seemed not to be a good choice as it requires two steps for global deprotection and the yield of the NaH/EtSH step was not high.

To construct a more convenient route, we decided to investigate another protecting group that could all be removed easily in one step.

2-Methoxyethoxymethyl ether (MEM) protecting group is a common and stable protecting group in organic synthesis against basic and oxidation conditions. It was widely applied in protection of hydroxyl groups and only weak acid was required for cleavage of this protecting group. Similar protection has been reported in literature and this protecting group was tried on **112** (**scheme 79 A**).[110]

Standard deprotonation of **112** with NaH and addition of MEMCl gave no reaction after 12h. The bis-protection of **112** with MEM-Cl group was unsuccessful (**scheme 79 B**).

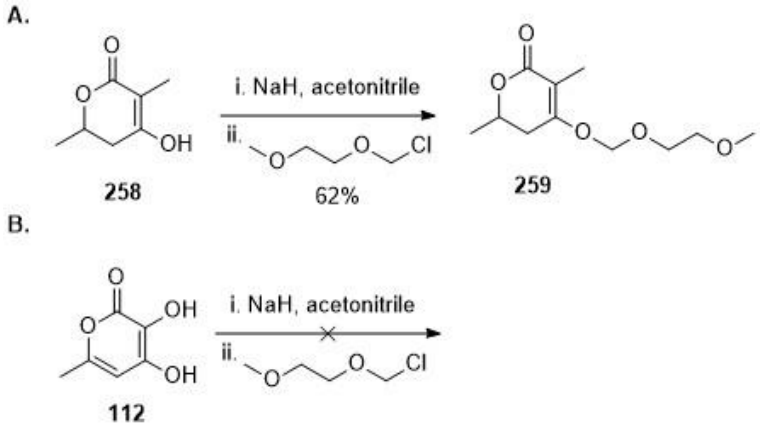

Scheme 79: **A**. MEM protection on similar structure **258**. **B**. unsuccessful MEM protection of **112**.

Trimethylsilyl (TMS) protecting group is also widely used in hydroxyl protection. The silane group is stable under basic and oxidation environment. The deprotection of TMS group is also convenient and it could be easily removed under acidic environment. Protection on similar structure has been reported in literature and the protection followed the same procedure (**scheme 80**). [111]

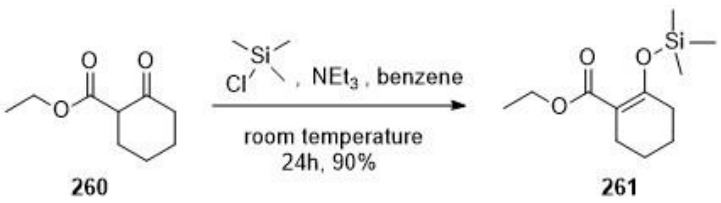

Scheme 80: TMS protection on similar structure from literature.

Diol **112** was reacted with TMSCl and triethylamine in DMF. At the end of the reaction, a new deep spot was shown on TLC with no starting material present. However, after aqueous work up, the new spot disappeared, and the starting material spot re-emerged. A direct column without workup did not give the desired product either and only starting material was collected. Presumably the silyl ethers were not hydrolytically stable and the TMS protection route was stopped.

Acetate ester protection has been used as a protecting group strategy in some syntheses involving strongly oxidizing environments. The acetate **262** was stable to chlorochromate oxidation and the reaction had a high yield of 84% (**scheme 81 A**).[112] An old isolated report in the literature reported that acetate protection was stable towards SeO_2, but the yield and detailed experiment procedure was not given (**scheme 81 B**).[113]

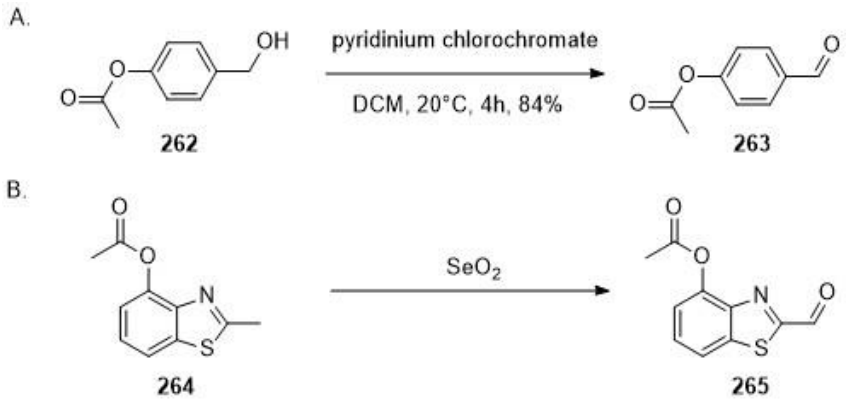

Scheme 81: Acetate protecting group against oxidation in literature.

The ester protection on **112** was successful with high yield (**scheme 82**). However, the protecting groups were unstable to the SeO_2 reaction conditions, giving an extremely low yield of **267** (5%).

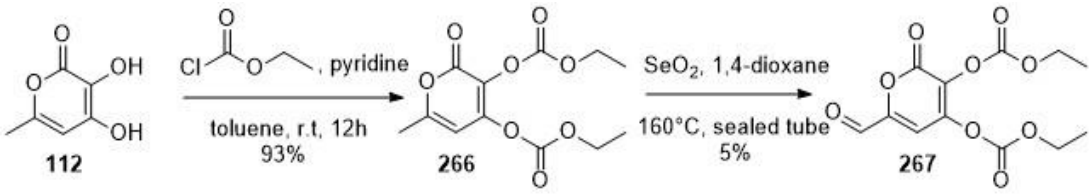

Scheme 82: Ester protection of **112** and SeO_2 oxidation of **266**

The *tert*-Butyldimethylsilyl (TBDMS) protecting group is more hydrolytically stable than the TMS group and it is usually used as a substitute for this group under aqueous conditions. Protection of a similar structure has been reported in the literature (**scheme 83**).[114]

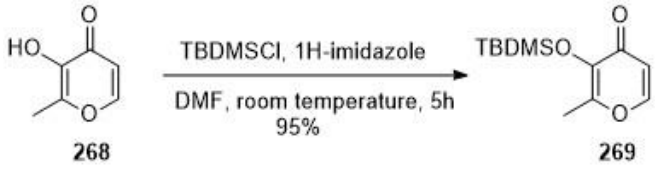

Scheme 83: TBDMS protection in literature

Two equivalents of TBDMSCl and double reaction time gave protected **270** in 90% yield. The OTBDMS group was also stable towards SeO_2 oxidation and gave **271** in 39% yield (**scheme 84**).

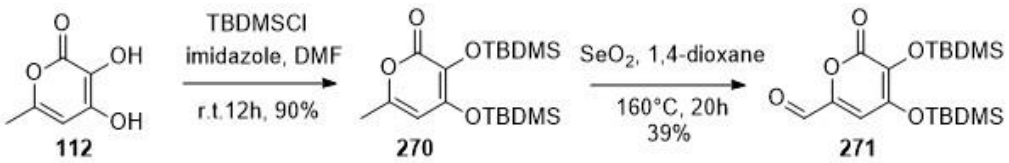

Scheme 84: Formation of TBDMS protected **271**.

The Wittig reagent was also modified by TBDMS protection. The methoxy group was switched to the OTBDMS group before the ylide synthesis (**scheme 85**). The procedure of preparing **206** followed the same route as before (**scheme 61**). The methoxy group of **206** was deprotected with BBr_3 in low yield and the hydroxyl group was subsequently re-protected with TBDMSCl, leading to silyl ether **273**. Attempted phosphonium salt formation by refluxing with PPh_3 led to the the TBDMS group in **273** being removed. Product **274** was confirmed by NMR and MS, but isolation of pure compound was unsuccessful. There are a lack of reports describing TBDMS protected Wittig reagents and the reason for TBDMS cleavage in this step remains unclear. Ylide formation was continued with the deprotected phosphonium salt and resulted in ylide **275**. [82, 87] Formation of **275** was confirmed by MS but isolation of pure **275** was unsuccessful. Wittig reaction of crude **275** generated many unwanted products and purification of the target alkene was unsuccessful. The isolation of pure **275** was repeated several times but the product always contained one major impurity in the aromatic region. Unfortunately, identification of the impurity by proton and ^{13}C NMR was unsuccessful. The route was stopped due to time limitation and a better protecting group will need to be found for this synthesis in future.

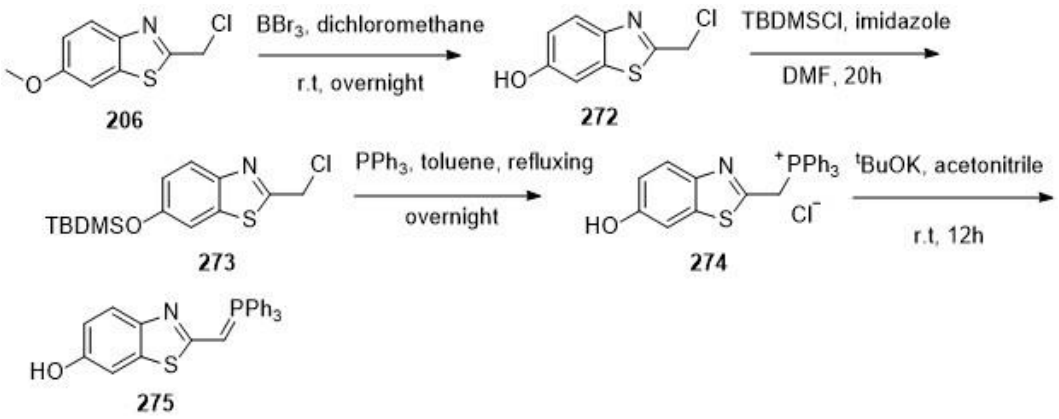

Scheme 85: Ylide **275** synthesis

4. Synthesis of *(E)*-3,4-dihydroxy-6-(2-(6-hydroxy-1H-benzo[d]imidazol-2-yl)vinyl)-2H-pyran-2-one (148)

Synthesis of (*E*)-4-(2-(6-hydroxybenzo[d]thiazol-2-yl)vinyl)benzene-1,2-diol (**148**) followed the same route as **147**, except for the functionality of the starting material and an alternative route was used to generate the benzimidazole ylide (**scheme 86**). [32, 87, 98]

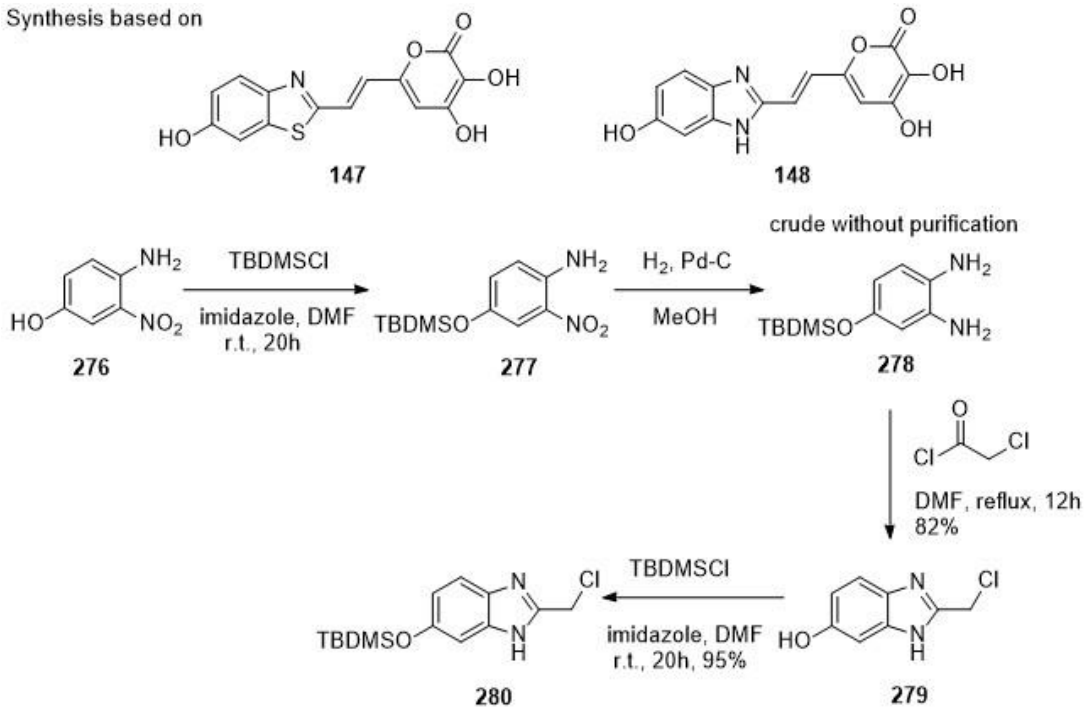

Scheme 86: Synthesis of benzimidazole **280**

TBDMS was used as the global protecting group because deprotection of the methoxy group in **246** was unsuccessful (**scheme 75**). The reactivity of the aryl-1,2-diamine was extremely high and the molecule changed colour in air from light pink to dark purple. Several attempts were made to isolate the reduction product of **277** by hydrogen and catalytic palladium on carbon. Although crude NMR and MS showed the formation of diamine **278**, isolation of the molecule by flash column chromatography was unsuccessful. A direct cyclization of the crude material was

investigated, which involved refluxing crude diamine with excess 2-chloroacetyl chloride. Surprisingly, the reaction was very clean and benzoimidazole **279** was isolated in high yield (82%) over 2 steps. It is common for 1,2-diamines to be reactive towards air and especially CO_2 in air and this telescoped procedure minimized the contact **278** with air.

The synthesis of **148** began at the end of the project and the rest of procedure was not completed. For future work, a stable protecting group for the Wittig reagent would have to be investigated first.

5. Synthesis of 3,4-dihydroxy-6-(6-hydroxybenzo[d]thiazol-2-yl)-2H-pyran-2-one (150)

Target molecule **150** (**Scheme 87 A**) is a heteroaromatic compound linked to pyrone by a single bond. There were less choices in retrosynthesis than the previous molecules (**147~149**) because the single bond between the heterocycles was less transformable than the double bond linker in **147**, **148** and **149**.

The first strategy was inspired by the procedure reported in 2002 by Chang, Kang, and Shifeng (**scheme 87 B**). [115]In this work the imine **281** was generated first by heating benzaldehyde and aminophenol **168**. There was a thermodynamic equilibrium between **281** and **282**. By addition of DDQ, all the ring closed material **282** could be oxidized into **283** at room temperature.

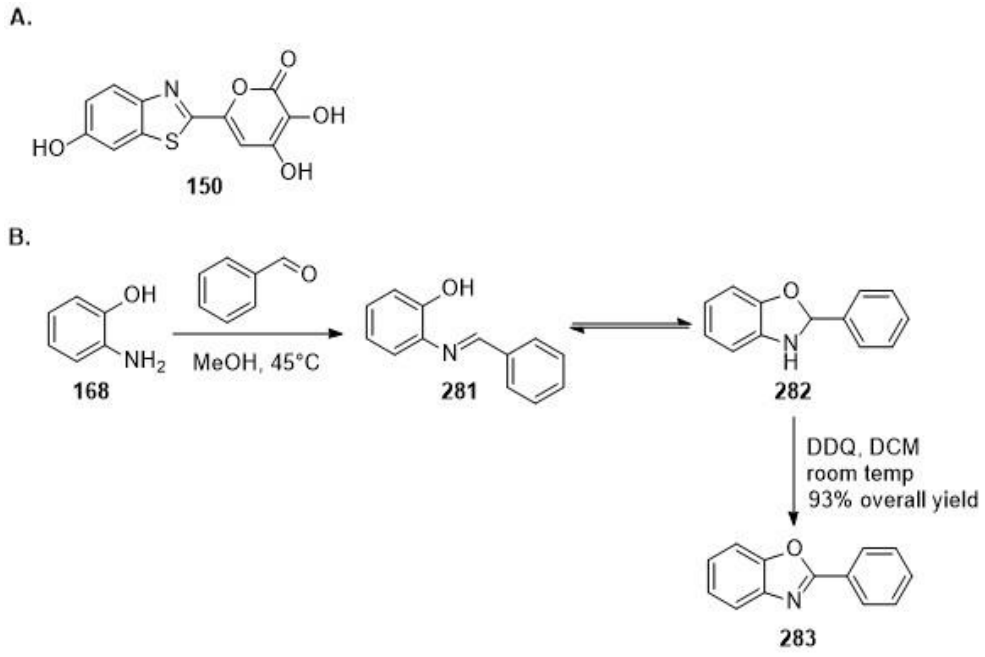

Scheme 87: Synthesis of 2-phenylbenzo[d]oxazole *via* DDQ cyclization.

In an analogous fashion retrosynthesis of **150** could utilize the DDQ cyclization (**scheme 88**). Although a similar oxidation on aminothiols has not reported before, the strategy may be applicable as the reactivities of aminophenol and aminothiol are not dissimilar. The target **150** was firstly protected with methyl groups. Then, disconnection of the thiazole ring gave ring opened product **284** which could be prepared from an aminobenzenethiol **205** and aldehyde **244**.

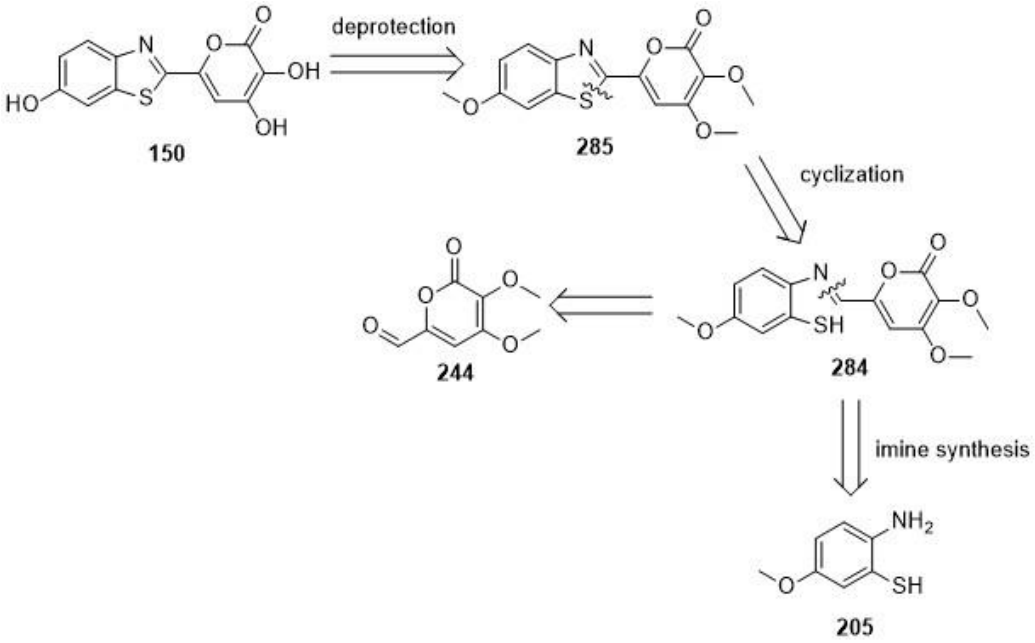

Scheme 88: Retrosynthesis of **150** *via* DDQ cyclization.

Other possible routes were considered. A classic disconnection was based on the self-condensation of ethyl acetoacetate. Past research reported several pyrone cyclizations of aromatic compounds. Ethyl 3,5-dioxo-5-phenylpentanoate (**288**) was first generated by condensation between **286** and **287** (**scheme 89**). [116] Cyclization of **288** took place at 150°C under neat conditions, leading to the desired product **289** in 92% yield.

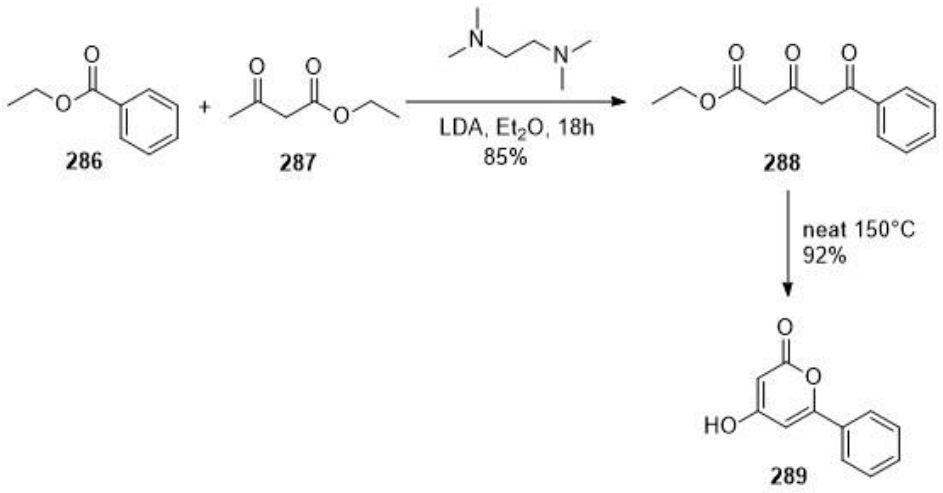

Scheme 89: Synthesis of **289** *via* pyrone cyclization.

According to this cyclization, our target molecule **150** was disconnected through the pyrone ring (**scheme 90**). The C-3 hydroxyl group was introduced by the use of a hypervalent iodine reagent as described in previous syntheses (**scheme 71 and 72**), leading to the intermediate molecules **294** and **293**. The molecule **292** was protected by the methyl group based on the availability of reagents in the lab. We thought that the deprotection of the methyl group with BBr_3 might possibly be low yielding and we were mindful that a new protecting group may have to be investigated in future. The pyrone of **292** could be generated by the self-condensation described in **scheme 91** and the ring-opening process leads to the acetoacetate **291**.Further disconnection of **291** by nucleophilic substitution leads to an acetyl and benzothiazole **190**.

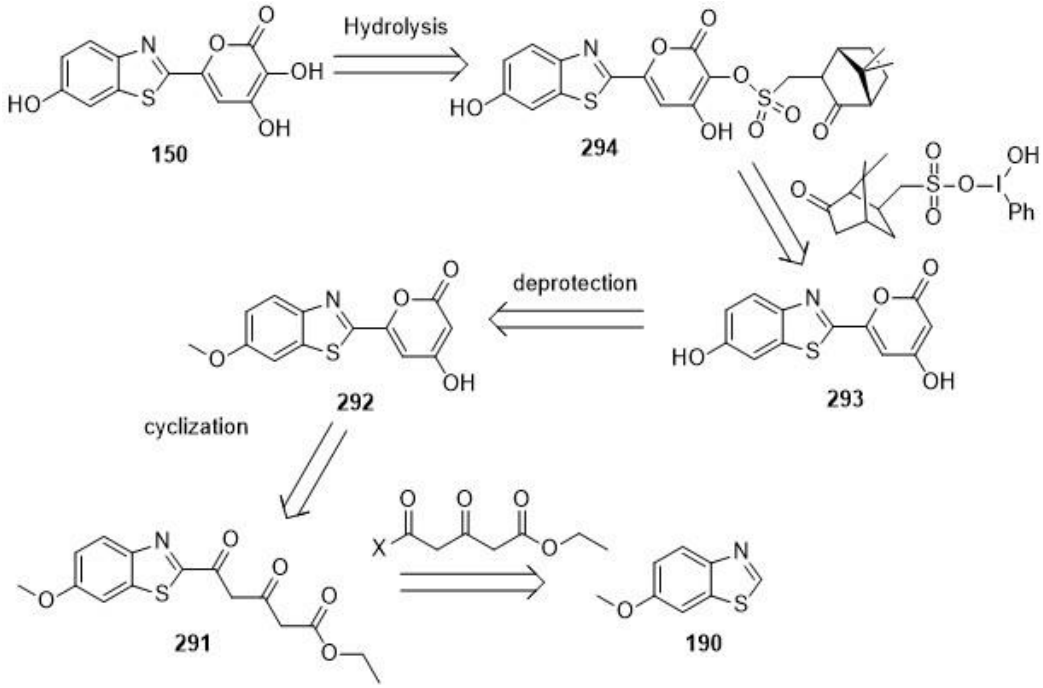

Scheme 90: Retrosynthesis of **150** *via* pyrone cyclization.

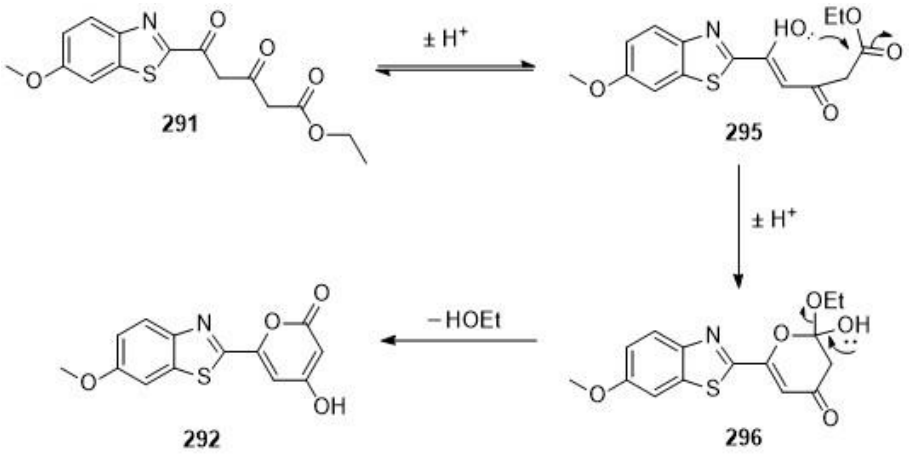

Scheme 91: Cyclization mechanism of **291**.

The synthesis of **150** began with testing the thiol cyclization reaction on a model compound (**scheme 92**). Aminobenzenethiol **167** and aldehyde **244** were heated at 55°C in acetonitrile for 12h to give imine **297**. Crude iminothiol **297** was then treated with DDQ to complete the cyclization. [116] The overall yield for the two steps was 60%.

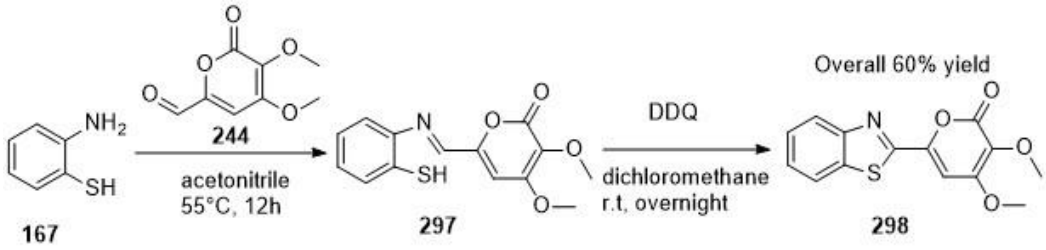

Scheme 92: Test cyclization on **167**

The mechanism of the DDQ step is as shown below (**scheme 93**). [117]The iminothiol **297** first cyclises to *N,S* acetal **299**. This reversible step must have a high equilibrium constant towards **297** as **299** was not observed in the proton NMR recorded. One proton is extracted by DDQ *via* a radical mechanism, generating radical intermediate **300**. Then, DDQ radical extraction of one more proton completes the cyclization to the aromatic benzothiazole.

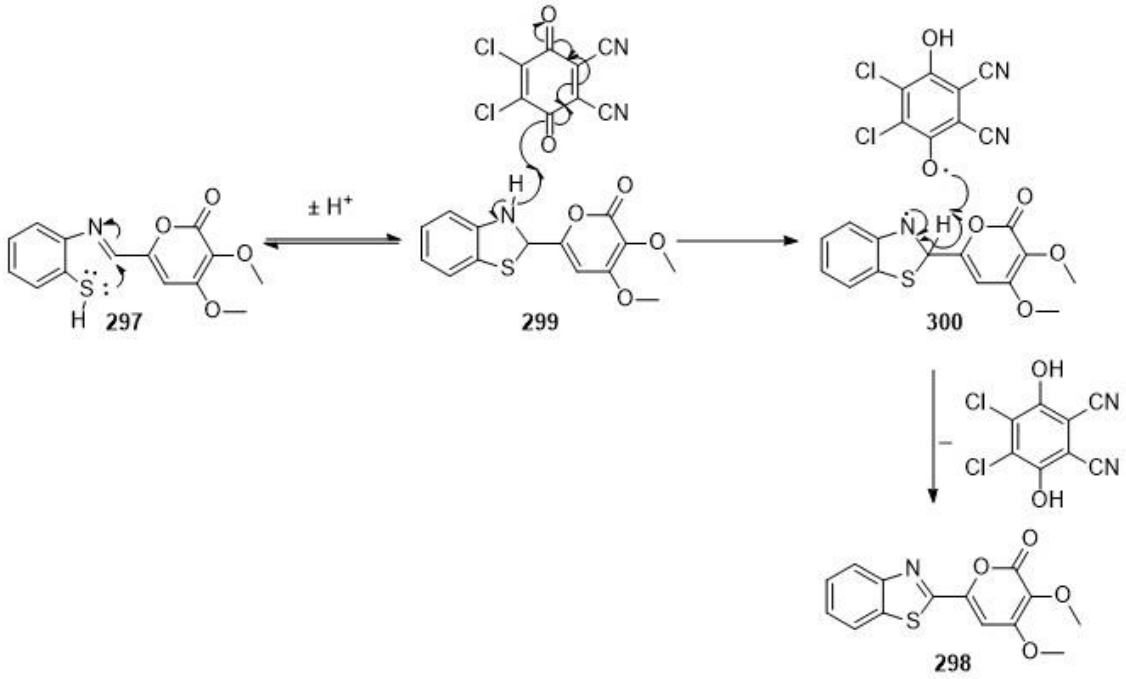

Scheme 93: DDQ cyclization mechanism of **297**.

Deprotection of the methyl ethers was attempted on model compound **298** following same procedure reported in literature (**scheme 94**). [82, 87] The procedure reported by Kaskova's was attempted first with excess equivalents of BBr_3, but only a singly deprotected product was observed. A two-step NaH/EtSH, then BBr_3 were then used to deprotect two methoxy groups on **298**. Although deprotection with NaH/EtSH had a relatively low yield (~20%), the BBr_3 step was very clean, and a direct workup gave the final product in high yield (90%).

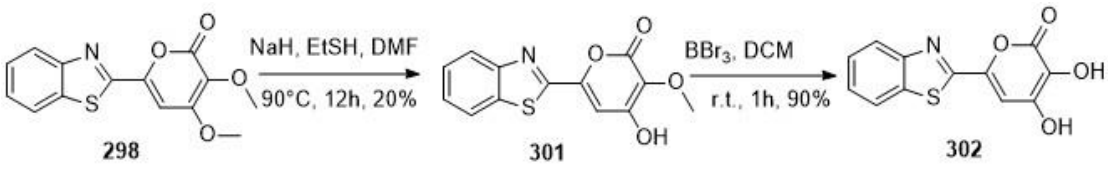

Scheme 94: Deprotection of **298** by NaH/EtSH and BBr_3

The same overall procedure was attempted on the real system (**scheme 95**). 2-amino-5-methoxybenzenethiol **205** was condensed with aldehyde **144** to give imine **303** which was used without purification. Intramolecular cyclization of crude **303** was successful in an overall yield of 50%.

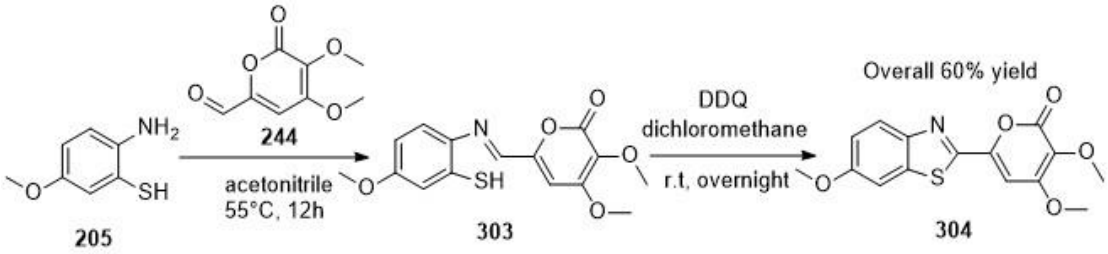

Scheme 95: Synthesis of **304** *via* DDQ oxidation.

Unfortunately, as we had seen previously for the attempted synthesis of **147** and **150** (**scheme 75** and **94**) using NaH/EtSH and then BBr_3, to deprotect all the three methyl groups, led to only two methoxy groups being removed (**scheme 96**). Based upon the

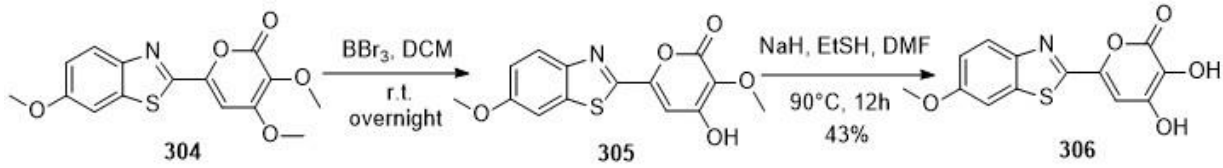

Scheme 96: Unsuccessful deprotection of **304**

results of deprotection, we decided to repeat the synthesis using TBDMS protected substrates. The synthesis restarted with TBDMS protection studies around the end of the project (**scheme 97**). The methyl ether of **205** was firstly unmasked with BBr_3 and then re-protected as its TBDMS silyl ether. The rest of the synthesis followed the same procedure as for the synthesis of **304** (**scheme 95**). The TLC showed disappearance of staring material and formed the same spot as **303** which was assumed to be the imine **352**. Unfortunately, the DDQ cyclization step gave a deep coloured baseline spot by TLC and isolation of pure product was unsuccessful. The reduction product of DDQ would generate side-product **308** and decomposition can lead to HCN. These may have possibly deprotected the OTBDMS groups forming a mixture of polar products. Further investigation was not performed due to the complexity of the crude NMR and the lack of available time.

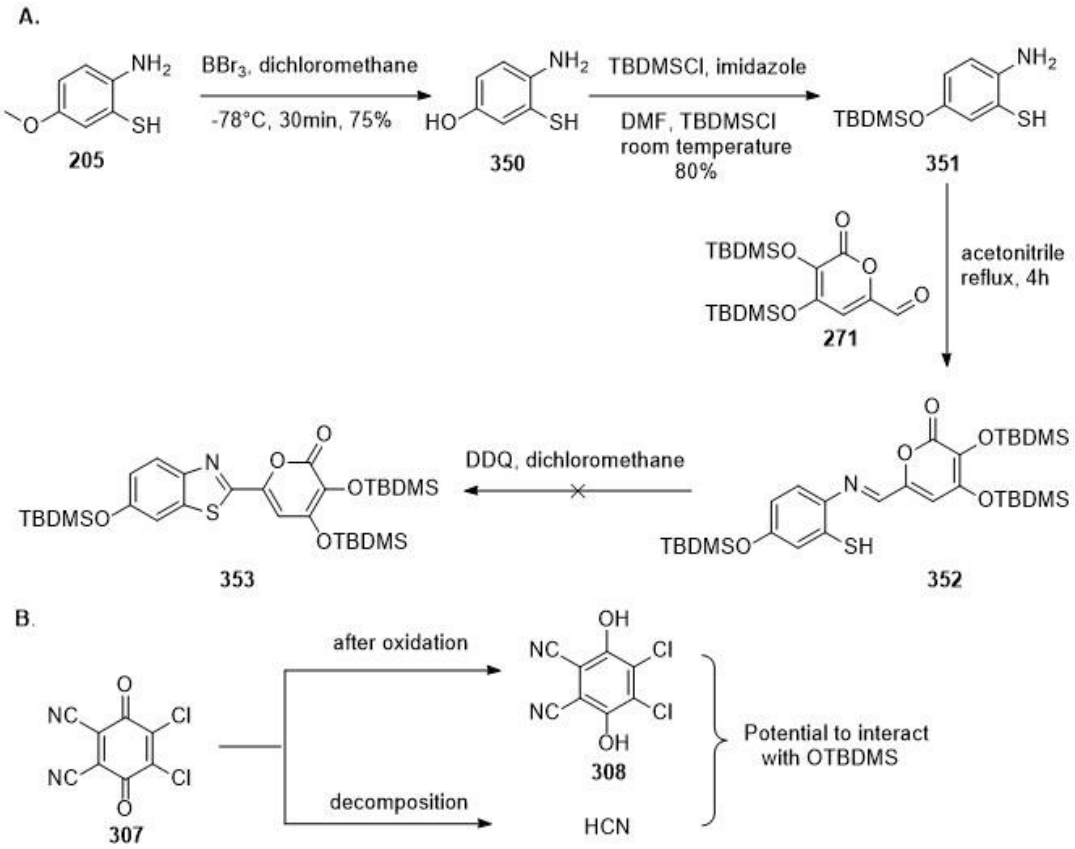

Scheme 97: A. Attempt synthesis of **353** *via* DDQ cyclization B. Side-products from DDQ which have potential to react with OTBDMS.

6. Synthesis of 2-(3,4-dihydroxyphenyl)-6,7-dihydroxy-5H-pyrano[2,3-d]thiazol-5-one (151)

From a survey of the literature there were a limited number of molecules with only similar structures to **151** (**scheme 98 B**). From Hao, Shu-Yi *et al*'s work, lactone **311** was generated from 1-(2-hydroxyphenyl)ethan-1-one (**309**)[118, 119] (**scheme 98 A**). Starting material **309** and diethyl carbonate were refluxed under strongly basic condition in toluene for 4.5h, and the reaction yielded lactone **311** in high yield (95%). To simplify our retrosynthesis, the heterocyclic part of **151** was treated as a lactone fused to a thiazole (**scheme 98 B**).

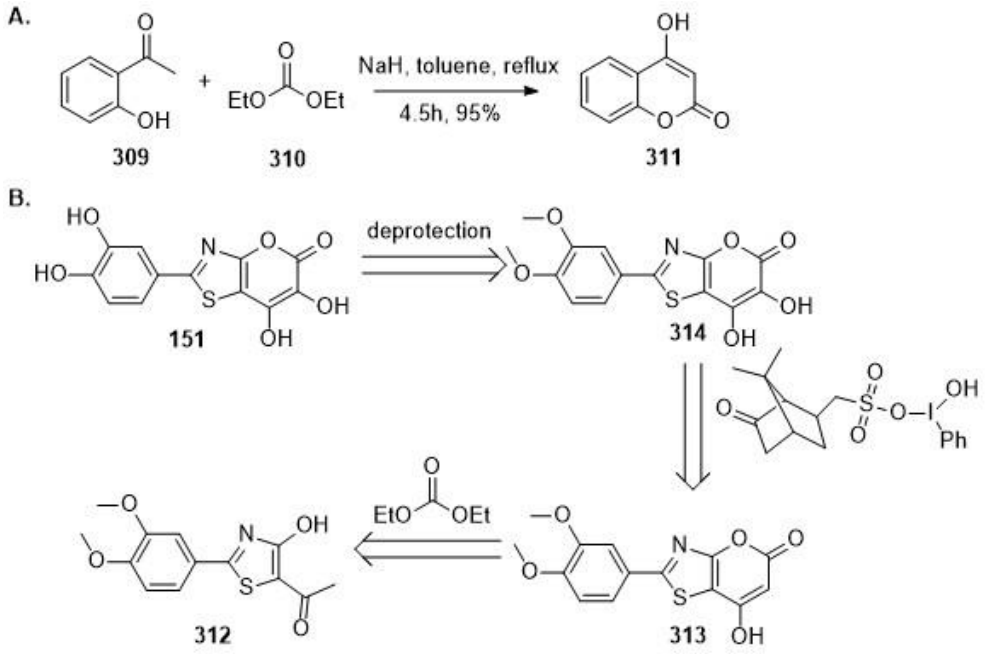

Scheme 98: **A.** Lactone **311** synthesis by Shu-Yi *et al*. **B.** First part of retrosynthesis of **151** based on Shu-Yi *et al*'s work.

Molecule **151** was firstly protected with methoxy groups to prevent side reactions giving **314**. The C-3 hydroxyl group in **314** could be introduced by a hypervalent iodine reagent we have used previously (**scheme 71**), and disconnection of pyrone ring lead back to thiazole **312**.

Synthesis of a benzothiazole with similar functional group arrangements has been reported by Bianchini *et al* (**scheme 99**). [120] Thioacetoamide **315** was heated first with diethyl 2-bromomalonate by microwave to generate benzothiazole **316** (75%). The molecule was then protected with MeI (95%) and hydrolyzed to give carboxylic acid **318** (95%). To transform the carboxylic acid group into a ketone carbonyl group, the molecule was converted into acyl chloride **319** (95%) and then Weinreb amide **320** (95%). Reaction between **320** and methyl Grignard reagent led to the desired methyl ketone **321** in good yield (95%). Deprotection with BBr_3 gave benzothiazole structure **322** which is similar to **312** (**scheme 98**).

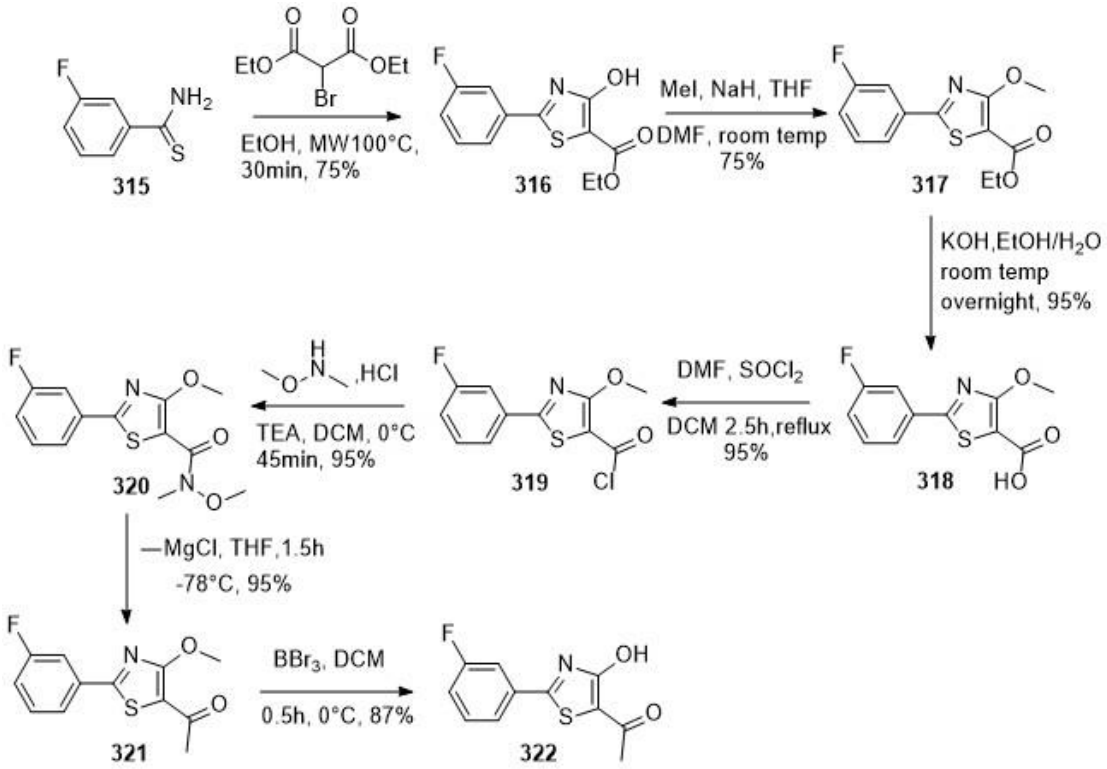

Scheme 99: Synthesis of **322** by Bianchini *et al*.

Following the route described in the literature (**scheme 99**), the second part of our retrosynthesis is described below (**scheme 100**).

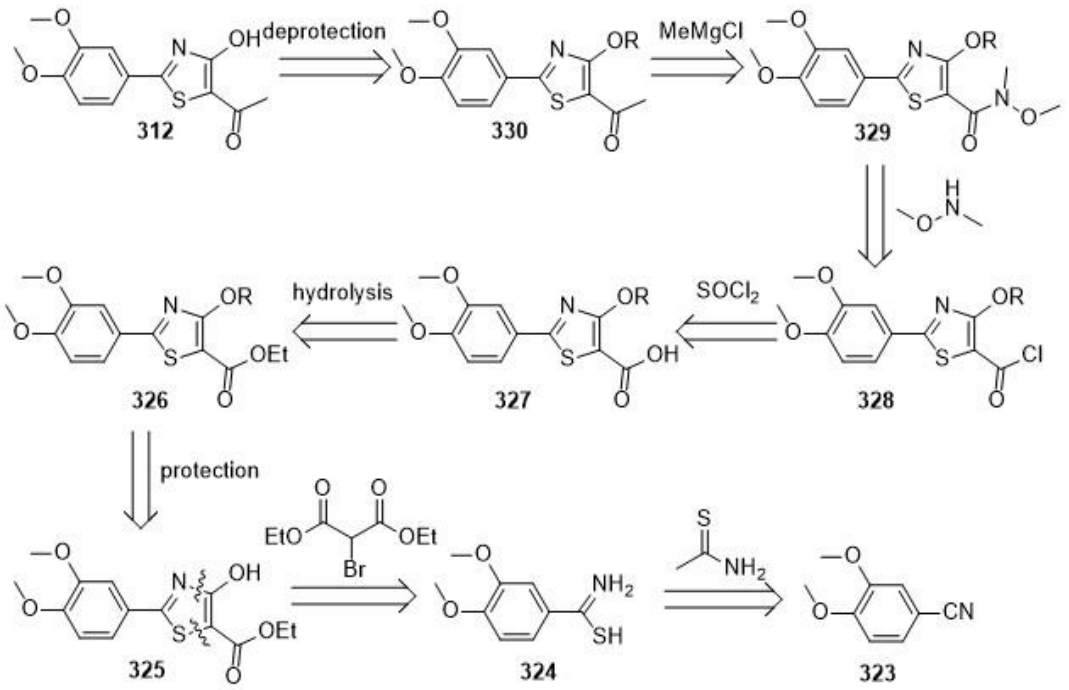

Scheme 100: Second part of retrosynthesis of **312** based on Bianchini *et al*.

Target molecule **312** should be protected with an orthogonal protecting group to the two methoxy groups. This could be derived from carboxylic acid **327** *via* carboxamide **329** and acetyl chloride **328**. Hydrolysis could transfer **327** to the ester **326** and disconnection of the protecting group R would lead to benzothiazole **325**. The synthesis of benzothiazole **325** could be prepared following the method reported by Bianchini *et al*, disconnecting the C-N and C-S bonds, leading to the symmetric ester diethyl 2-bromomalonate and thioamide **324**. The final functional group interconversion of **324** by ethanethioamide gave the commercially available molecule **323**.

The synthesis began with functional group interconversion of **323** (**scheme 101**). A weak acidic environment was used to generate H_2S from thioacetamide and direct attack of H_2S on the nitrile group gave the aminobenznethiol **324** (yield 79%, literature yield 75%).[121] Cyclization of **324** with diethyl 2-bromomalonate gave the desired thiazole ring **325** in 88% yield.

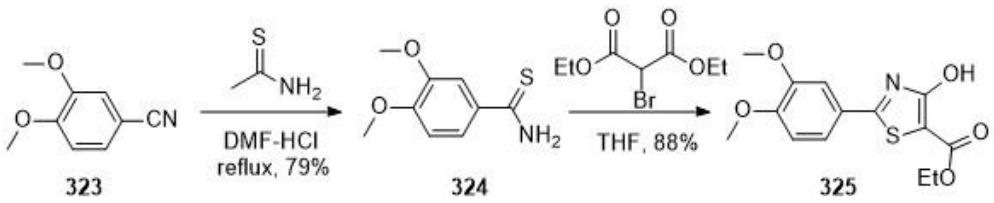

Scheme 101: Synthesis of heterocycle **325**.

Because it required 9 more steps to convert **325** into **151** and several reagents were not available in the lab, the synthetic route after **325** was changed due to time limitation and booking of reagents. It was hard to complete the original route and a shortened route was attempted (**scheme 102**).

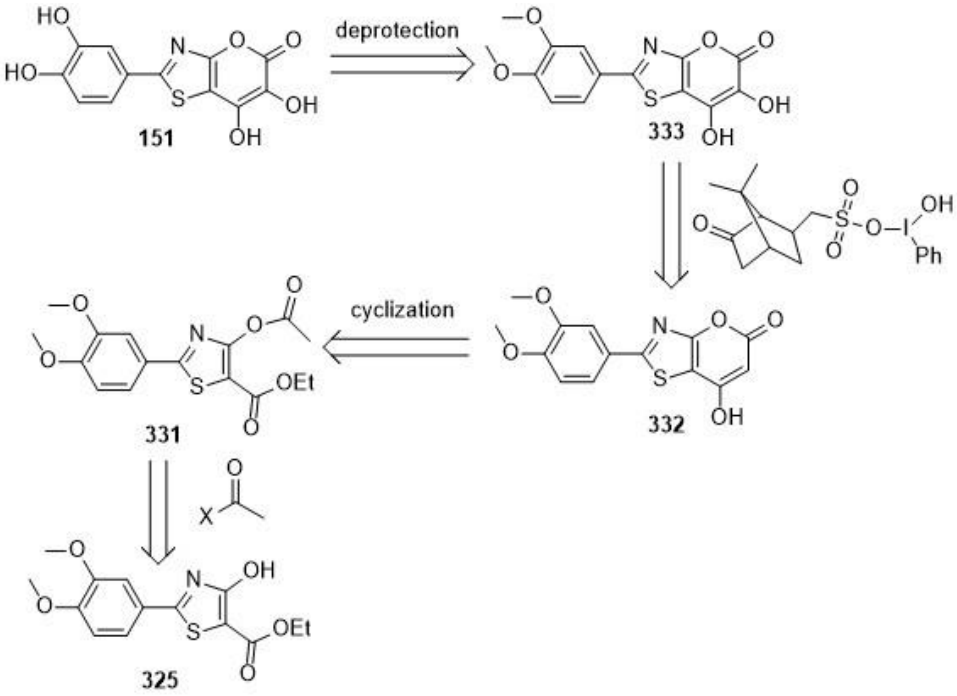

Scheme 102: Shorten retrosynthesis of **151**.

The retrosynthesis followed same procedure up until intermediate **332**. A cyclization was proposed to disconnect the pyrone ring based on Pauly's work (**scheme 103 A**),[122] leading to the ester **331**. Disconnection of the acetyl group in **331** leads back directly to **325** previously prepared (**scheme 101**).

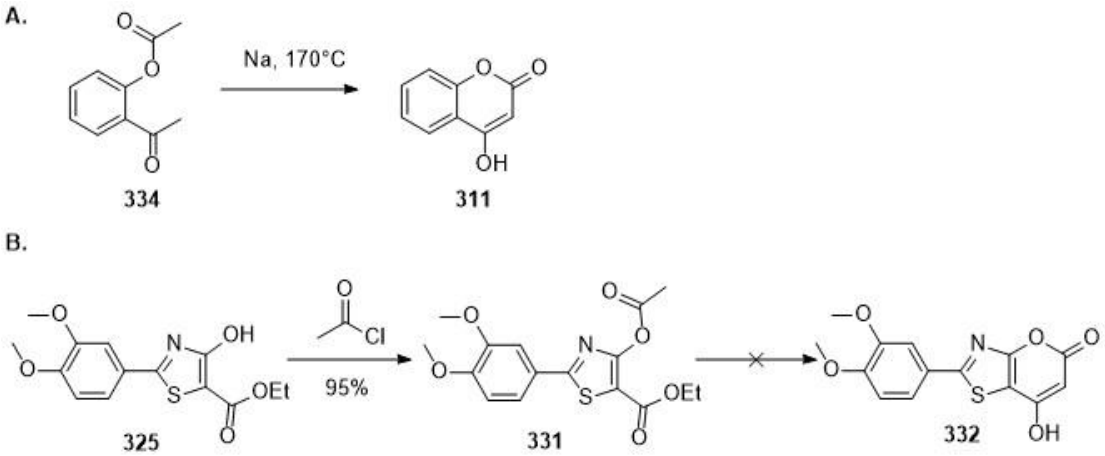

Scheme 103: **A.** Pauly's pyrone cyclization. **B.** Synthesis based on Pauly's work.

The synthesis proceeded with acylation of **325** to give **331** in a good yield (95%). The first attempt at cyclization with NaOH under anhydrous conditions was unsuccessful and the reaction gave mainly starting material **325** by hydrolysis. In later attempts, bulky organic soluble bases DBU, and ^{t}BuOK in EtOAc were used to avoid acyl substitution of the ester group by hydroxide ion. No reaction was observed by TLC and NMR of the crude reaction mixtures (**scheme 104**).

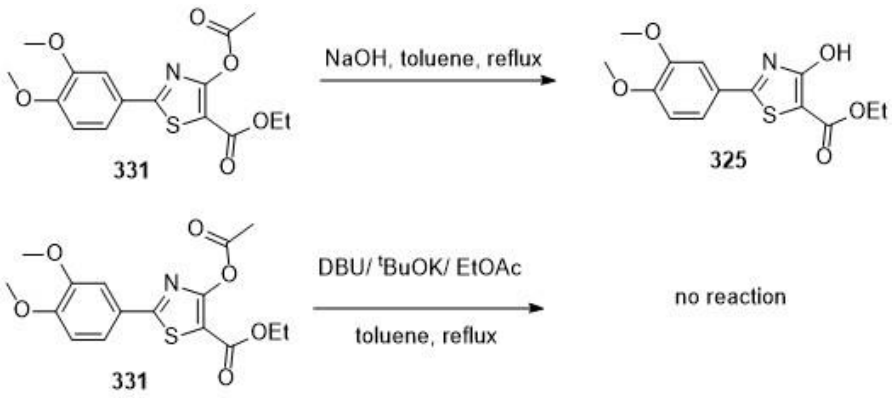

Scheme 104: Unsuccessful basic cyclization of **331**.

An improved structure **335** for cyclization was synthesized (**scheme 105 A**). The malonate **335** could be more easily deprotonated and become a good nucleophile for the cyclisation reaction (**scheme 105 B**). Cyclization reaction of **335** was attempted under anhydrous and basic conditions, but no product was observed.

The cyclization of **331** and **335** would be by *6-exo-trig* cyclisation which follows Baldwin's rules. The stability of thiazole carboxylic ester might be high due to conjugation and may deter the initial nucleophilic attack onto the C=O bond. The attempt synthesis of **151** by the shorter route was unsuccessful and the investigation of **331** and **335** cyclization was stopped at the end of the project. For future research, the attempted synthesis of **151** should be performed based on Bianchini *et al*'s route (**scheme 100**).

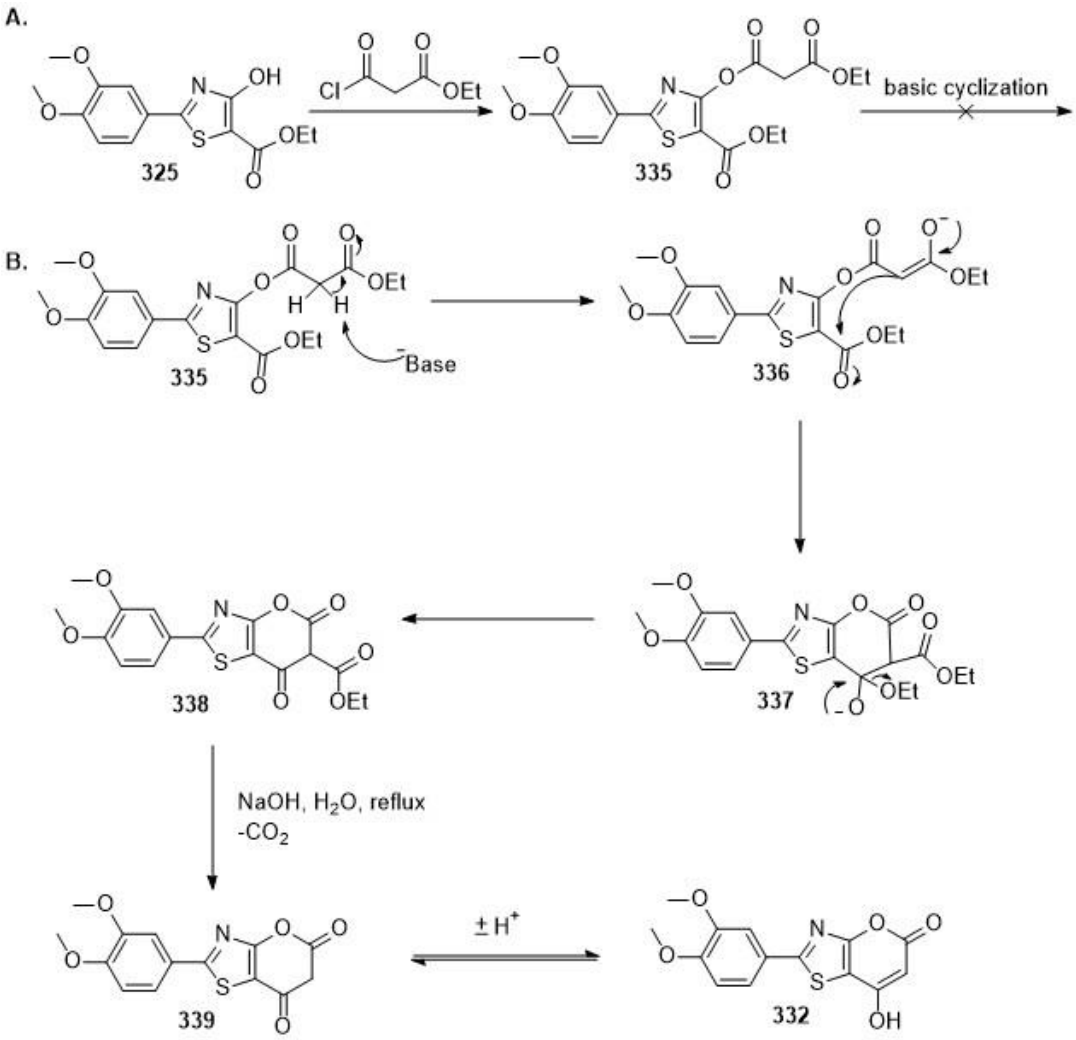

Scheme 105: A. Unsuccessful basic cyclization of **325**. B. Proposed mechanism of **335** cyclization.

7. Conclusion and future work

7.1 Synthesis of *trans* chimeric fungal luciferin

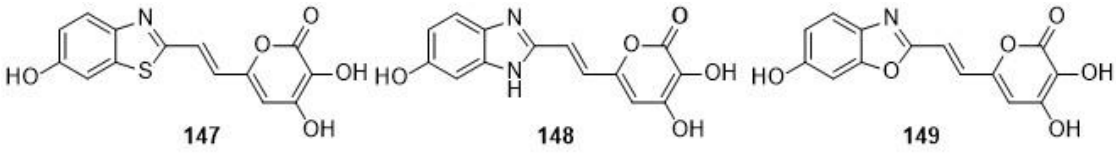

Scheme 106: Synthetic targets **147**, **148** and **149**.

The investigation of trans chimeric fungal luciferin synthesis began with $Mg(OMe)_2$ condensation but the attempt between molecules **188** and **127** was unsuccessful. The same procedure was repeated between molecules **106** and **127** to generate *trans* alkene **147** (**scheme 107**). There might be reactivity difference between **106** and **188** which lead different outcomes of the condensation reactions and a new route was investigated to generate *trans* chimeric fungal luciferins.

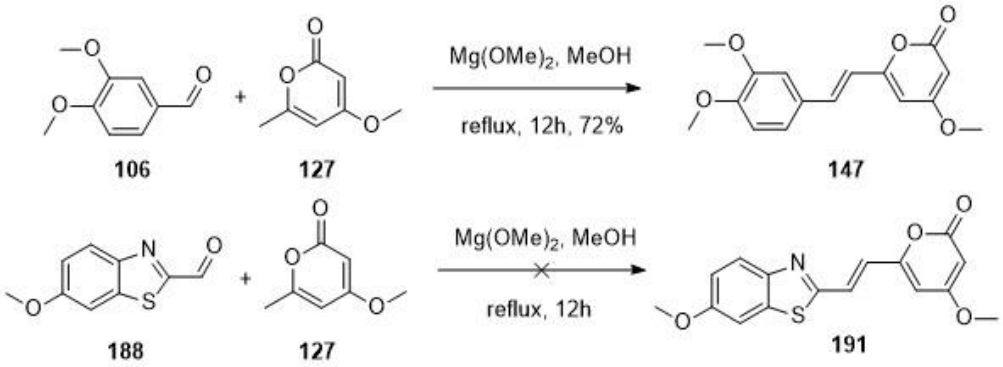

Scheme 107: Successful condensation of **106** and unsuccessful condensation of **188**

The second synthesis was based on the Wittig reagent and the overall route of *trans* chimeric fungal luciferin was constructed in high yield (**scheme 109**). Aldehyde **144** was generated by a novel route based on hypervalent iodine reagent and Riley oxidation. Wittig reaction between **207** and **244** gave **245** in high yield with negligible *cis* product. The only problematic step was deprotection of the last of the three methoxy groups. The literature recorded that methoxy groups could have very high stability towards many reagents and sometimes it is hard to remove multiple methoxy

groups from the same molecule. Reagents including NaH/EtSH, BBr_3 and pyridine-HCl were attempted but only two of three methoxy groups were cleavable. Synthesis towards other trans chimeric fungal luciferin **148** and **149** was also reconstructed due to protecting group selection. Protecting groups such as MEM, TMS, acetyl and TBDMS were tested and the TBDMS group was chosen to be the global protecting group. The synthesis of the TBDMS protected aldehyde **271** was successful. However, the TBDMS protection on the Wittig reagent **273** was cleaved during refluxing with PPh_3 in toluene (**scheme 108 B**). TBDMS protected Wittig reagents are not well documented in the literature and the reason for decomposition remains unclear. Other protecting groups such as OBn could be attempted to give a more stable ylide because they are only cleavable under reductive conditions. Final deprotection of the three hydroxyl groups needs to be accomplished in order to complete the synthesis of *trans* chimeric fungal luciferin **147**. The synthesis of the other *trans* chimeric fungal luciferins **148** and **149** can also be finished with the same protecting group strategy.

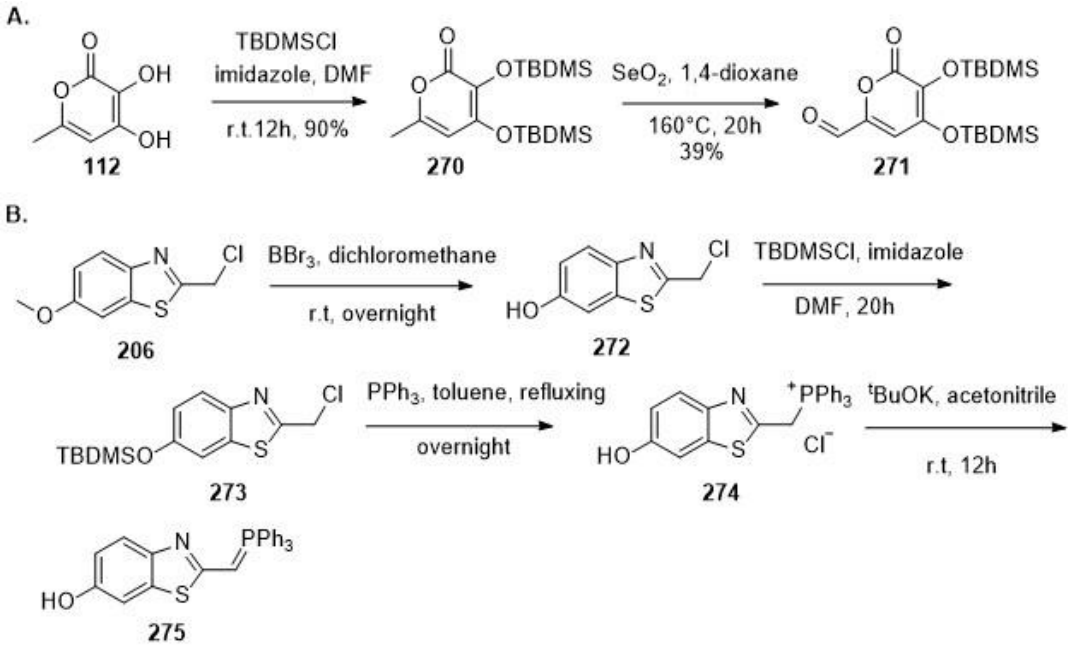

Scheme.108: A. TBDMS protected aldehyde **271** synthesis. B. Decomposition of TBDMS protected Wittig reagent.

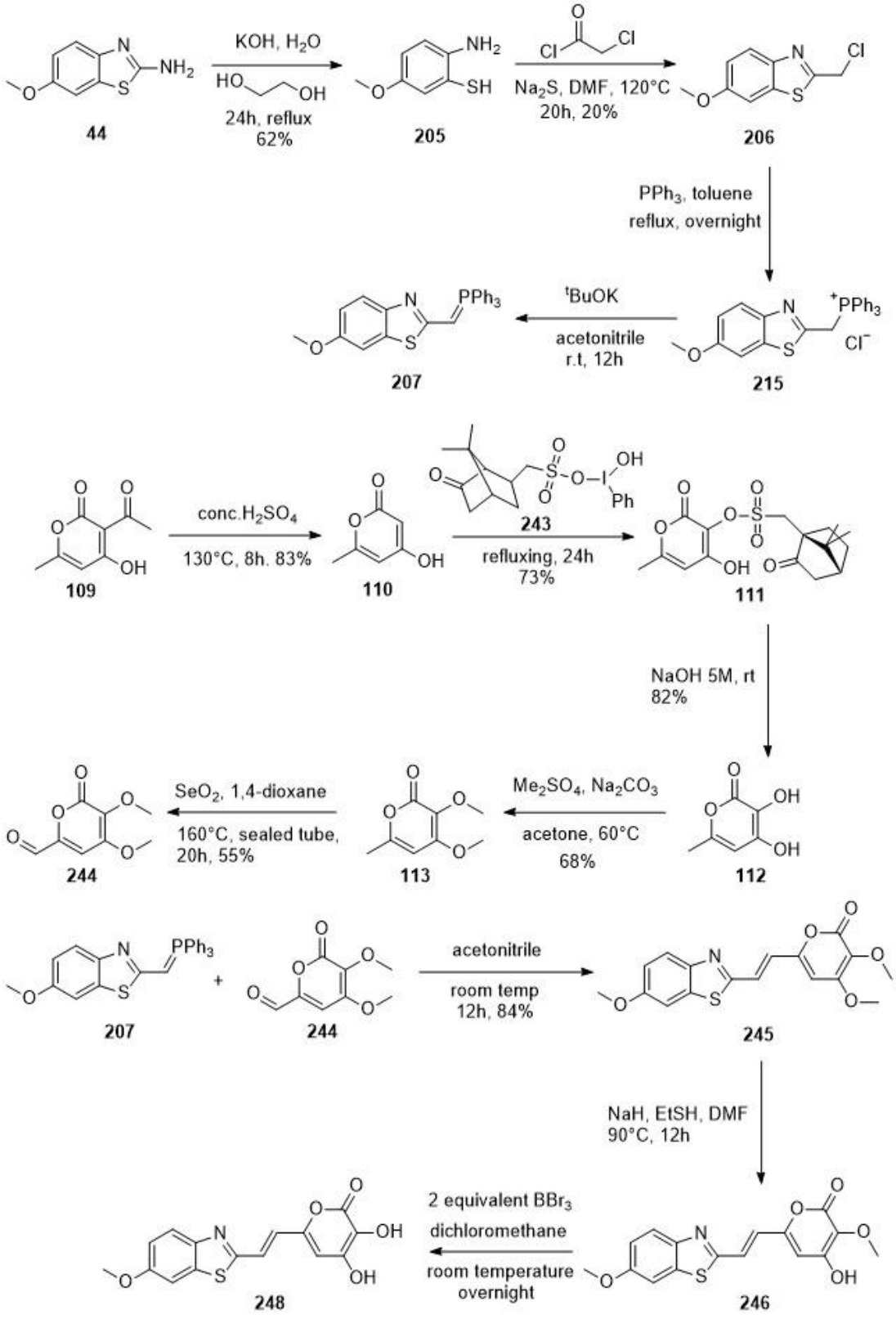

Scheme 109: General route of trans chimeric fungal luciferin **147** synthesis.

7.2 Synthesis of chimeric fungal luciferin 150

The attempted synthesis of chimeric fungal luciferin **150** *via* DDQ oxidation was successful, but the methoxy group deprotection step was again problematic (**scheme 110**). The TBDMS protecting group was surveyed instead, but it was cleaved during DDQ oxidation and yield of the cyclized aromatic product was extremely low. Other protecting groups such as OBn could be tested instead because it is stable towards acidic and oxidative conditions. A general procedure towards chimeric fungal luciferin skeleton of **150** was achieved, but more work needs to be done into protecting group selection.

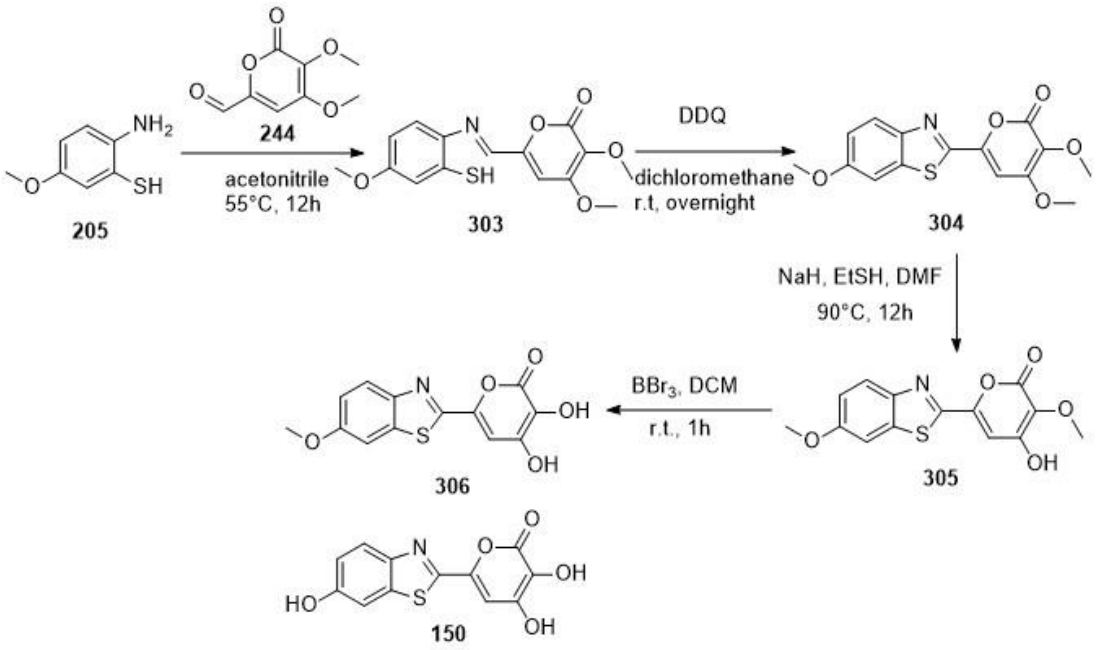

Scheme 110: Synthesis of chimeric fungal luciferin **150**

7.3 Synthesis of chimeric fungal luciferin 151

The synthesis of chimeric fungal luciferin **151** failed at the cyclization step. The route was shortened due to time limitations and was unsuccessful. In future research, the synthesis should follow the longer route reported in the literature (**scheme 111**). [120]

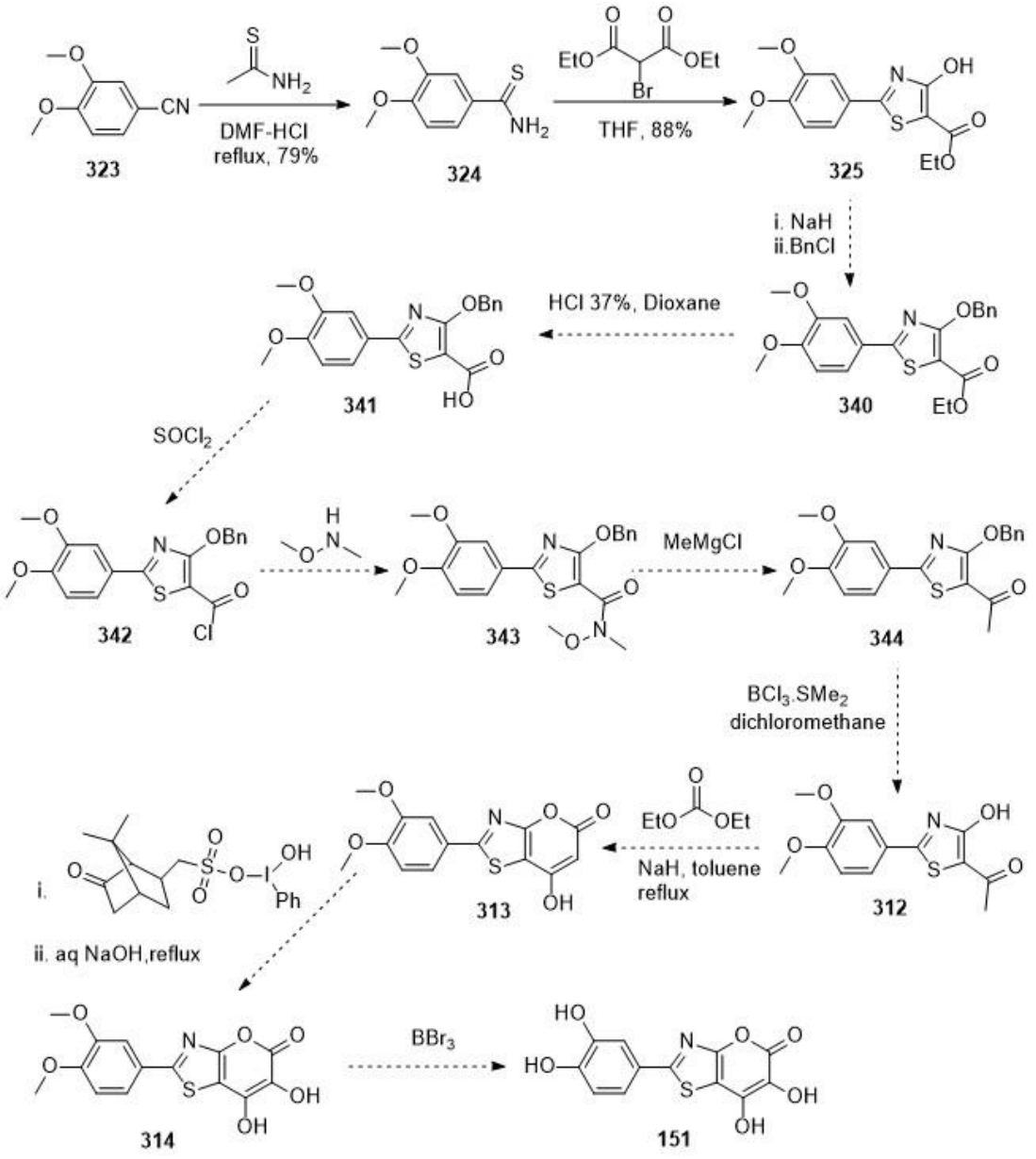

Scheme 111: Future plan of **151** synthesis.

7.4 Synthesis of chimeric fungal luciferin 152

The synthesis of **152** (**scheme 38**) was not attempted due to time limitation. A similar molecule **147**, the fungal luciferin before hydroxylation, was synthesized and the synthesis of pyridinone analogue from molecule **345** was also successful (**scheme 112 A**). For future synthesis, molecule **152** will follow the same route as molecule **147** except the starting material is molecule **346** and **347** with a global protecting group (**scheme 112 B**). The amino-oxygen exchange could be performed at the end of the synthesis.

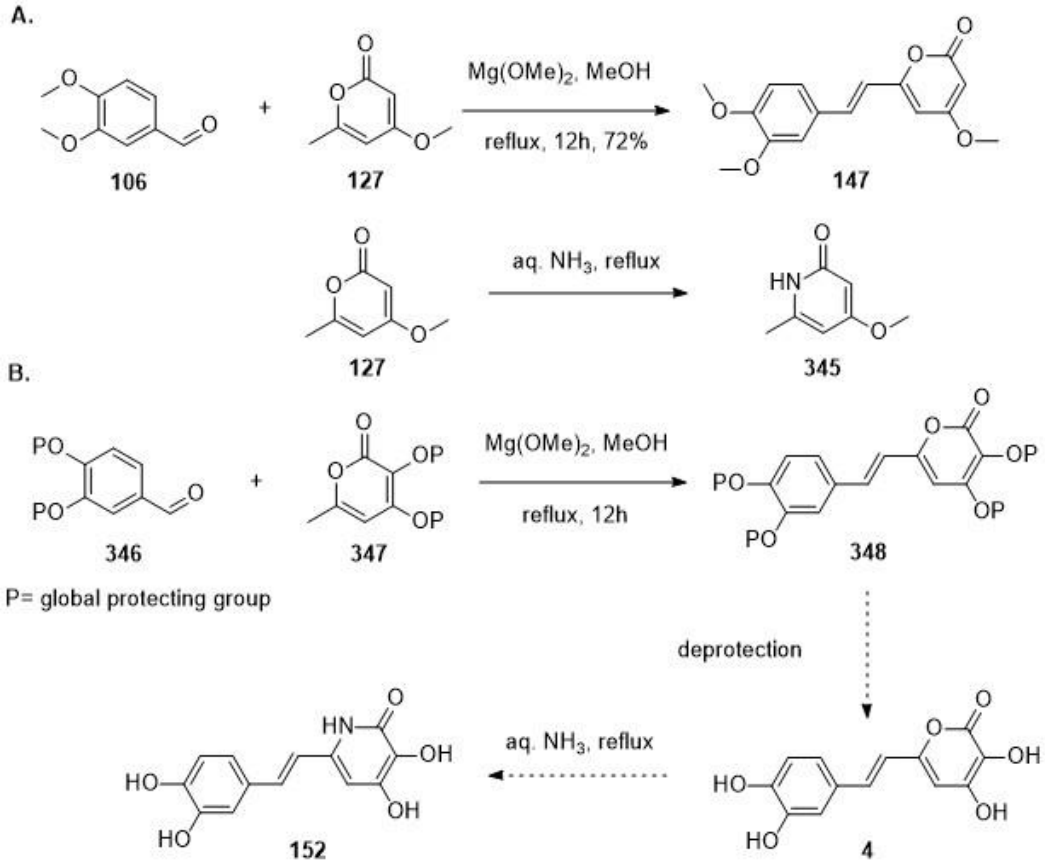

Scheme 112: A.Successful synthesis of **147** and amino-oxygen exchange of **127**.

B.Future synthesis of **152**.

7.5 Conclusion and future research

The project has constructed three novel synthetic procedures to synthesis the skeletons of chimeric fungal luciferins **147**~**152** and most of the synthetic steps were successful and high yielding. The strategy of combining Riley oxidation and Wittig reaction gave a convenient route to synthesize *trans*-linked pyrone structures. The deprotection of all the methoxy groups was unsuccessful under several deprotection conditions. Many efforts were made in finding new protecting groups and the TBDMS group was found to be a good choice. The syntheses were continued with TBDMS protection, but it was found unstable in DDQ cyclization and Wittig reaction. The overall result of protecting groups against reactions are summarized in **table 2**. The benzyl protecting group is not selected as first choice because it has potential to be oxidized during the Riley oxidation step. The *t*-butyl ether is considered to be the second good choice as it has similar stability as OMe group and could be removed with H_3PO_4 under mild conditions.[142] For future research, we aim to find a protecting group which is stable under Riley oxidation and Wittig reaction for **147**~**149**, and that can be removed without affecting the *trans*-alkene. For molecule **150**, a protecting group which resists acidic and oxidative conditions is required for the DDQ cyclisation reaction. There was no problematic reaction in the syntheses of **151** and **152**, but unfortunately the investigation was stopped due to time limitation. The synthesis of these molecules will follow the same procedure as detailed in the future work section.

Protecting groups/Reactions	Protection	Riley oxidation	DDQ cyclization	Wittig Reaction	Deprotection
OMe	Successful	Successful	Successful	Successful	Unsuccessful
OTMS	Unsuccessful	N	N	N	N
OTBDMS	Successful	Successful	Unsuccessful	Unsuccessful	N
OAc	Successful	Low yield	N	N	N
OMEM	Unsuccessful	N	N	N	N
OBn	N	Potential to be oxidized	N	N	N
O^{t}Bu	N	N	N	N	N

Table 2: Protecting group against reactions during synthesis of **147~152**. **N** means "not tried"

8. Experimental procedure:

All The experiments were performed in glassware cleaned by acetone and dried in the oven. All reaction temperatures recorded were oil bath/sand bath temperature. Room temperature means a temperature range between 19-24°C. 0°C was achieved by ice-water bath and -78°C was achieved by mixing dry ice and acetone. Nitrogen atmosphere was achieved by removing air in a flask by vacuum with needle and charging with a nitrogen balloon three times. Hydrogen reactions were performed with a balloon charged with hydrogen. The sealed tube used was Ace pressure tube (bushing type, Back seal, capacity 100 mL, L × O.D. 17.8 cm × 38.1 mm) bought from Sigmaaldrich. The microwave used was Anton Paar, Monowave 400 reactor. The chemical shift for 1H NMR was recorded in parts per million (ppm) relative to residual $CHCl_3$, and the coupling constant was calculated in Hertz (Hz). 13C NMR was recorded as proton decoupled spectra at 100MHz with 3200 scans on 400MHz spectrometer. Infrared spectra (IR) were recorded by Perkin Elmer spectrum 100 Ft-IR (ATR mode). Accurate mass measurements were performed using ASAP-HESI ionisation connected to a Q Exactive Plus mass spectrometer. Melting points were recorded by DigitMelt MPA 161 SRS. Thin layer chromatography (TLC) was performed on Merk aluminium backed DC 60 F254 0.2mm pre-coated plates. The melting point was recorded at the temperature when the solid melted completely. The flash chromatography adsorbent was silica unless stated otherwise. All reagents were used directly as received from the chemical company. Anhydrous solvent (DMF, toluene and THF) were taken from the solvent tower, where degassed solvent was passed through two columns of activated alumina and 7 micron filter under 4 bar pressure with nitrogen protection.

4-hydroxy-6-methyl-2H-pyran-2-one (110)

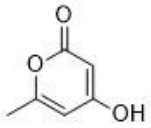

Dehydroacetic acid (8.40g, 50.0 mmol) was dissolved in conc H_2SO_4 (30mL) and heated at 130°C for 8h. After cooling down, the mixture was poured into ice water (150mL) and stirred for 10min. The precipitate was collected by filtration and washed with water (50mL). The solid residue was dried under vacuum to obtain product as a white solid (6.30g, 41.5mmol, 83%).

^{1}H NMR (400MHz, dmso-d_6) δ5.96(1H, s, 5-*H*), δ5.21(1H, s, 3-*H*), δ2.17(3H, s, C*H*$_3$). m.p 165.7°C

Data in agreement with literature values[125]

2,4-dimethylbenzenediazonium tetrafluoroborate (226)

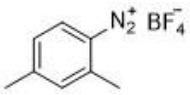

2,4-dimethylaniline (1.97g, 16.5mmol) in isopropanol (2.50mL) was added to a solution of 50% aq HBF_4 (27.4mmol 3.50mL). The mixture was cooled to 0°C and a solution of $NaNO_2$ (1.45g, 21.0 mmol) in water (5mL) was added dropwise. The mixture was stirred for 30min at 0°C. The precipitate was filtered and washed with Et_2O (3 x 30mL). The product was collected as a red solid (3.45g, 15.7mmol, 95%).

^{1}H NMR (400MHz, dmso-d_6) δ8.50 (1H, d, J= 8.5Hz, ArC*H*), δ7.68 (1H, s, ArC*H*), δ7.42 (1H, d, J=8.5Hz, ArC*H*), δ2.68 (3H, s, ArC*H*$_3$), δ2.53 (3H, s, ArC*H*$_3$).

Data in agreement with literature values[126]

4-hydroxy-6-methyl-3-nitro-2H-pyran-2-one (232)

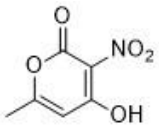

To a cold solution of 4-hydroxy-6-methyl-2H-pyran-2-one (10.0g, 79.3mmol) in H_2SO_4 (25mL) was added a mixture of H_2SO_4 (4.3mL) and HNO_3 (84mL) over 10min. After stirring for 30min, the mixture was poured into ice-water and the precipitate was collected by filtration, washed with cold water (3 x 10mL) and dried to obtain product as a white solid (12.2g, 71.4mmol, 90%)

^{1}H NMR (400MHz, dmso-d_6) δ6.10 (1H, s, C=C-*H*), δ2.21(3H, s, C*H*$_3$)

Data in agreement with literature values[127]

4-methoxy-6-methyl-2H-pyran-2-one (127)

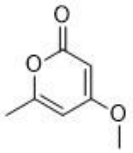

To a stirring mixture of 4-hydroxy-6-methyl-2H-pyran-2-one (1.26g, 10.0mmol) and potassium carbonate (4.14g, 30.0mmol) in acetone (20mL), dimethyl sulfate (3.78g, 2.84mL, 30.0mmol) was added dropwise. The mixture was stirred at room temperature for 12h. After completion of the reaction, sat.aq.$NaHCO_3$ (20mL) was added into the mixture and then extracted with EtOAc (3x20mL). Organic layers were combined and dried over $MgSO_4$, concentrated under vacuum and a flash column (1:1 EtOAc/petroleum ether) was used to obtain product as a pale yellow solid (1.33g, 9.50mmol, 95%).

^{1}H NMR (400MHz, $CDCl_3$) δ5.76(1H, s, 5-*H*), δ5.39(1H, s, 3-*H*), δ3.78(3H, s, OC*H*$_3$), δ2.19(3H, s, C*H*$_3$). m.p 69.3°C

Data in agreement with literature values[128]

iodosylbenzene (126)

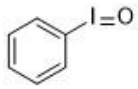

Phenyl-l3-iodanediyl diacetate (3.22g, 10.0mmol) was added slowly into a solution of 3N aq.NaOH (15mL) over 5min period with vigorous stirring. The precipitate was stirred with a rod for 15min. Then the reaction was stand for 45min. Water (10mL) was added and the mixture was stirred vigorously. The crude solid was collected by filtration. The wet solid was triturated in water (2 x 20mL) and chloroform (7.5mL). The product was obtained as a yellow solid (2.18g, 9.90mmol, 99%).

^{1}H NMR (400MHz, MeOD) δ8.04(2H, m, ArC*H*), δ7.57(3H, m, ArC*H*)

Data in agreement with literature values[129]

(4-hydroxy-6-methyl-2-oxo-2H-pyran-3-yl)(phenyl)iodonium (235)

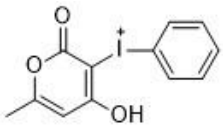

To a solution of iodosylbenzene (2.20g, 10.0mmol) in DMF (25mL) was added $POCl_3$ (2.29, 15.0mmol) and dehydroacetic acid (1.68g, 10.0mmol). The reaction mixture was stirred for 2h and then poured into ice-cold water. The mixture was filtered and washed with chloroform, recrystallized from EtOAc and acetic acid to afford a white crystal (2.88g, 8.80mmol, 88%.)

Data in agreement with literature values: ^{1}H NMR (400MHz, MEOD) δ7.79(2H, m, ArC*H*), δ7.55(1H, m, ArC*H*), δ7.42(2H, m, ArC*H*), δ5.65(1H, s, C=C*H*), δ2.05(3H, s, CH_3)

Data in agreement with literature values[107]

Hydroxy(phenyl)-l3-iodaneyl ((1*S*,4*R*)-7,7-dimethyl-2-oxobicyclo[2.2.1]heptan-1-yl)methanesulfonate (243)

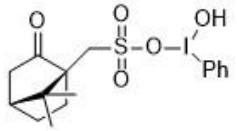

To a stirring mixture of [bis(acetoxy)iodo]benzene (19.3g, 30.0mmol) in acetonitrile (200mL) and water (10mL), (*1S*)-(+)-10-Camphorsulfonic acid (8.12g, 35.0mmol) was added slowly. The mixture was stirred at room temperature for 1h and the solvent was removed under vacuum. The resulting yellow solid was washed with 3:1 EtOAc/ petroleum ether solution (100mL x 2) and dried to obtain product as a white crystal (12.9g, 28.5mmol, 95%).

^{1}H NMR (400MHz, $CDCl_3$) δ8.23 (1H, d, J= 7.6Hz, Ar*H*), δ7.72~7.59 (4H, m, Ar*H*), δ2.92 (1H, d, J= 14.7Hz, O_3SCH_2), δ2.63(2H, t, J= 9.8Hz, O=CCH_2), δ2.49(1H, d, J= 14.7Hz, O_3SCH_2), δ2.23(1H, dt, J= 7.6Hz, 3.72Hz, CH_2CHCH_2), δ 1.95~1.78 (m, 2H, $CHCH_2CH_2$), δ 1.32~1.24 (m, 2H, $CHCH_2CH_2$), δ 1.03 (3H, s, CH_3), δ 0.73 (3H, s, CH_3),

Data in agreement with literature values[70]

3- ((10-Camphorsulfonyl)oxy)-4-hydroxy-6-methyl-α-pyrone (111)

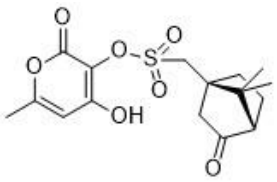

A mixture of 4-hydroxy-6-methyl-2H-pyran-2-one (2.77g, 22.0mmol) and hypervalent iodol reagent (9.00g, 20.0mmol) was dissolved in acetonitrile (150mL) and stirred at refluxing for 24h. After cooling down, the mixture was concentrated and a flash column (1:1 EtOAc/petroleum ether) was used to obtain product as a yellow solid (5.20g, 14.6mmol, 73%)

^{1}H NMR (400MHz, dmso-d_6) δ6.16(1H, s, 5-*H*), δ3.85(1H, d, J=15.0Hz, SO_3CH-*H*), δ3.65(1H, d, J=15.0Hz, SO_3CH-*H*), δ2.49~2.21 (2H, m, O=CCH_2), δ2.19(3H, s,

C*H*$_3$), δ2.08(1H, s, O=C-C*H*), δ1.95(2H, m, CHC*H*$_2$CH$_2$), δ1.56(1H, m,CH$_2$CH-*H*), δ1.45(1H, m,CH$_2$CH-*H*), δ1.03(3H, s,C*H*$_3$), δ0.73(3H, s,C*H*$_3$)

Data in agreement with literature values[70]

3,4-dihydroxy-6-methyl-2H-pyran-2-one (112)

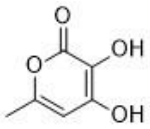

3- ((10-Camphorsulfonyl)oxy)-4-hydroxy-6-methyl-α-pyrone. (6.70g, 18.8mmol) was added into a solution of sodium hydroxide (55.0g, 1.38mol) in water (250mL). The mixture was stirred at 90°C for 1h and 70°C for 12h. After cooling down, the mixture was neutralized to pH~7 by concentrated HCl and acetic acid. Water was removed under vacuum and the solid residue was extracted by EtOAc (3 x 100mL). The organic layers were combined, dried over $MgSO_4$, concentrated under vacuum and a flash column (1:1 EtOAc/petroleum ether ~ pure EtOAc) was used to obtain product as a yellow solid (2.40g, 16.9mmol, 90%).

^{1}H NMR (400MHz, dmso-d$_6$) δ10.55 (1H, brs, O-*H*), δ8.38(1H, brs, O-*H*), δ5.96(1H, s,C-5*H*), δ2.10 (3H, s, C*H*$_3$)

Data in agreement with literature values[50]

3,4-dimethoxy-6-methyl-2H-pyran-2-one (113)

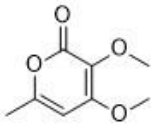

To a stirring mixture of 3,4-dihydroxy-6-methyl-2H-pyran-2-one (1.26g, 10.0mmol) and potassium carbonate (4.14g, 30.0mmol) in acetone (20mL), dimethyl sulfate (6.30g, 4.73mL, 50.0mmol) was added dropwise. The mixture was stirred at room temperature for 12h. After completion of the reaction, sat.aq.$NaHCO_3$ (40mL) was added into the mixture and then extracted with EtOAc (3x20mL). Organic layers were combined and dried over $MgSO_4$, concentrated under vacuum and a flash column (1:1

EtOAc/petroleum ether) was used to obtain product as a pale yellow solid (1.34g, 7.90mmol, 79%).
^{1}H NMR (400MHz, $CDCl_3$) δ5.93(1H, s, 5-*H*), δ3.95(3H, s, OC*H*$_3$), δ3.78(3H, s, OC*H*$_3$), δ2.23(3H, s, C*H*$_3$). Data in agreement with literature values[51]

Ethyl (6-methyl-2-oxo-2H-pyran-4-yl) carbonate (234)

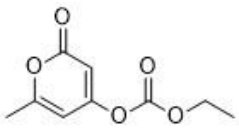

To a mixture of 4-hydroxy-6-methyl-2H-pyran-2-one (0.126g, 1.00mmol) and pyridine (0.053mL) in toluene (10mL) was added ethyl chloroformate (0.730g, 6.70mmol). The mixture was stirred at room temperature for 12h. Water (5mL) was added and the organic layer was separated, washed with aq HCl (5%, 5mL) and aq NaOH (5%, 5mL). The organic layer was dried over $MgSO_4$ and solvent was removed under vacuum. The product was a pale yellow oil (0.212g, 0.990mmol, 99%).
^{1}H NMR (400MHz, $CDCl_3$) δ6.11(1H, s, C-3*H*), δ6.00(1H, s, C-5*H*), δ4.30 (2H, q, J= 7.1Hz, OC*H*$_2$CH$_3$), δ2.23(3H, s, C*H*$_3$), δ1.35(3H, t, J= 7.1Hz, CH$_2$C*H*$_3$). ^{13}C NMR (100MHz, $CDCl_3$) δ163.7 (HC=*C*O), δ163.6 (O*C*=O), 163.1 (CH$_3$*C*O), δ150.7 (O*C*=O), δ100.6 (C=*C*H), δ100.2 (CO_2C=*C*), δ77.5 (O*C*H$_2$CH$_3$), δ20.9 (C=C*C*H$_3$), δ14.7 (CH$_2$*C*H$_3$). IR Vmax (solid) 3089 (alkene C-H), 2986 (alkane C-H), 2938 (alkane C-H), 1731 (C=O), 1643 (C=C), 1573 (C=C). HRMS (m/z+ 1) Expected: 199.06010 Found 199.0594.

Diethyl (6-methyl-2-oxo-2H-pyran-3,4-diyl) bis(carbonate) (266)

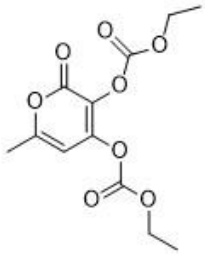

To a mixture of 3,4-dihydroxy-6-methyl-2H-pyran-2-one (0.142g, 1.00mmol) and pyridine (0.1mL) in toluene (20mL) was added ethyl chloroformate (1.46g, 13.4mmol). The mixture was stirred at room temperature for 12h. Water (10mL) was added and the organic layer was separated, washed with aq. HCl (5%, 10mL) and aq NaOH (5%, 10mL). The organic layer was dried over $MgSO_4$ and solvent was removed under vacuum. The product was a pale yellow oil (0.266g, 0.930mmol, 93%).

^{1}H NMR (400MHz, $CDCl_3$) δ6.00(1H, s, C-5*H*), δ4.35 (4H, m, OCH_2CH_3), δ2.28(3H, s, CH_3), δ1.35(6H, m, CH_2CH_3). ^{13}C NMR (125MHz, $CDCl_3$) δ100.9 (C=*C*H), δ100.2 (CO_2C=C), δ66.5 (OCH_2CH_3), δ66.1 (OCH_2CH_3), δ20.0 (C=CCH_3), δ14.2 (CH_2CH_3). IR Vmax (solid) 3095 (alkene C-H), 2986 (alkane C-H), 1735 (C=O), 1665 (C=C), 1593 (C=C). HRMS (m/z+ 1) Expected: 287.07614 Found 287.0758.

3,4-dimethoxy-2-oxo-2H-pyran-6-carbaldehyde (267)

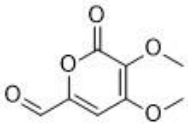

Method A: A mixture of 3,4-dimethoxy-6-methyl-2H-pyran-2-one (0.340g, 2.00mmol) and selenium dioxide (1.19g, 10.0mmol) in 1,4-dioxane (10mL) was heated at 180°C by microwave for 1.5h. After cooling down, the mixture was filtered, quenched with sat. aq. $NaHCO_3$ (25mL) and extracted with dichloromethane (3 x 20mL). The organic layers were combined, dried over $MgSO_4$ and concentrated. A flash column (1:3 EtOAc/petroleum~ 1:1 EtOAc/petroleum) was used to obtain product as an orange solid (0.202g, 1.10mmol, 55%).

Method B: In a sealed tube under nitrogen atmosphere, a mixture of 3,4-dimethoxy-6-methyl-2H-pyran-2-one (0.340g, 2.00mmol) and selenium dioxide (1.19g, 10.0mmol) in 1,4-dioxane (15mL) was heated at 160°C by sand bath for 20h. After cooling down, the mixture was filtered, quenched with sat. aq. $NaHCO_3$ (25mL) and extracted with dichloromethane (3 x 20mL). The organic layers were combined, dried over $MgSO_4$ and concentrated. A flash column (1:3 EtOAc/petroleum~ 1:1 EtOAc/petroleum) was used to obtain product as an orange solid.
Dimethyl sulfate and water caused a significant decrease on yield of final product. Check the NMR of starting material if the product was a dark orange oil.
^{1}H NMR (400MHz, $CDCl_3$) δ9.54(1H, s, O=C-*H*), δ6.98(1H, s, C-5*H*), δ4.14 (3H, s, OCH_3), δ3.85(3H, s, OCH_3). ^{13}C NMR (125MHz, $CDCl_3$) δ182.4 (*C*=O), δ159.2 (O*C*=O), δ149.2 (O*C*=C), δ133.8(C=*C*OMe), δ126.8(C=*C*H), δ105.5(C=*C*OMe), δ60.6 (O*C*H_3), δ58.1 (O*C*H_3), δ20.0 (C=C*C*H_3). IR Vmax (solid) 3085 (alkene C-H), 2942 (alkane C-H), 2843 (alkane C-H), 1685 (C=C), 1641 (C=C). HRMS (m/z+ 1) Expected: 185.04445 Found 185.0443. m.p 110.1°C

4-methoxy-2-oxo-2H-pyran-6-carbaldehyde (197)

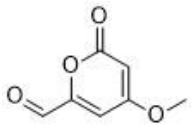

Prepared *via* **Method A** or **Method B** procedure. 4-methoxy-6-methyl-2H-pyran-2-one (0.140g, 1.00mmol), selenium dioxide (0.560g, 5.00mmol) and 1,4-dioxane (8mL). Purified by flash column (1:3 EtOAc/petroleum ether ~ 1:1 EtOAc/petroleum ether) to give product as an orange solid (0.097g, 0.630mmol, 63%).
1H NMR (400MHz, CDCl3) δ9.55 (1H, s, O=C*H*), δ6.70 (1H, s, C5-*H*), δ5.76 (1H, s, C3-*H*), δ3.89 (1H, s, OCH_3). m.p 156.7°C Data in agreement with literature values[124]

4-methoxy-2-oxo-2H-pyran-6-carboxylic acid (349)

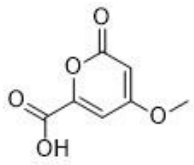

To a mixture of 4-methoxy-2-oxo-2H-pyran-6-carbaldehyde (0.154g, 1.00mmol) in 2-methylpropan-1-ol (25mL) and 2-methylbut-2-ene (10mL), a solution of $NaClO_2$ (1.00g, 11.0mmol) and NaH_2PO_4 (1.00g, 8.30mmol) in water (10mL) was added dropwise. The mixture was stirred at room temperature overnight. The solvent was removed and the residue was washed with Et_2O (2 x 10mL). The organic layer was combined and dried to obtain product as a white solid (0.125g, 0.680mmol, 68%). 1H NMR (400MHz, dmso-d_6) δ6.48 (1H, s, C5-*H*), δ5.62 (1H, s, C3-*H*), δ3.88 (3H, s, OC*H*$_3$). ^{13}C NMR (100MHz, dmso-d_6) δ171.0 (C=*C*OCH$_3$), δ163.9 (O*C*=O), δ160.9 (*C*OOH), δ 158.9 (O*C*CO$_2$H), δ 101.7 (C=*C*H), δ89.8 (CO$_2$=*C*H), δ56.3 (O*C*H$_3$), IR Vmax (solid) 3538 (O-H), 3256 (alkene C-H), 3106-3086 (alkane C-H), 1692 (C=O), 1650 (C=O), 1626 (C=C), 1569 (C=C); HRMS (m/z+ 1) Expected: 171.0289 Found 171.0288

3,4-bis((*tert*-butyldimethylsilyl)oxy)-6-methyl-2H-pyran-2-one (270)

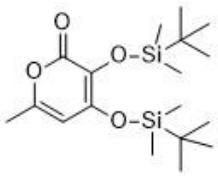

To a stirred mixture of 3,4-dihydroxy-6-methyl-2H-pyran-2-one (1.39g, 9.80mmol) and imidazole (2.16g, 39.2mmol), in DMF (20mL), TBDMSCl (4.00g, 26.5mmol) was added slowly. The mixture was stirred at room temperature for 12h. After completion of the reaction, sat.aq.$NaHCO_3$ (20mL) was added into the mixture and then extracted with Et_2O (3x20mL). Organic layers were combined and dried over $MgSO_4$, concentrated under vacuum and a flash column (1:1 EtOAc/petroleum ether) was used to obtain product as a white solid (3.33g, 9.00mmol, 90%). ^{1}H NMR

(400MHz, $CDCl_3$) δ5.67(1H, s, 5-*H*), δ2.19(3H, s, CH_3), δ0.97 (9H, s, CH_3), δ0.91 (9H, s, CH_3), δ0.29 (6H, s, SiCH_3), δ0.24 (6H, s, SiCH_3). ^{13}C NMR (125MHz, $CDCl_3$) δ163.4 (SiO*C*=C), 154.2 (CH_3*C*=C), 152.3 (O*C*=O), δ127.0 (SiO*C*C=O), δ103.3 (C=*C*HC), δ25.4 (C*C*H_3), δ19.6 (CH_3*C*CH_3), δ18.6 (CH_3*C*CH_3), δ1.2 (Si*C*H_3), - δ3.6(Si*C*H_3), IR Vmax (solid) 2957 (alkane C-H)2957 (alkane C-H), 2926 (alkane C-H), 2855 (alkane C-H), 1687 (alkene C=C), HRMS (m/z+ 1) Expected: 371.2068 Found 371.2060, m.p 120.9°C

3,4-bis((*tert*-butyldimethylsilyl)oxy)-2-oxo-2H-pyran-6-carbaldehyde (271)

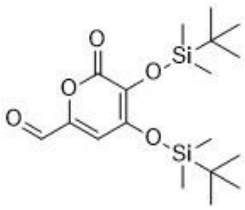

Prepared *via* **Method A** or **Method B** procedure. 3,4-bis((*tert*-butyldimethylsilyl)oxy)-6-methyl-2H-pyran-2-one (0.384g, 1.00mmol), selenium dioxide (0.560g, 5.00mmol) and 1,4-dioxane (8mL). Purified by flash column (1:3 EtOAc/petroleum ether ~ 1:1 EtOAc/petroleum ether) to give product as an orange solid (0.150g, 0.390mmol, 39%).

^{1}H NMR (400MHz, $CDCl_3$) δ9.45 (1H, s, O=C*H*), δ6.74(1H, s, C5-*H*), δ0.99 (9H, s, CH_3), δ0.93 (9H, s, CH_3), δ0.29 (6H, s, SiCH_3), δ0.26 (6H, s, SiCH_3). ^{13}C NMR (125MHz, $CDCl_3$) δ182.0 (O=*C*H), δ160.5 (SiO*C*=C), 149.2 (O*C*=C), 146.7 (O*C*=O), δ134.9 (SiO*C*C=O), δ112.6 (C=*C*HC), δ25.8 (C*C*H_3), δ18.8 (CH_3*C*CH_3), δ-3.5 (Si*C*H_3). IR Vmax (solid) 2926 (alkane C-H), 1647 (alkene C=C), 1571 (cyclic alkene C=C), HRMS (m/z+ 1) Expected: 385.18610 Found 385.1854, m.p 129.5°C

(*E*)-6-(3,4-dimethoxystyryl)-4-methoxy-2H-pyran-2-one (147)

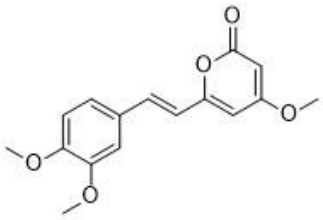

Magnesium metal (0.104g) was added into anhydrous MeOH (10mL) and refluxed for 2h until all solid residue was dissolved. 4-methoxy-6-methyl-2H-pyran-2-one (0.200g, 1.40mmol) and 3,4-dimethoxybenzaldehyde (0.282g, 1.70mmol) were added into the milky mixture and refluxed for 12h. After cooling down, solvent was removed under vacuum and the solid residue was neutralized to pH~7 by acetic acid. The mixture was then dissolved in water (20mL) and extracted by dichloromethane (3 x 15mL). The organic layers were combined, dried over $MgSO_4$ and concentrated under vacuum. A flash column (1:1 EtOAc/petroleum) was used to obtain product as a pale yellow solid (0.291g, 1.01mmol, 72%).

^{1}H NMR (400MHz, $CDCl_3$) δ7.50 (1H, d, J= 15.9 Hz, ArC*H*=CH), δ7.06(1H, dd, J= 8.3, 1.9Hz, Ar*H*), δ7.01 (1H, d, J=1.9Hz, Ar*H*), δ6.87 (1H, d, J= 8.3Hz, Ar*H*), δ6.45 (1H, d, J=15.9 Hz, CH=C*H*-C-O), δ 5.91(1H, s, C-5*H*), δ 5.47(1H, s, C-3*H*), δ 3.91 (3H, s, OCH_3), δ 3.89 (3H, s, OCH_3), δ 3.82 (3H, s, OCH_3).

Data in agreement with literature values[130]

2-(chloromethyl)benzo[d]thiazole (170)

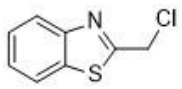

A mixture of 2-aminobenzenethiol (0.125g, 1.00mmol) and 2-chloroacetyl chloride (0.167g, 1.50mmol) in DMF (5mL) was stirred at 50°C for 1h and 120°C for 20h. After cooling down, sat. aq. $NaHCO_3$ (10mL) was added into mixture and extracted with EtOAc (3x 15mL). The organic layers were combined, dried over $MgSO_4$, concentrated under vacuum. A flash column (1:4 EtOAc/ petroleum ether) was used to obtain product as an orange oil (0.156g, 0.850mmol, 85%) which solidify at room temperature.

^{1}H NMR (400MHz, $CDCl_3$): δ8.03 (1H, d, J= 8.9Hz, Ar*H*), δ7.91 (1H, d, J= 8.9Hz, Ar*H*), δ7.53 (1H, m, Ar*H*), δ7.44 (1H, m, Ar*H*), δ4.90 (2H, s, ArCH_2Cl) Data in agreement with literature values[131]

(benzo[d]thiazol-2-ylmethyl)triphenylphosphonium chloride (173)

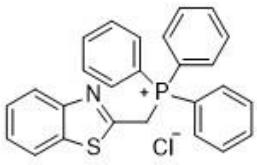

A mixture of 2-(chloromethyl)benzo[d]thiazole (0.213g, 1.00mmol) and triphenylphosphine (0.393g, 1.50mmol) in toluene (10mL) was stirred at refluxing overnight. After cooling down, solvent was removed under vacuum. The solid residue was washed with pure EtOAc (2x 10mL), dried and the product was a solid (0.352g, 0.790mmol, 79%).

1H NMR (400MHz, $CDCl_3$): δ8.07 (1H, d, J= 7.5Hz, Ar*H*), δ7.91~7.73 (16H, m, Ar*H*), δ7.49 (1H, m, Ar*H*), δ6.08 (2H, d, J= 16.0Hz, ArC*H*2PPh3+), δ3.33 (3H, s, OC*H*3) Data in agreement with literature values[132]

2-((triphenyl-l5-phosphaneylidene)methyl)benzo[d]thiazole (176)

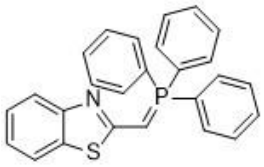

A mixture of (benzo[d]thiazol-2-ylmethyl)triphenylphosphonium chloride (0.445g, 1.00mmol) and ^{t}BuOK (0.168g, 1.50mmol) in acetonitrile was stirred at room temperature for 12h. After completion of reaction, water (10mL) was added into the mixture and extracted with EtOAc (3x 10mL). The organic layers were combined, dried over MgSO4, and solvent was removed under vacuum. The product was obtained as an orange soild (0.389g, 0.950mmol, 95%).

1H NMR (400MHz, $CDCl_3$): δ7.76~ 7.47(16H, m, Ar*H*), δ6.98 (1H, s, Ar*H*), δ6.78 (1H, m, Ar*H*), δ3.58 (1H, d, J= 17.8Hz, ArC*H*=PPh_3) HRMS (m/z+ 1) Expected: 410.11268 Found 410.1125 Data in agreement with literature values[132]

2-amino-5-methoxybenzenethiol (205)

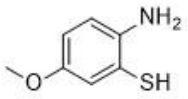

6-methoxybenzo[d]thiazol-2-amine (1.50g, 8.32mmol), ethylene glycol (2.02g, 33.3mmol) and the mixture of 50% w/ v KOH (10mL) was refluxed for 48h. After cooling, scraps were removed by filtration and conc HCl and acetic acid was used to neutralize solution to pH ~7. The orange mixture was extracted with EtOAc (3x 15mL) and organic layers were combined, dried over $MgSO_4$, concentrated under vacuum. A flash column (1:4 EtOAc/ petroleum ether) was used to obtain product as an orange oil (2.99g, 19.3mmol, 58%).

^{1}H NMR (400MHz, $CDCl_3$): δ6.76 (2H, m, Ar*H*), δ6.50 (1H, dd, J= 8.4, 5.9Hz, Ar*H*), δ3.74(3H, s, CH_3). Data in agreement with literature values[133]

2-aminobenzo[d]thiazol-6-ol (354)

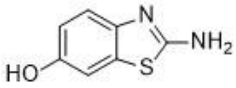

6-methoxybenzo[d]thiazol-2-amine (18.0g, 100mmol) was suspended in 40% HBr (140mL) and the mixture was stirred at 120°C for 4h. The system was cooled to 0°C and the pH of filtered cake was adjusted to 8~9 with sat.aq.$NaHCO_3$ solution. The residue was filtered and dried by vacuum at 40°C for 8h to obtain white solid as product (14.8g, 89.0mmol, 89%).

^{1}H NMR (400MHz, dmso-d_6): δ9.12 (2H, m, O*H*&NH), δ7.34 (1H, s, N*H*), δ7.12(2H, m, ArC*H*), δ6.64 (1H, s, ArC*H*). Data in agreement with literature values[134]

4-amino-3-mercaptophenol (350)

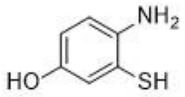

To a solution of 2-amino-5-methoxybenzenethiol (0.318g, 2.00mmol) in dichloromethane at -78°C was added BBr_3 (7mL, 1M in CH_2Cl_2, 7mmol) dropwise. The mixture was stirred for 30min and raised to room temperature. Methanol (10mL) was added dropwise to quench the mixture. The mixture was concentrated and the precipitated solid was dissolved in 1:1 EtOAc/MeOH. A flash column was used to obtain product as a black solid (0.127g, 1.5mmol, 75%).
^{1}H NMR (400MHz, $CDCl_3$) δ8.75 (1H, s, S*H*), δ6.47(2H, m, ArC*H*), δ6.27 (1H, d, J= 8.2Hz, ArC*H*), δ5.65 (1H, s, N*H*), ^{13}C NMR (100MHz, $CDCl_3$) δ151.6 (Ar*C*), δ139.5 (Ar*C*), 130.7 (Ar*C*), 112.8 (Ar*C*), δ111.0 (Ar*C*), δ109.0 (Ar*C*) HRMS (m/z+ 1) Expected: 142.03211 Found 142.0322
^{1}H NMR different, but ^{13}C NMR and MS agreed with literature values[135]

2-(chloromethyl)-6-methoxybenzo[d]thiazole (206)

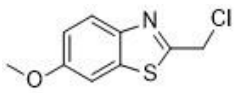

A mixture of 2-amino-5-methoxybenzenethiol (0.155g, 1.00mmol), 2-chloroacetyl chloride (0.167g, 1.50mmol), Na_2S (0.0780g, 1.00mmol) in DMF (5mL) was stirred at 50°C for 1h and 120°C for 20h. After cooling down, sat. aq. $NaHCO_3$ (10mL) was added into mixture and extracted with EtOAc (3x 15mL). The organic layers were combined, dried over $MgSO_4$, concentrated under vacuum. A flash column (1:4 EtOAc/ petroleum ether) was used to obtain product as an orange oil which solidify at room temperature (0.126g, 0.590mmol, 59%).
^{1}H NMR (400MHz, $CDCl_3$): δ7.89 (1H, d, J= 8.9Hz, Ar*H*), δ7.32 (1H, s, Ar*H*), δ7.10 (1H, d, J= 9.0Hz, Ar*H*), δ4.90 (2H, s, ArCH_2Cl), δ3.91 (1H, s, OCH_3) Data in agreement with literature values[136]

((6-methoxybenzo[d]thiazol-2-yl)methyl)triphenylphosphonium chloride (215)

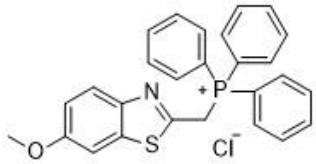

A mixture of 2-(chloromethyl)-6-methoxybenzo[d]thiazole (0.213g, 1.00mmol) and triphenylphosphine (0.393g, 1.50mmol) in toluene (10mL) was stirred at refluxing overnight. After cooling down, solvent was removed under vacuum. The solid residue was washed with pure EtOAc (2x 10mL), dried and the product was a pale brown solid. The product was used without further purification.

^{1}H NMR (400MHz, dmso-d_6): δ7.92~7.63 (18H, m, Ar*H*), δ6.02 (2H, d, J= 21.0Hz, ArC*H*$_2$PPh$_3^+$), δ3.80 (3H, s, OC*H*$_3$), ^{13}C NMR (125MHz, dmso-d_6) δ157.7 (N=*C*-S), δ155.9 (Ar*C*), δ146.4 (Ar*C*), δ136.7 (Ar*C*), δ134.9 (Ar*C*), δ133.3 (Ar*C*), δ130.2 (Ar*C*), δ123.1 (Ar*C*), δ119.6 (Ar*C*), δ118.6 (Ar*C*), δ117.9 (Ar*C*), δ116.1 (Ar*C*), δ114.7 (Ar*C*), δ55.8 (O*C*H$_3$), δ27.1 (*C*-PPh$_3$), IR Vmax (solid) 3055 (alkene C-H), 2832 (alkane C-H), 1601 (aromatic C=C), ^{31}P NMR (400MHz, dmso-d_6) δ25.8 (C-*P*Ph$_3^+$), HRMS (m/z+ 1) Expected: 453.0230 Found 453.02271, m.p 110.8°C

6-methoxy-2-((triphenyl-l5-phosphaneylidene)methyl)benzo[d]thiazole (207)

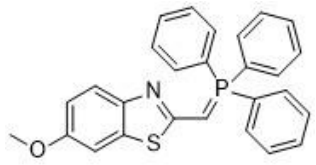

A mixture of ((6-methoxybenzo[d]thiazol-2-yl)methyl)triphenylphosphonium chloride (0.475g, 1.00mmol) and ^{t}BuOK (0.168g, 1.50mmol) in acetonitrile was stirred at room temperature for 12h. After completion of reaction, water (10mL) was added into the mixture and extracted with EtOAc (3x 10mL). The organic layers were combined, dried over $MgSO_4$, and solvent was removed under vacuum. The product was obtained as a pale yellow soild (0.349g, 0.800mmol, 53%).

^{1}H NMR (400MHz, dmso-d_6): δ7.75~ 7.56(16H, m, Ar*H*), δ7.14~ 6.62 (2H, m, Ar*H*), δ3.68 (3H, s, OC*H*$_3$). ^{31}P NMR (400MHz, CDCl$_3$): δ11.53 (1H, s, C=*P*Ph$_3$), ^{13}C NMR

(125MHz, dmso-d_6) δ164.1 (N=*C*-S), δ156.9 (Ar*C*), δ147.4 (Ar*C*), δ136.6 (Ar*C*), δ133.2 (Ar*C*), δ132.1 (Ar*C*), δ131.6 (Ar*C*), δ130.3 (Ar*C*), δ128.8 (Ar*C*), δ122.4 (Ar*C*), δ115.0 (Ar*C*), δ104.8 (Ar*C*), δ55.7 (O*C*H_3), δ19.6 (*C*=PPh_3), IR Vmax (solid) 3055 (alkene C-H), 2933 (alkane C-H), 1599 (aromatic C=C), 1558 (aromatic C=C), ^{31}P NMR (400MHz, dmso-d_6) δ11.5 (C=*P*Ph_3), HRMS (m/z+ 1) Expected: 440.1228 Found 440.12325, m.p 87.5°C

2-amino-5-((*tert*-butyldimethylsilyl)oxy)benzenethiol (351)

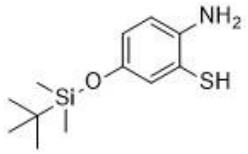

To a mixture of 4-amino-3-mercaptophenol (0.141g, 1.00mmol) and imidazole (0.0680g, 1.00mmol) in DMF (5mL) was added TBDMSCl (0.102g, 1.00mmol) at room temperature. The mixture was stirred for 24h and extracted with Et_2O (3 x 20mL). The organic layers were combined, dried over $MgSO_4$ and filtered. After volatile materials were removed in vacuum, the product was used without purification.

^{1}H NMR (400MHz, $CDCl_3$): δ7.42 (1H, d, J=10.0Hz, Ar*H*), δ6.62 (1H, d, J=10.0Hz, Ar*H*), δ6.50 (1H, s, Ar*H*), δ1.83 (6H, s, 2x SiCH_3), δ 1.56 (9H, s, CCH_3)

4-((*tert*-butyldimethylsilyl)oxy)-2-nitroaniline (277)

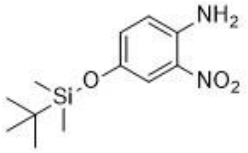

To a mixture of 4-amino-3-nitrophenol (0.154g, 1.00mmol) and imidazole (0.0680g, 1.00mmol) in DMF (5mL) was added TBDMSCl (0.102g, 1.00mmol) at room temperature. The mixture was stirred for 24h and extracted with Et_2O (3 x 20mL). The organic layers were combined, dried over $MgSO_4$ and filtered. After volatile materials were removed in vacuum, the product was used without purification.

^{1}H NMR (400MHz, $CDCl_3$): δ7.33 (1H, s, Ar*H*), δ7.22 (2H, s, NH_2), δ7.06 (1H, d, J= 9.1Hz, Ar*H*), δ6.94 (1H, d, J= 9.1Hz, Ar*H*), δ0.93 (9H, s, CCH_3), δ0.16 (6H, s, 2x SiCH_3)

Data in agreement with literature values[32]

4-((*tert*-butyldimethylsilyl)oxy)benzene-1,2-diamine (278)

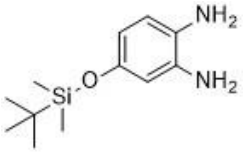

To a solution of 4-((*tert*-butyldimethylsilyl)oxy)-2-nitroaniline (1.75g, 6.52mmol) in MeOH (15mL) was added 10% Pd-C (0.550g) as a slurry in MeOH (5mL) at room temperature. The solution was degassed with N_2, charged with H_2 for 3 times. The mixture was stirred under H_2 atmosphere by balloon for 7h. The mixture was filtered and the filtrate was concentrated in vacuum to obtain product as a purple oil. The mixture oxidized immediately in air and was used without purification for next step.

2-(chloromethyl)-1H-benzo[d]imidazol-6-ol (279)

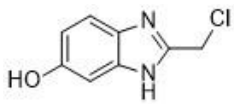

A mixture of 4-((*tert*-butyldimethylsilyl)oxy)benzene-1,2-diamine (0.238g, 1.00mmol) and 2-chloroacetyl chloride (0.167g, 1.50mmol) in DMF (5mL) was stirred at 50°C for 1h and 120°C for 20h. After cooling down, sat. aq. NaHCO3 (10mL) was added into mixture and extracted with EtOAc (3x 15mL). The organic layers were combined, dried over MgSO4, concentrated under vacuum. A flash column (1:4 EtOAc/ petroleum ether) was used to obtain product as a yellow solid (0.149g, 0.820mmol, 82%).

^{1}H NMR (400MHz, dmso-d_6): δ10.37(1H, s, O*H*), δ7.50 (1H, d, J= 8.8Hz, Ar*H*), δ7.33 (1H, s, Ar*H*), δ7.13 (1H, d, J= 8.7Hz, Ar*H*), δ4.29 (2H, s, CH_2Cl). ^{13}C NMR (125MHz, dmso-d_6) δ165.1 (N=*C*-NH), δ155.1 (Ar*C*), δ143.3 (Ar*C*), δ127.6 (Ar*C*), δ122.0 (Ar*C*), δ121.3 (Ar*C*), δ110.7 (Ar*C*), δ42.9 (*C*H_2Cl), δ19.6 (*C*=PPh_3), IR Vmax (solid) 3265 (N-H), 3006 (alkene C-H), 2955 (alkane C-H), 1648 (C=C), 1593 (aromatic C=C), HRMS (m/z+ 1) Expected: 183.03197 Found: 183.03197, m.p 191.4°C

2-(chloromethyl)-6-methoxy-1H-benzo[d]imidazole (351)

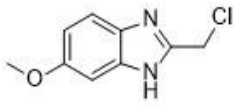

To a mixture of 2-(chloromethyl)-1H-benzo[d]imidazol-6-ol (0.183g, 1.00mmol) in acetonitrile (10mL), K_2CO_3 (0.165g, 0.176mmol) and dimethyl sulfate (0.237mL, 2.96mmol) were added under stirring. The mixture was stirred at room temperature overnight. After completion of the reaction, sat.aq.$NaHCO_3$ (40mL) was added into the mixture and then extracted with EtOAc (3x20mL). Organic layers were combined and dried over $MgSO_4$, concentrated under vacuum and a flash column (1:1 EtOAc/petroleum ether) was used to obtain product (0.169g, 0.740mmol, 74%,).
^{1}H NMR (400MHz, $CDCl_3$): δ8.65 (1H, d, J= 9.3Hz, Ar*H*), δ7.71 (1H, s, Ar*H*), δ7.24 (1H, m, Ar*H*), δ4.23 (2H, s, CH_2Cl), δ3.88 (3H, s, OCH_3). Data in agreement with literature values[32]

2-(chloromethyl)-6-nitrobenzo[d]thiazole (352)

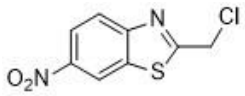

To a solution of 2-amino-5-nitrobenzenethiol (0.170g, 1.00mmol) in toluene (10mL), 2-chloroacetyl chloride (0.123g, 1.10mmol) was added dropwise at room temperature. The mixture was stirred for 48h. After completion of reaction, the mixture was concentrated directly and the residue was dissolved in hot acetone. A column (EtOAc/petroleum ether 1:1) was used to obtain product as a yellow solid (0.207g, 0.910mmol, 91%).
^{1}H NMR (400MHz, $CDCl_3$): δ8.79 (1H, s, Ar*H*), δ8.37 (1H, d, J= 8.9Hz, Ar*H*), δ7.84 (1H, d, J= 8.9Hz, Ar*H*), δ4.36 (2H, s, ArCH_2Cl), ^{13}C NMR (100MHz, dmso-d_6) δ172.3 (Ar*C*), δ165.9 (Ar*C*), δ163.4 (Ar*C*), δ122.7 (Ar*C*), δ120.5 (Ar*C*), δ118.5 (Ar*C*), δ42.0 (*C*H_2Cl). Data was different from literature values[137]

2-((triphenyl-l5-phosphaneylidene)methyl)benzo[d]thiazol-6-ol (275)

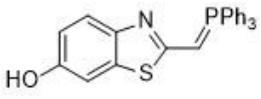

A mixture of 6-((*tert*-butyldimethylsilyl)oxy)-2-(chloromethyl)benzo[d]thiazole (0.313g, 1.00mmol) and triphenylphosphine (0.393g, 1.50mmol) in toluene (10mL) was stirred at refluxing overnight. After cooling, the mixture was evaporated on vacuum. The residue was dissolved in acetonitrile and ^{t}BuOK (0.168g, 1.50mmol) was added. The mixture was stirred at room temperature for 12h. After completion of reaction, water (10mL) was added into the mixture and extracted with EtOAc (3x 10mL). The organic layers were combined, dried over $MgSO_4$, and solvent was removed under vacuum. The crude solid was columned but isolation of pure product was unsuccessful.

HRMS (m/z+ 1) Expected: 426.10760 Found: 426.1074

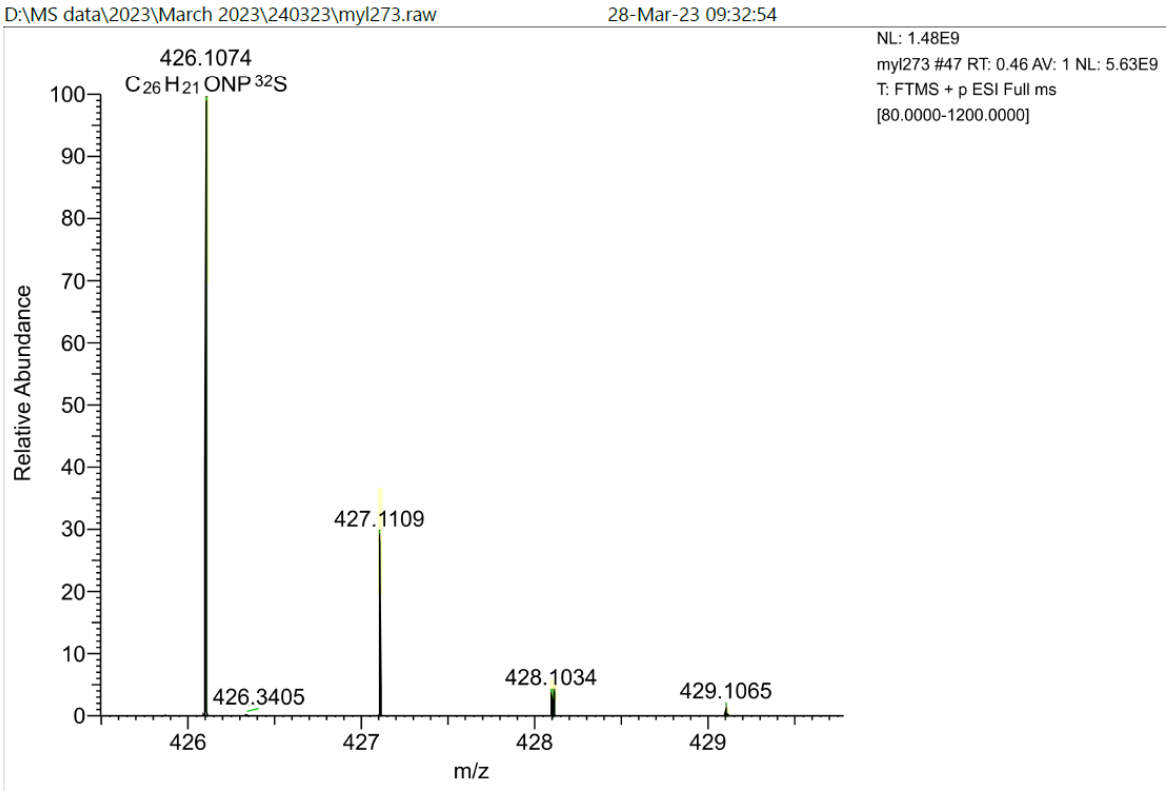

(*E*)-3,4-dimethoxy-6-(2-(6-methoxybenzo[d]thiazol-2-yl)vinyl)-2H-pyran-2-one (246)

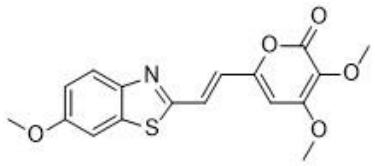

To a mixture of 3,4-dimethoxy-2-oxo-2H-pyran-6-carbaldehyde (0.184g, 1.00mmol) in toluene (10mL) was added 6-methoxy-2-((triphenyl-l5-phosphaneylidene)methyl)benzo[d]thiazole (0.439g, 1.00mmol) at room temperature. The mixture was stirred for 4h and water (15mL) was added into the reaction mixture. The mixture was extracted with dichloromethane (3x 15mL), the organic layers were combined, dried over $MgSO_4$, concentrated under vacuum. A flash column (1:1 EtOAc/ petroleum ether) was used to obtain product as a pale yellow solid (0.290g, 0.84mmol, 84%).

^{1}H NMR (400MHz, dmso-d_6): δ7.90 (1H, d, J= 8.9Hz, Ar*H*), δ7.70 (1H, s, Ar*H*), δ7.40 (1H, d, J= 15.8Hz, Ar*H*C=C), δ7.30 (1H, d, J= 15.8Hz, C=C*H*CO), δ6.38 (1H, s, C-5*H*) δ3.95 (3H, s, OCH_3), δ3.85 (3H, s, OCH_3), δ3.71 (3H, s, OCH_3). ^{13}C NMR (125MHz, dmso-d_6) δ161.8 (N=*C*-S), δ160.9 (O*C*=C), δ160.0 (O*C*=O), δ152.2 (aromatic *C*), δ148.0 (aromatic *C*), δ137.7 (aromatic *C*), δ136.4 (aromatic *C*), δ128.5 (ArH*C*=C), δ126.1 (ArC=*C*H), δ125.9 (C=*C*OCH$_3$), δ123.8 (aromatic *C*), δ116.8 (C=*C*OCH$_3$), δ104.8 (aromatic *C*), δ101.9 (C=*CH*), δ59.6 (O*C*H$_3$), δ57.4 (O*C*H$_3$), δ55.8 (O*C*H$_3$), IR Vmax (solid) 3084 (alkene C-H), 3002 (alkene C-H), 2962 (alkane C-H), 1688 (C=C), 1651 (C=C), 1564 (aromatic C=C), HRMS (m/z+ 1) Expected: 346.0734 Found: 346.07437, m.p 105.5°C

(*E*)-6-(((2-mercaptophenyl)imino)methyl)-3,4-dimethoxy-2H-pyran-2-one (284)

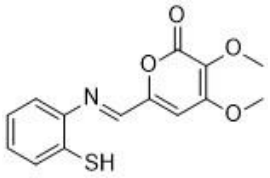

To a mixture of 3,4-dimethoxy-2-oxo-2H-pyran-6-carbaldehyde (0.184g, 1.00mmol) in acetonitrile (10mL), 2-aminobenzenethiol (0.125g, 1.00mmol) was added dropwise. The mixture was heated at 55°C for 12h. After cooling, the mixture was concentrated under vacuum and a direct column (1:1 EtOAc/petroleum ether) was used to obtain product as solid. The product was used without further purification. ^{1}H NMR (400MHz, dmso-d_6): δ7.04 (2H, m, J= 8.9Hz, Ar*H*), δ6.91 (1H, t, J= 8.0Hz , Ar*H*), δ6.70 (1H, d, J= 8Hz, Ar*H*), δ6.56 (1H, s, C=C*H*CO), δ3.89 (1H, s, OCH_3), δ3.63 (1H, s, OCH_3). ^{13}C NMR (100MHz, dmso-d_6) δ158.8 (ArN=*C*H), δ158.6 (O*C*=O), δ146.9 (Ar*C*-N), δ125.7 (Ar*C*H), δ124.2 (Ar*C*H), δ121.4 (C=*C*-OMe), δ119.4 (Ar*C*H), δ110.4 (Ar*C*H), δ109.6 (C=*C*-OMe), δ95.0 (C=*C*H), δ59.4 (O*C*H_3), δ57.4 (O*C*H_3), IR Vmax (solid) 3349 (S-H), 3063 (alkene C-H), 2935 (alkane C-H), 1724 (C=O), 1641 (C=C), HRMS (m/z+ 1) Expected: 292.0638 Found 292.0638, m.p 107.5°C

6-(benzo[d]thiazol-2-yl)-3,4-dimethoxy-2H-pyran-2-one (298)

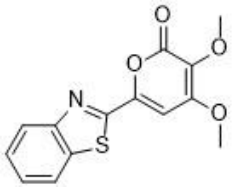

To a mixture of (*E*)-6-(((2-mercaptophenyl)imino)methyl)-3,4-dimethoxy-2H-pyran-2-one (0.291g, 1.00mmol) in dichloromethane (10mL), DDQ (0.227g, 1.00mmol) was added with stirring. The mixture was stirred at room temperature overnight. After completion of reaction, sat.aq.$NaHCO_3$ (10mL) was added into the mixture and extracted with EtOAc (3 x 10mL). The organic layers were combined, dried over $MgSO_4$, concentrated under vacuum and a column was used to obtain product as an orange solid (0.173g, 0.600mmol, 60%).

^{1}H NMR (400MHz, $CDCl_3$): δ8.08 (1H, d, J= 8.1Hz, Ar*H*), δ7.99 (1H, d, J= 8.0Hz, Ar*H*), δ7.58 (1H, t, J= 7.7Hz, Ar*H*), δ7.49 (1H, t, J=7.8Hz , Ar*H*), δ7.39 (1H, s, C=C*H*C), δ4.13 (1H, s, OCH_3), δ3.95 (1H, s, OCH_3). ^{13}C NMR (100MHz, $CDCl_3$) δ159.9 (N=*C*S), δ159.1 (O=*C*-O), δ153.6 (Ar*C*-N), δ149.9 (C=*C*-O), δ136.1 (Ar*C*-S), δ130.6 (C=*C*-OMe), δ127.2 (Ar*C*H), δ126.4 (Ar*C*H), δ123.9 (Ar*C*H), δ122.3 (C=*C*OMe), δ97.2 (C=*C*H), δ60.5 (O*C*H_3), δ57.8 (O*C*H_3). IR Vmax (solid) 3054 (alkene C-H), 2946 (alkane C-H), 1712 (C=O), 1632 (C=C), HRMS (m/z+ 1) Expected: 290.04816 Found 290.0480, m.p 105.3°C

6-(benzo[d]thiazol-2-yl)-3-hydroxy-4-methoxy-2H-pyran-2-one (301)

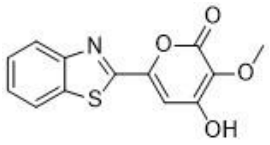

To a mixture of 60% NaH protected with oil (0.0770g, 2.00mmol) in DMF (5mL), EtSH (0.186g, 0.220mL, 3.00mmol) was added dropwise and stirred for 10min. After all the solid was dissolved, 6-(benzo[d]thiazol-2-yl)-3-hydroxy-4-methoxy-2H-pyran-2-one (0.275g, 1.00mmol) was added and the mixture was stirred at 90°C for 12h. After completion of reaction, the mixture was heated at 115°C and dried under wind. Acetic acid was added into solid residue to neutralize pH~7. The solid residue was washed with chloroform and filtrates were combined, dried over $MgSO_4$. The solvent was removed under vacuum and the solid was recrystallized in diethyl ether to obtain product as a dark brown solid. Isolation of pure product was unsuccessful.
^{1}H NMR (400MHz, dmso-d_6): δ8.21 (1H, d, J= 8.0Hz, Ar*H*), δ8.19 (1H, d, J= 8.2Hz, Ar*H*), δ7.62 (1H, m, Ar*H*), δ7.51 (2H, m, Ar*H*&C-5*H*), δ4.02 (3H, s, OCH_3), ^{13}C NMR (125MHz, dmso-d_6) δ149.8 (Ar*C*-N), δ144.5 (Ar*C*H), δ126.2 (Ar*C*H), δ123.2 (C=*C*-OMe), δ122.8 (Ar*C*H), δ110.4 (Ar*C*H), δ99.1 (C=*C*-OH), δ95.0 (C=*C*H), δ57.2 (O*C*H_3) IR Vmax (solid) 3092 (alkene C-H), 3010 (alkene C-H), 1705 (C=O), 1649 (C=C), HRMS (m/z+ 1) Expected: 276.03251 Found: 279.0929

6-(benzo[d]thiazol-2-yl)-3,4-dihydroxy-2H-pyran-2-one (302)

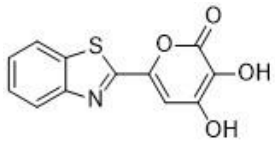

To a mixture of 6-(benzo[d]thiazol-2-yl)-3,4-dimethoxy-2H-pyran-2-one (0.289g, 1.00mmol) in dichloromethane (5mL), 1M BBr_3 (1.10mL, 1.10mmol) was added dropwise. The mixture was stirred at room tmerpature for 1h. After completion of reaction, water (10mL) was added into reaction mixture and the aqueous layer was extracted by chloroform (1x 10mL). The organic layers were combined, dried over $MgSO_4$, and the solvent was removed under vacuum. A column (pure EtOAc~ 1:3 MeOH/EtOAc) was used to obtain product as a brown solid (0.235g, 0.900mmol, 90%).

1H NMR (400MHz, dmso-d_6): δ8.27 (1H, m, Ar*H*), δ7.67 (2H, m, Ar*H*), δ7.21 (1H, s, C=C-*H*),^{13}C NMR (125MHz, dmso-d_6) δ159.3 (N=*C*S), δ159.1 (O=*C*-O), δ153.2 (Ar*C*-N), δ149.8 (C=*C*-O), δ144.5 (Ar*C*-S), δ134.8 (C=*C*-OMe), δ129.1 (Ar*C*H), δ127.3 (Ar*C*H), δ126.2 (Ar*C*H), δ122.8 (C=*C*OMe), δ99.1 (C=*C*H), HRMS (m/z+ 1) Expected: 262.01685 Found 262.0169

3,4-dimethoxy-6-(6-methoxybenzo[d]thiazol-2-yl)-2H-pyran-2-one (304)

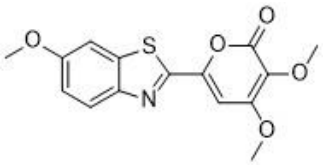

To a mixture of 3,4-dimethoxy-2-oxo-2H-pyran-6-carbaldehyde (0.184g, 1.00mmol) in acetonitrile (10mL), 2-amino-5-methoxybenzenethiol (0.155g, 1.00mmol) was added dropwise. The mixture was heated at 55°C for 12h. After cooling down, the solvent was removed under vacuum and the residue was dissolved in dichloromethane (10mL). DDQ (0.227g, 1.00mmol) was added into the mixture and stirred at room temperature overnight. After completion of reaction, sat.aq.$NaHCO_3$ (10mL) was added into the mixture and extracted with EtOAc (3 x 10mL). The organic layers

were combined, dried over $MgSO_4$, concentrated under vacuum and a column (1:3 EtOAc/ petroleum ether) was used to obtain product as an orange solid (0.160g, 0.500mmol, 50%).

^{1}H NMR (400MHz, $CDCl_3$): δ7.95 (1H, d, J= 9.0Hz, Ar*H*), δ7.39 (1H, s, Ar*H*), δ7.31 (1H, s, OC=C*H*), δ7.16 (1H, d, J=9.0Hz, Ar*H*), δ4.11 (1H, s, OCH_3), δ3.93 (1H, s, OCH_3) , δ3.71 (1H, s, OCH_3). ^{13}C NMR (125MHz $CDCl_3$) δ159.9 (N=*C*S), δ158.9 (O=*C*-O), δ158.4 (Ar*C*-N), δ156.4 (C=*C*-O), δ150.2 (Ar*C*-S), δ137.8(C=*C*-OMe), δ130.1 (Ar*C*H), δ124.5 (Ar*C*H), δ117.5 (Ar*C*H), δ103.9 (C=*C*OMe), δ96.2 (C=*C*H), δ60.5 (O*C*H_3), δ57.8 (O*C*H_3), δ56.0 (O*C*H_3). IR Vmax (solid) 2927 (alkane C-H), 1712 (C=O), 1628 (C=C), 1602 (C=C), HRMS (m/z+ 1) Expected: 320.5872 Found 320.579, m.p 105.5°C

3,4-dihydroxy-6-(6-methoxybenzo[d]thiazol-2-yl)-2H-pyran-2-one (306)

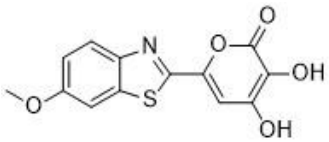

To a mixture of 60% NaH protected with oil (0.154g, 4.00mmol) in DMF (5mL), EtSH (0.372g, 0.440mL, 6.00mmol) was added dropwise and stirred for 10min. After all the solid was dissolved, 6-(benzo[d]thiazol-2-yl)-3-hydroxy-4-methoxy-2H-pyran-2-one (0.275g, 1.00mmol) was added and the mixture was stirred at 90°C for 12h. After completion of reaction, the mixture was heated at 115°C and dried under wind. Acetic acid was added into solid residue to neutralize pH~7. The solid residue was washed with chloroform and filtrates were combined, dried over $MgSO_4$. The solvent was removed under vacuum and the solid was recrystallized in diethyl ether to obtain product as a dark orange solid (0.125g, 0.430mmol, 43%).

^{1}H NMR (400MHz, dmso-d_6): δ10.04 (1H, s, O-*H*), δ7.85(1H, d, J= 8.9Hz, Ar*H*), δ7.43 (1H, s, Ar*H*), δ7.01 (1H, d, J= 9.0Hz, Ar*H*), δ6.63 (1H, s, C=C-*H*), δ3.89 (1H, s, OCH_3). ^{13}C NMR (125MHz, dmso-d_6) δ159.3 (N=*C*-S), δ156.7 (O-*C*=C), δ149.1 (O=*C*-O), δ146.8 (Ar*C*H), δ136.8 (Ar*C*H), δ127.4 (C=*C*OMe), δ124.4 (HO*C*=C), δ117.3 (Ar*C*H), δ106.9 (Ar*C*H), δ100.6 (C=*C*H), δ59.4 (O*C*H_3), IR Vmax (solid) 3092 (alkene C-H), 3010 (alkane C-H), 1705 (C=O), 1650 (C=C), HRMS (m/z+ 1) Expected: 320.5872 Found 320.579, m.p 125.3°C

6-methoxybenzo[d]thiazole (190)

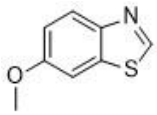

To a solution of 6-methoxybenzo[d]thiazol-2-amine (1.17g, 6.50mmol) in THF (15mL), isopentylnitrite (1.52g, 13.0mmol) was added under N_2. The mixture was stirred at 70°C for 2h. Then water (50mL) was added and the aqueous layer was extracted with EtOAc (3x 35mL). The organic layers were combined, dried over $MgSO_4$, concentrated under vacuum. A flash column (1:1 EtOAc/ petroleum ether) was used to obtain product as an orange oil which solidify at room temperature (0.870g, 5.27mmol, 81%).

^{1}H NMR (400MHz, $CDCl_3$): δ8.81 (1H, s, N=C*H*S), δ7.98 (1H, d, J= 9.0Hz Ar*H*), δ7.36 (1H, d, J= 3.0Hz, Ar*H*), δ7.11 (1H, dd, J=9.3Hz, 2.4Hz, Ar*H*), δ3.87 (1H, s, OCH_3). m.p 45.3°C Data in agreement with literature values[138]

6-methoxybenzo[d]thiazole-2-carbaldehyde (188)

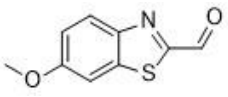

To a mixture of 6-methoxybenzo[d]thiazole (0.305g, 1.85mmol) in anhydrous THF (5mL) was added n-BuLi (2.5M in hexane, 0.960mL, 2.40mmol) dropwise at -78°C. The resulting solution was stirred at -78°C for 30min. Anhydrous DMF (0.540g, 7.40mmol) was then added dropwise at -78°C. The mixture was then raised to room temperature and stirred for 1h. After completion, the mixture was quenched with NH_4Cl at 0°C and extracted with dichloromethane (3 x 10mL). The organic layer was then washed with brine (2 x 15mL), dried over $MgSO_4$, concentrated under vacuum. A flash column was used to obtain product as a pale yellow solid (0.108g, 0.560mmol, 30%).

^{1}H NMR (400MHz, $CDCl_3$): δ10.11 (1H, s, O=C*H*), δ8.12 (1H, d, J= 9.1Hz, Ar*H*), δ7.39 (1H, s, Ar*H*), δ7.21 (1H, d, J= 9.1Hz, Ar*H*), δ3.93 (1H, s, OCH_3). m.p 78.5°C
Data in agreement with literature values[139]

3,4-dimethoxybenzothioamide (323)

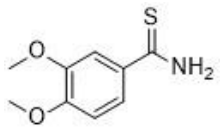

A mixture of 3,4-dimethoxybenzonitrile (2.70g, 14.0mmol) and thioacetamide (2.11g, 28.0mmol) in 10% HCl-DMF solution (15mL) was stirred at refluxing for 15h. After cooling, the reaction mixture was poured onto ice. The precipitate was filtered and washed with diethyl ether (20mL). The crude product was recrystallized from EtOAc to give product as a pale solid (2.18g, 11.1mmol, 79%).
^{1}H NMR (400MHz, $CDCl_3$): δ7.63 (1H, s, Ar*H*), δ7.53 (1H, brs, N-*H*), δ7.39 (1H, d, J= 8.4Hz, Ar*H*), δ7.15 (1H, brs, O-*H*), δ6.85 (1H, d, J= 8.4Hz, Ar*H*), δ3.93 (6H, s, OCH_3). m.p 187.4°C
Data in agreement with literature values[140]

Ethyl 2-(3,4-dimethoxyphenyl)-4-hydroxythiazole-5-carboxylate (325)

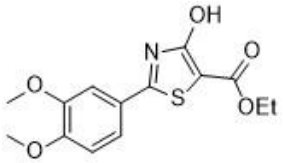

To a mixture of 3,4-dimethoxybenzothioamide (1.00g, 5.00mmol) in toluene (10mL), diethyl 2-bromomalonate (1.19g, 5.00mmol) and pyridine (0.0790g, 1.00mmol) was added. The mixture was stirred at 60°C for 8h. After cooling down, the mixture was concentrated and a direct column (1:2 EtOAc/petroleum ether) was used to obtain product as an orange solid (1.36g, 4.40mmol, 88%).
^{1}H NMR (400MHz, $CDCl_3$): δ9.96 (1H, brs, O*H*), δ7.58 (1H, s, Ar*H*), δ7.54 (1H, d, J=8.4Hz, Ar*H*), δ6.91 (1H, d, J= 8.4Hz, Ar*H*), δ4.41 (2H, q, J= 7.1Hz, OCH_2CH_3), δ3.68 (1H, s, OCH_3), δ3.52 (1H, s, OCH_3), 1.26 (3H, t, J= 7.1Hz, CH_2CH_3). ^{13}C NMR (100MHz, $CDCl_3$) δ170.3 (N=*C*S), δ169.7 (O=*C*-O), δ152.4 (Ar*C*OH), δ149.4 (Ar*C*OH), δ146.3 (S*C*=C), δ141.5 (N*C*OH), δ127.5(Ar*C*H), δ125.7 (Ar*C*H), δ120.2 (Ar*C*H), δ111.1 (Ar*C*H), δ109.3 (Ar*C*H), δ61.7 (OCH_2CH_3), δ56.2 (OCH_3), δ14.4

(CH_2CH_3). IR Vmax (solid) 3405 (O-H), 3105 (C=C-H), 2985-2836 (C-C-H), 1713 (C=O), 1576 (Ar), 1524 (Ar), 1438 (Ar); HRMS (m/z+ 1) Expected: 310.0744 Found 310.0744

9. References

1. R. Boyle, *Philosophical Trans*, 1668, **2**, 605
2. L. John, *J. Siberian Federal University. Bio*, 2008, **1**, 194-205
3. K. Alexander. N, K. Vasilisa. V, E. Maxim. K, Z. Sayana. V, R. Anastasia. V, T. Felix. N, F. Ludmila. A, *Int. J. Mol. Sci*, 2023, **24**, 2144
4. J. Tianyu, D. Lupei, and L. Minyong, *Photochem. Photobio. Sci*, 2016, **15**, 466-48
5. N. Hideshi, W. Chun, I. Satoshi, M. Akio, *J. Am. Chem. Soc.*, 2001, **123**, 1523-1524
6. T. Goto, M. Isobe, D.A. Coviello, Y. Kishi, S. Inoue, *Tetrahedron*, 1973, **29**, 2035-2039
7. Tsuji.F.I, Barnes. A.T. and Case, J. F, *Nature (London)*, 1972, **237**, 515-516
8. V. Vadim. R, U. Akira, V. Wladia, O. Yoshihiro, *Photochem. Photobio*, 2002, **76**, 538-544
9. V. Martha and D. Iglesias-Rodriguez, *Microorganisms*, 2013, **1**, 3-25
10. S. Osamu, *J. Bioluminescence and Chemiluminescence*, 1995, **10**, 91-101
11. L. John, F. Müller and A. J. W. G. Visser, *Photochem. Photobio.*, 2019, **95**, 679-704
12. K. Alexey. A, S. Karen. S, M. Yuliana. A, M. Marina, S. Ekaterina O, M. Nadezhda. M, S. L. Gonzalez, G. Andrey. Y, V. Andrey, P. Konstantin. V, P. Valentin. N, R. Natalja. S, C.Tatiana. V, F. Liliia. I, G. Elena. B, Z. Rustam, T. Aleksandra. S, K. Zinaida. M, S. Victoria, A. Maxim, A. Tatiana. O, P. Inna. S, E. Fedor. M, Z. Andrey. G, M. Alexander. S, D. Sergey. V, M. Tatiana. Y, K. Eugene. P, W. Hans. E, O. Anderson. G, O. Yuichi, B. Ekaterina, B. Ekaterina.

A, G. Toni, S. Cassius. V, L. Sergey, S. Ivan. V, G. Josef . I , K. Fyodor. A, Y. Ilia. V, *Proc. Natl. Acad. Sci - Pnas*, 2018, **115**, 12728-12732

13. F. Aubin, and K. S. Sarkisyan, *Curr. genetics*, 2019, **65**, 877-882
14. W.D. McElroy, J.W. Hastings, J. Coulombre, V. Sonnenfeld, *Arch. Biochem. Biophys*, 1953, **46**, 399-416
15. A. Louis M, R. I. Weed and S. B. Troup, *Analyt. Biochem*, 1966, **17**, 268-277
16. Harber. M. J and A. W. Asscher, *J. Antimicrobial Chemotherapy*, 1977, **3**, 35-41
17. W. G. S.E. Brolin and L. Juhlin, *J. Colloid and Interface Sci*, 1980, **73**, 287-289
18. R. George. T, *Photochem. Photobio*, 1978, **27.4,** 405–421
19. Barry. J. D, Heitman, J. M, Lane, C. R, *J. Applied. Phys*, 1979, **50**, 7181-7185
20. Mueller-Klieser. W and S. Walenta, *The Histochem. J*, 1993, **25**, 407-420
21. S. Julia. L and T. C. Zhu, *J. Biophotonics*, 2011, **4**, 773-787
22. C. Maria. Maddalena, G. Denise, M. Héctor, M. Elisa, *Biosensors (Basel)*, 2022, **12**, 742
23. L. Xueyan, Y. Nakajima, K. Niwa, V. R. Viviani, Y. Ohmiya, *Protein. Sci*, 2010, **19**, 26-33
24. S. T. Adams, D. M. Mofford, G. S. K. K. Reddy, S. C. Miller, *Angew. Chem. Int. Ed*. 2016, **55**, 4943
25. H. Takashi, H. Yosuke, O. Kazuhiro, M. Shojiro, N. Haruki, Y. Minoru, H. Daisuke, *J. Am. Chem. Soc*, 2009, **131**, 2385-2396
26. P. Konstantin. V, P. Valentin. N, B. Mikhail. S, M. Konstantin. S, R. Natalja. S, K. Zinaida. M, T. Aleksandra. S, P. Alexei. I, B. Vladimir. S, R. Emma. K, M. Svetlana. E, O. Yuichi, O. Yumiko, A. Alexander S, L. Sergey, G. Josef I, Y. Ilia. V. *Angew. Chemie (Int. ed.)*, 2015, **54**, 8124-8128

27. B. Bruce. R, B. Curran. E, S. Tara. L, F. Danielle. M, G. Andrew. M, V. David. J, B. Gary. W, *J. Am. Chem. Soc*, 2015, **137**, 7592-7595

28. Horecker, B.L, *J. Bio. Chem*, 1943, **148**, 173-183

29. E. H. White, F. McCapra, G. F. Field, W. D. McElroy, *J. Am. Chem. Soc*., 1961, **83**, 2402-2403

30. W. Emil. H, F. McCapra, and G. F. Field. *J. Am. Chem. Soc.*, 1963, **85**,337-343

31. I. Satoshi, O. Rika, M. Chihiro, K. Masahiro, H. Kazutoshi, N. Mitsuhiro, A.Yoshiharu, K. Satoshi, H. Takashi, M. Shojiro, N. Haruk, *Tetrahedron*, 2013, **69**, 3847-3856

32. Anderson, J. C, Amit. P. J and Aisha. J.S, *Tetrahedron*, 2019, **45**, 347-356.

33. M. David. M, A. Spencer. T, R. G. S. K. Kumar, R. G. Randheer, M. Stephen. C, *J. Am. Chem. Soc.*, 2015, **137**, 8684-8687

34. E. Melanie S, C. Joanna. P, A. Jr. Spencer. T, R. Gadarla. R, P. Miranda. A, A. Neil, P. Jennifer. A, M. Stephen. C, *Nature methods*, 2014, **11**, 393-395

35. M. David. C, P. Miranda. A, S. Rachel. C, P. Jennifer. A, *J. Am. Chem. Soc*, 2012, **134**, 7604-7607

36. S. Ioka, T. Saitoh, S. Iwano, K. Suzuki, S. A. Maki, A. Miyawaki, M. Imoto, S. Nishiyama, *Chem. Eur. J*. 2016, **22**, 9330

37. M. Giuseppe, C. Paolo, M. Adriana, S. Enzo, *Synlett*, 2009, **16**, p. 2682 - 2684

38. J. Metzger and H. Planck, *Chim. Ind. (Paris)*, 1956, **75**, 930.

39. M. F. G. Stevens, C. J. McCall, P. Lelieveld, P. Alexander, A. Richter, *J. Med. Chem*, 1994, **37**, 1689

40. E.H. White, H. Wörther, G. F. Field, W.D. McElroy, *J. Org. Chem*, 1965, **30**, 2344-2348

41. E.H. White, H. Worther, H.H. Seliger, W.D. McElroy, *J. Am. Chem. Soc*, 1966, **88**, 2015-2019

42. Y. Toya, M. Takagi, H. Nakata, N. Suzuki, M. Isobe, T. Goto, *Bull. Chem. Soc. Jpn.*, 1992, **65**, 392-395

43. N. Suzuki, T. Nomoto, Y. Toya, N. Kanamori, B. Yoda, A. Saeki, *Biosci. Biotechnol. Biochem*, 1993, **57**, 1561-1562

44. D.C. McCutcheon, W.B. Porterfield and J.A. Prescher, *Org. & Biomol. Chem*, 2015, **13** ,2117-2121

45. J. Amit P, G. Helen, A. James. C, P. Martin. A, *Angew. Chemie. (Int. ed.)*, 2014, **53**,13059-13063

46. Airth. R. L and W. D. McElory. *J. Bacteriology*, 1959, **77**, 249-250

47. Kuwabara. S and E.C Wassink, *Bioluminescence in Progress*, 2015, 233-246

48. O. Anderson G and C. V. Stevani, *Photochem. Photobio. Sci*, 2009, **8**, 1416-1421

49. P. Kseniia. A, B. Anastasia. V, B. Olga. A, C. Tatiana. V, M. Nadezhda. M, K. Sergey. I, T. Aleksandra. S, M. Alexander. S, Y. Ilia. V, S. Karen. S, *Int. J. Mol. Sci*, 2023, **24**, 1317

50. K. Zinaida. M, D. Felipe. A, P. Valentin. N, P. Konstantin. V, T. Aleksandra. S, R. Natalja. S, M. Konstantin. S, G. Elena. B, K. Alexey, B. Nadezhda. S, B. Mikhail. S, A. Alexander. S, G. Josef. I, L. Sergey, S. Yoshiki, K. Shusei, P. Ernani, D. Paolo, W. Hans. E, P. Tatiana. A, C. Rodrigo. P, O. Anderson. G, O. Yuichi, B. Erick. L, S. Cassius. V, Y. Ilia. V, *Sci. Adv*, 2017, **3**, 1602847-1602847

51. T. Yapei, T. Milos, S. Simone, V. B. Willem J.H, F. Marco. W, *J. Bio. Chem*, 2020, **295**, 16013-16022

52. M. Tatiana, M. Alexander. S, S. L. Gonzalez, M. Nadezhda. M, C. Tatiana. V, G. Elena. B, K. Tatiana. A, P. Kseniia. A, S. Ekaterina. S, F. Liliia. I, C. Sofia. V, T. Aleksandra. S, G. Yaroslav. V, N. Vadim. V, D. Sergey. A, S. Pavel. V, S. Dmitry, M. Olesya. A, S. Victoria. O, D. Sergey. M, B. Andrey. I, P. Alexander. S, C.Vladimir. V, D. Sergey. V, K. Fyodor. A, Y. Ilia. V, S. Karen. S, *Nature. Biotech*, 2020, **38**, 944-946

53. K. Arjun, S. Colby. G , C. James. C, L. Nayoung, S. Sydney, W. Cecily, S. Ryan, R. Furva, I. Takato, V. Daniel. F, *eLife*, 2020, **9**, web

54. M. Matthew. A, and D. H. Wise, *Oecologia*, 2019, **191**, 587-599

55. K. Huei-Mien and I. J. Tsa, *Curr. Opin. Green. Sustainable Chem*, 2022, **33**, 100570

56. C. Martin, N. L. Eimear, K. Paul, L. Heather, C. Julia, L. Brian, D. Brian, H. Danny, G. Ester, L.Theo, A. A. Martyn, G. Yusufjon, H. Kevin, C. Pedro, H. Mark, W. Barnaby. E, C. F. Rafaela, W. K. Meng, N. Tuula, *Plants, People, Planet*, 2020, **2.5**, 371–388.

57. D. Dennis E, A. G. Oliveira and C. V. Stevani, *Photochem. Photobio. Sci*, 2008, **7**, 170-182

58. B. Kendra, M. P. A. Coetzee and D. Hoffmeister, *Mol. Plant. Pathology*, 2011, **12**, 515-534

59. Pu. A. P, M. S. E and Bondar V. S, *Chemicals & Chem*, 2017, 886

60. C. Audrey. L. C, D. Dennis E, T. Yee-Shin, M. M. Yusoff, S. Vikineswary, *Fungal Diversity*, 2015, **70**, 149-187

61. W. Philip, D. Steven, W. Tom, A. Andrew. D, *IMA Fungus*, 2016, **7**, 229-234

62. D. Dennis E, P. Brian A, L.D. Jean, S. Cassius V, N. Eiji, *Mycologia*, 2010, **102**, 459-477

63. S. Gary B, Accounts of chemical research, 1979, **12**, 366-373

64. Y. Ling and Y. Liu, *J. Physical. Chem*. B, 2020, **124**, 7682-7693

65. G. Angelo, F. Pooria, M. M. Daniel, L. Marcus, L. Roland, R. S. Daniel, *Chem : A. Eur. J.*, 2019, **25**, 5202-5213

66. S. Jimmie P, A. K Schrock and G. B Schuster, *J. Am. Chem. Soc*. 1982, **104**, 1041-1047

67. Briviba. K, Saha-Möller, C. R. Adam, W. Sies. H, *Biochem. Mol. Bio, Int*., 1996, **38**, 647-651

68. W. Ming-Yu, and L. Ya-Jun, *J. Org. Chem*, 2021, **86**, 1874-1881

69. I. Kim. N, Q. Stephan, D. B. Melanie, W. Dennis S., K. Jan, S. Philipp, L. Ute, Z. Ralf, M. Ulf, S. Katrin, M. Christian, O. Klaus, G. Jochen S., H. J. Kerstin, *Chembiochem : A. Eur. J. Chem. Bio*, 2021, **22**, 398-407

70. H. Evangelia, A. Varvoglis, and M.Bakola-Christianopoulou, *J. Org. Chem*, 1990, **55**, 315-318

71. Bacardit. R., Moreno-Manas. M and Pleixats, R, *J. Heterocyclic Chem.*, 1982, **19**, 157 - 160

72. Bubyrev. A. I, Tsarkova. A. S, Kaskova. Z. M., *Russ J. Bioorgan. Chem*, 2019, **45**, 183-185

73. G. Cristina, L. Raúl, F. Diana, S. Diego, N. Isabelle, *J. Org. Chem*, 2020, **85**, 5503-5510

74. C. Steven. K, B. Koen, M. Evelyne, D. S. Stefaan. C, S. Niek. N, *J. Fluorescence*, 2013, **23**, 909-920

75. S. T. Adams, D. M. Mofford, G. S. K. K. Reddy, S. C. Miller, *Angew. Chem. Int. Ed*. 2016, **55**, 4943-4946

76. K. Nobuo, S. Tsuyoshi, I. Yuma, I. Satoshi, O. Rika, N. Haruki, H. Takashi, M. Atsushi, S. Koji, N. Shigeru, M. Shojiro A, *Tetrahedron. Lett*, 2018, **59**, 1087-1090

77. K. Takahiro, I. Satoshi, K. Masahiro, M. Shun, K. Tetsuya, N. Haruki, M. Shojiro, K. Shinae, *Nat. Commun.*, 2016, **7**, 11856-11856,

78. R. G. Randheer, W. C. Thompson, and S. C. Miller, *J. Am. Chem. Soc*, 2010, **132**, 13586-13587

79. G. Samer, G. S. Popat, G. Liang, D. Sayantan, G. Sara, G. Ori, S. Omri, H. Nir, B. Phil S, S. Doron, *Int. ed. in English; Angew. Chemie, (Int ed.)*, 2022, **61**, e202202187-n/a

80. L. Chanjuan, C. Bao, Sai, Z. Huihao, G. Qiong, X. Jun, *Eur. J. Med. Chem.* 2018, **143**, 114-122

81. C. Jonathan, S. Warren and N. Greeves, *Organic Chemistry*. Oxford University Press, 2012.

82. R. M. Goreti, V. M. Hugo,S. Isabel C, S. Isabel, O. Tiago F, P. Antonio, *Bioorg. Med. Chem*, 2011, **19**, 7698-7710

83. R. Raphaël, R. Jeffery, A. Varinder. K, H. Jeremy. N, *J. Am. Chem. Soc*. 2005, **127**, 13468-13469

84. Current Patent Assignee: National Institutes For Quantum and Radiological Science and Technology - EP3932405, 2022, A1 Location in patent: Paragraph 0137, 0139

85. K. Momochika, N. Keisuke, M. Takashi, Y. Izumi, I. Masahiro, K. Keiko, N. Munetomo, M. Yoshiki, *Bio. Med. Chem. Lett.*, 2017, **27**, 2401-2406

86. R. Michael. G. N, C. Robert. W, A. John. R, B. Frances. A, C. Susan. M,H. Peter, I. Catherine, L. Matt, M. Ruth. M, M. Andrew, M. Kevin. W, N. Robert, M. Alison. J, T. David, T. Sally-Anne, W. Keith. A, C. José L, *J. Med. Chem.*, 2005, **48**, 1367-1383

87. D. Alessandro, F. Giancarlo, F. Marco, M. Alessandro, P. Paola, *Tert*, 1988, **44**, 2021-2031

88. P. Kwakye, Z. Xue Y, E. Suresh V.K,E. Jagan R, S. Vincent, R. Bryan L,A. Seth Y, *Bioorg. Med. Chem.*, 2012, **20**, 1671-1678

89. F. Zhanxiong, L. Pei-Chun, Y.Yu-Liang, Y. Feng-Ling, C. Yi-Lin, L. Yulin, H. Kuo-Feng, W. Shih-Hsiung, *J. Med. Chem*, 2010, **53**, 7967-7978

90. C. Bao, L. Yongsheng, K. Ming, F. Sai, G. Qiong, X. Jun, W. Laiyou. *Chem. Bio. Drug. Design*, 2015, **86**, 1121-1130

91. Stephenson. L. M, and D. R. Speth, *J. Org. Chem*, 1979, **44**, 4683-4689

92. DeWolfe. R. H, and W. G Young, *Chem. Reviews*, 1956, **56**, 753-901

93. Waitkins. G. R, and C. W. Clark. *Chem. Reviews*, 1945, **36**, 235-289

94. H. Steven. S, Q. Li and A. L. L East, *J. Physical. Chem*. 2005, **109**, 10975-10981

95. H.Yiran, C. Hong-Jun, B. Nilantha, S. Liang, T. Diana, R. Buck E., M. Liviu M, *Chem. Sci. (Cambridge)*, 2020, **11**, 7789-7799

96. F. Brian. E, G. Ashvinikumar. V, T. John. S, G. Bindu, M. Raj, X. Hai-Yun, K. S. David, H. Wen-Ching, N. Derek, S. Thomas E, Y. Dan, G. Marco M, L. Matthew V, V. Gregory D, *Bioorgan. Med. Chem. Lett*, 2006, **16**, 1532-1536

97. W. Ashley. A, M. C. Bagley and A. D. Westwell, *Tetrahedron*, 2011, **67**, 7743-7747

98. R. M. Goreti, V. M. Hugo,S. Isabel C, S. Isabel, O. Tiago F, P. Antonio, *Bioorg. Med. Chem.*, 2011, **19**, 7698-7710

99. R. Morais, Goreti, V. M. Hugo, S. Isabel C, S. Isabel, O. Tiago F, P. Antonio, *Topics in Cur. Chem.* (2016), 2021, **379**, 38-38, Article 38

100. O. Dmitrii. L, N. Diana. I, S. Alexander. S, M. Oleg. E, F. Vladislav. V, U. Sergey. A, S. Alena. E, K. Mikhail. Y, S. Vyacheslav. Y, *Molecules* (Basel, Switzerland), 2022, **27**

101. K. Aleksey. V, L. Nan, H. Richard. P, G. Glen C, C. Kevin. P, S. Nadiya, S. Jacob. J, *Organ. Lett*, 2006, **8**, 191-193

102. O. Takayuki, M. Keisuke, I. Fumitaka, H. Tatsuya, Y. Masahito, K. Hideo, *Bullet. Chem. Soc. Japan*, 2020, **93**, 1540-1551

103. N. Aayesha and S. R. Adapa, *Organ. Prep. Proce. Int*, 1999, **31**, 573-575

104. S. Jordi, S. R. Maria, V. Adelina, C. J. Francisco, N. Carmen, *Tetrahedron*, 2013, **69**, 2655-2659

105. M. Albert, and K. Krohn, *Chemische Berichte*, 1970, **103**, 2729-2743

106. Current Patent Assignee: Kyung-In Synthetic Corporation- EP1367099, 2003

107. K. Thomas, G. Korbuly and E. P. M. für, *Chemie*, 1983, **114**, 303

108. K. Talon M, C. Heidi A, K. Andrew L, L. Richard L, *Eur. J. Org. Chem*, 2015, **2015**, 7460-7467

109. Kulkarni, Kadam, Mane, D. Uday. V, Wadgaonkar, *J. Chem. Research. - Part S*, 1999, **6**, 394 - 395

110. B. Svante, F. Magnus, L. Hans, S. Anders, *J. Am. Chem. Soc*, 2003, **125**,11942-11955

111. L. Peter and T. Schneider, *Syn. Lett*, 2000, **2000**, 497-500

112. P. E. Bit and K. Jeong, *Chem. Commun (Cambridge, England)*, 2015, **51**,9197-9200

113. Minale,L. *Gazzetta Chimica Italiana*, 1970, **100**, 870 – 879

114. B. Jacob. J, G. Jacob. P, L. Chunyin. M, S. Jessica. L, G. John. R, M. T. Andrew, *J. Org. Chem.*, 2019, **84**, 10306-10320

115. C. Junbiao, K. Zhao and S. Pan, *Tetrahedron Lett*, 2002, **43**, 951-954

116. O. Grace, J. C. Chukwujekwu and F. R. van Heerden, *Synthetic. Commun.*, 2020, **50**, 726-734

117. A. Meshari. A, R. Q. Alam, M. N. Abdul, J. Rabab. S, A. Abdulrahman. A, S. Amina, N. Nafeesa, M. E. Ullah, A. Reem. I, M. Ziad, A. Saleh. A, *RSC. Adv*., 2021, **47**, 29826-29858

118. J. Jae-Chul, Y. Jung, and O. Park, *Synthetic.Commun*, 2001, **31**, 1195-1200

119. H. Shu-Yi, F. Shi-Liang, W. Xing-Rong, W. Zhichao, C. Shi-Wu, H. Ling, *Bioorg. Med. Chem. Lett*, 2019, **29**, 2129-2135

120. B. Gianluca, T. Mara, L. Samuele, S. Anna, B. Silvia, Z. Lorena, L. Chiara, N. Rubina, A. Andrea, *J. Med. Chem*, 2021, **64**, 16820-16837

121. C. Masatoshi, N. Hisashi, T. Isao, K. Kazuyoshi, K. Hajime, S. Kazuo, T. Fujio, M. Toyoki, T. Michiaki, Y. Youichi, *J. Med. Chem*, 1995, **38**, 353-358

122. P. Lockemann, *Chemische Berichte*, 1915, **48**, 30

123. Current Patent Assignee: Haisco Pharmaceutical Group CO., LTD. - WO2017/218960, 2017

124. F. Sai, C. Lei, Y. Miao, C. Bao, L. Yongsheng; M. Susan L, L. Kuo-Hsiung, G. Qiong, X. Jun, *Org. Biomol. Chem*, 2015, **13**, 4714-4726

125. N. Rahul R, K. Vijay V, B. Sachin S, S. Devanand B, *Euro. J. Med. Chem*, 2005, **40**, 1325-1330

126. G. Zsombor, B. Ferenc, T. Orsolya, P. Milán, N. Zoltán;T. Balázs L, *Eur. J. Org. Chem*, 2017, **2017**, 2112-2117
127. P. Allan. M, G. Medha. J, K. Daisuke, D. John, K. Yunjeong, C. Kyeong-Ok, M. Izumi, J. Lee-Way, H. Duy. H, *Synthesis (Stuttgart)*, 2014, **46**,2179
128. E. Franz, S. Karl-Heinz, *Chemische Berichte*, 1984, **117**, 3270-3279
129. X. Feng, L.Yuqin, H. Xin, F. Xinjie, L. Zhuofei, J. Hongshuo, Q. Jingyi, C. Wenyi, S. Zhizhong. *Adv. Syns. Catalysis*, 2019, **361**, 520-525
130. M. Stephen. T, K. Marcel, B. Helena. I, B. Peter. D.W, C. Brent. R, *Bioorg. Med. Chem*., 2012, **20**,1482-1493
131. L. Bo, L. Ding, Z. An-Ling, G. Jin-Ming, *Molecules*, 2018, **23**, 2457
132. Knott, E. B. *J. Chem. Soc*, 1965, 3793
133. Y. Fujimoto, S. Kanazaki, M. Nishino, S. Koike, *Chem. Pharma. Bullet*, 1992, **40**, 2055 ~2061
134. Z. Yu-Shen, S. Linlin, F. Lianrong, C. Xiran, Z. Xinju, H. Xin-Qi, S. Mao-Ping. *Chinese.Chem. Lett*, 2022, **33**, 1497-1500
135. Kindai University - WO2022/196819, 2022, A1, Page 0045
136. Zavarzin. I. V, Karabaeva. L. K, Shimkina, N. G, Shorunov. S. V, Yarovenko. V. N, Platonova. I. V, Kobeleva. O. I, Valova. T. M, Barachevskii. V. A. Krayushkin. M. M, *Chem. Heterocyclic. Compounds*, 2012, **47**, 1445 ~1452
137. K. Takayuki, I. Akira, N. Yasuhiro, T. Yoshio, Y. Hisashi, S. Seishi, O. Nobuhisa, O. Kaoru, *Chem. Pharma. Bullet*, 1997, **45**, 297-304
138. L. Ethan. J, V. Amy. L, H. Bao, K. Jayson. J, S. Scott. E, D. Stephen. G, *Org. Biomolecular. Chem*, 2017,**15**, 2246-2252
139. Current Patent Assignee: National Institutes For Quantum and Radiological Science and Technology - EP3932405, 2022, A1

140. C. Masatoshi, N. Hisashi, T. Isao, K. Kazuyoshi, K. Hajime, S. Kazuo, T. Fujio, M. Toyoki, T Michiaki, Y. Youichi, *J. Med. Chem.*, 1995, **38**, 353-358

141. O. Yuichi, S. Yoshiki, M. Gabriel. N. R, C. Rodrigo. P, P. Tatiana. A, W. Hans. E, K. Shusei, N. Masashi, O. Anderson. G, D. Felipe. A, P. Ernani, Y. Ilia. V, S. Cassius. V, *Photochem. Photobiolo. Sci*, 2017, **16**,1435-144

142. L. Bryan, B. Martin, B. R, C. Charles K.-F, C. Stephen. T, K. Takushi, K. Nandell, K. William, L. Tung, L. Kyle. R, M. Brian, M. Ronald, N. Lisa, W. Silke, W. Michael, W. John, Z. Zhijun, Z. Zhongli, *J. Org. Chem*, 2006, **71**, 9045-9050

143. M. Z. Zhdankin and Viktor V, *Arkivoc*, 2012, **1**, 432-490

144. McCauley, J. Irene, *Synlett*, 2012, **23**, 2999-3000

145. H. Xianqiang, R. Nianxin, L. Pengfei, S. Guodong, L. Qiang, X. Nana, C. Chuansheng, C. Jichui, Y. Bingchuan, L. Dacheng, Z. Changqiu, D. Jianmin, W. Bo, *Org. Lett*, 2018, **20**, 3332 - 3336

146. Khaligh, N. G, *Dyes and pigments*, 2017, **139**, 556-560

147. Itoh. T, Matsuya. Y, Nagata. K, Ohsawa. A, *Tetrahedron Lett*, 1996, **37**, 4165-4168

148. Itoh. T, Matsuya. Y, Nagata. K, Ohsawa. A, *Chem. Pharma. Bullet*, 1997, **45**, 1547-1549